Quantifying the costs of transport networks' components

Dissertation zur Erlangung des Grades eines Doktors der Wirtschaftswissenschaft

eingereicht an der Fakultät für Wirtschaftswissenschaften der Universität Regensburg

vorgelegt von: Maximilian Braun

Berichterstatter:

Prof. Dr Andreas Otto

PD Dr. Florian Kellner

Tag der Disputation:

07.07.2022

Table of Contents

List of Figures

List of Tables

1. Introduction

During the process of moving freight from origin to destination, consignors can choose from a set of different modes of transportation. The most common methods of moving goods across geographical distances discussed in literature and used in practice are airfreight, sea freight, rail freight, road freight or the so-called intermodal split. The existence of different modes results from inherent characteristics, advantages and disadvantages each mode has depending on a specific weight, volume, worth and distance that must be covered for any given shipment. The choice of transport mode can also be seen from the perspective of maximizing or minimizing one specific variable or the simultaneous optimization of a set of decision variables. Examples of decision variables mentioned in literature are flexibility, costs, velocity, sustainability, quality, frequency or reliability [1,2]. Determining the right mode of transportation is considered a complex process due to the amount of possible combinations in characteristics every available mode contributes and their combined impact on a desirable decision variable outcome [3].

When talking about last mile logistics, the dominant mode of transport is road freight [4,5]. The importance of road freight transportation for Business-to-Business (B2B) and Business-to-Customer (B2C) use cases can be explained due to their shared requirement of high flexibility which is necessary to reach all recipients within a distribution network to provide door-to-door service [6]. As long as the recipients' locations are connected to a public road network – which holds true for most of the populated areas worldwide – there is a possibility to deliver freight via road transportation. Within the context of this thesis, road freight transportation is limited to the main task of moving freight via vehicles throughout a road network. Loading and unloading, more generally considered as handling, is therefore not part of this research. Based on its importance to basic economic and social transactions, the research community is studying the topic of road freight transportation very extensively.

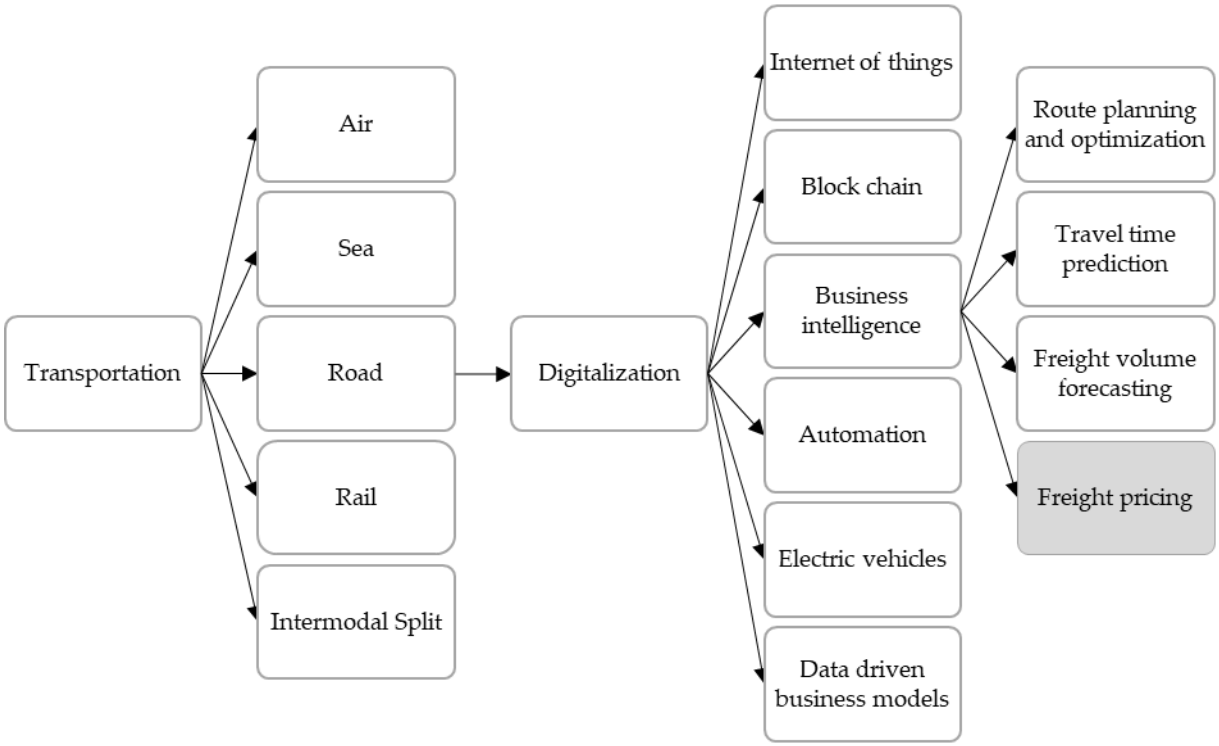

Figure 1 Overview of selected digitalization trends in the field of road freight transportation. This figure does not account for completeness but is limited to recent focus in literature.

Examining recent publications within the field, a broad body of literature relating to the keyword "Digitalization" can be found. To understand the concept of digitalization, the root of its appearance and its impact on road freight transportation, the following section will give a suitable definition and discuss the trends established in this field of research.

To begin with, key concepts of digitalization relevant within the road freight transportation context are defined by slightly modifying existing definitions found in literature. In general, Digitalization is considered an opportunity to improve efficiency, reduce costs, increase service levels and enable new business models driven by new technologies [7]. Technologies are defined as all tools, machines, data and information by which we produce and use them [8]. With operative margins being very small, the road freight industry always searches for ways to improve efficiency, reduce costs or increase service levels. Consequently, Digitalization is meant to be one the biggest key factors for road freight businesses being profitable in the future. To get an idea of the progress the road freight industry has made towards Digitalization, a closer look will be taken at the most important technologies. Taking recent literature into account, seven main technologies can be identified which are depicted in Figure 1.

1.1.1. Internet of things

Internet of things (IoT) refers to the connection of digital and physical assets which are often equipped with sensors and intelligence [9,10]. A sensor is an electronic component which observes and transmits a specific state of its environment. An exemplary application of IoT in road freight transportation is the concept of a so-called "digital twin". A digital twin is a detailed digital model of a real-world object which is used to monitor, analyze and simulate different states of the underlying, physical object [11]. In the context of road freight transportation, this means that the real-world object is usually the vehicle used to deliver the freight. This vehicle can be equipped with various sensors, e.g. Global Positioning System (generally referred to as GPS) sensors, axle load monitoring sensors, fuel consumption monitoring sensors, headwind sensors or cargo space temperature sensors [12]. All sensors transmit data to a centralized data center, where further data analysis is performed. Practical applications of results generated from these analyses vary significantly. GPS data allows for freight tracking and improved customer service [6] as well as monitoring the drivers' behavior to give real-time information about excessive speeding in an attempt to prevent fatal accidents [13]. Aside from that, real-time route optimization based on GPS data can be performed to avoid traffic congestion and save operational time [14,15]. In combination with fuel consumption sensors, GPS data can be used to identify optimal fuel purchasing based on price and location [16]. Optimal speed profiles and gearing can be determined by analyzing wind sensor data [17]. Combining data from axle load monitoring sensors and GPS modules enables predictive maintenance of vehicles to prevent failure during operation and increase operational efficiency [12,13]. In addition to that, temperature sensors allow for monitoring the state of the cargo hold to identify and react to unintended storage conditions [6].

1.1.2. Block Chain

Another well-studied technology in the field of road freight transportation is block chain technology. A block chain is defined as a distributed database in the form of a decentralized ledger that is stored and replicated among all network participants [18]. Every ledger records encrypted transactions in a trustless environment [19]. Therefore block chains are immutable, transparent, secure, decentralized, irreversible and consensus-based [20]. The primary issues addressed via block chain technology within the context of road freight are related to collaborations across business entities. These collaborations are often lacking in terms of trust and communication standards [21]. Block chain technology might contribute to address these issues by providing a shared and transparent platform to unify communication among different stakeholders along global supply chains in a standardized format [22,23]. This platform can also be a key factor when looking at the network of IoT devices. On top of streamlining communication, block chain provides a way to securely save sensor data without any possibility for malicious manipulation by any stakeholder. Freight owners can therefore be sure to get trustworthy information

about their freight and its environment [19,24]. When talking about collaboration between two or more parties in logistics, the scientific community mentions the term "control tower" as a new concept to eliminate trust issues among involved parties when collaborating horizontally [25]. The control tower is an independent third party that consolidates loads from different shippers, delegates load to carriers and distributes potential gains to the participants. The parties' biggest concerns in the context of control towers are fairness and neutrality [4]. A block chain where everyone can securely save data and transparently comprehend underlying mechanisms can help overcome these issues and help secure the benefit of a control tower for everyone involved. Another opportunity to integrate block chain in road freight transportation are so-called smart contracts. Smart contracts can replace analogous and repetitive paperwork by saving all relevant data immutably on the block chain. In addition to that, specific transactions can be executed automatically when certain conditions are met [26]. These smart contracts are stored in a user-specific setting on the block chain [18]. For example, saving information on the block chain about the unloading of freight at the recipient location can replace the confirmation signature and automatically trigger a payment.

1.1.3. Automation

In the context of this thesis, the term automation is defined as the implementation of electric or mechanical devices in business processes to reduce human labor [27]. Consequently, the primary factor of human labor that is to be reduced within road freight transport is the task of manually driving the vehicle. The body of literature proposes various ideas on how to implement automation in road freight transportation. An opportunity to completely replace human labor is to change the mode from road freight transportation with vehicles to drone delivery. Several prototypes of comparable concepts are already implemented by major companies like DHL, Swiss Post and UPS [28]. When taking the business models of these companies into account, one major disadvantage of drone deliveries is apparent: It is applicable only to small and light freight, especially parcels. Drones are physically and legally incapable of delivering bulky goods or pallets. The drones' major advantage is the saving of human resources and therefore reducing the costs.

Another interesting research topic is the concept of truck platooning. Platooning describes a group of trucks constantly communicating with each other to autonomously drive in column, resulting in a significant decrease of air resistance, in turn decreasing fuel consumption for all following trucks [29–31]. To achieve these effects, only the first truck within a platoon is controlled by a human driver. Algorithms control the following vehicles to keep the distance between the trucks as low as possible while retaining or increasing the level of safety. The results of less drag, vehicle-to-vehicle distance and higher safety levels are lower fuel consumption, better working conditions for drivers and less accidents [17,32]. Fewer accidents and lower fuel consumption directly result in decreasing operational costs. Better working conditions for drivers could help to attract more people to apply for jobs as driver shortage is a main problem in the trucking industry today [33–36]. Furthermore, platooning could lead to less air pollution by burning less fossil fuel [37]. When talking about platooning, the driver is not entirely replaced. In contrast to that, the technology of driverless vehicles is widely called automated or autonomous vehicles. As the name suggests, automated or autonomous vehicles conduct the manual task of operating a vehicle without the support and guidance of a human operator. These vehicles can be separated by size into two categories: Autonomous delivery vehicles which are trucks without drivers and driverless pods which are small self-driving delivery robots [38]. When asking companies about the expected benefits of automated vehicles in the context of road freight transportation, the answers can be broken down to the following key message: Automated vehicles can help to reduce staff shortages and personnel costs which is in line with other automation scenarios [39].

1.1.4. Electric vehicles

A widely discussed topic due to increasing environmental awareness within societies are electric vehicles. Electric vehicles are defined as motorized means of transport which are fueled by electricity

and operated by humans. In this context, two types of vehicles are commonly investigated: Electric four-wheeled vehicles and electric bicycles [40]. The goal of the implementation of electric vehicles remains the same for most of the use cases. Switching from vehicles powered by fossil fuels to vehicles powered by renewable energy is meant to help reach decarbonization goals set by politics and society [41,42]. The technology of electric vehicles per se is studied extensively [43–47] whereas concrete implementations in freight transportation still present a significant gap in contemporary research [48]. Most electric transport vehicles and their documented use cases are designed around urban areas. Often, they are not adaptable to suburban or rural areas due to the predominant requirement of widespread charging infrastructures. To solve this problem, new design concepts based on specific needs of suburban and rural deliveries are realized [49]. Another limitation of electric vehicle implementation is the reduced range capacity until charging is needed. In contrast to combustion engine vehicles, charging a battery takes significantly longer than refueling a gas tank. The vehicle is blocked for a longer time and cannot be used for profitable purposes. A suggested solution is opportunity charging. Opportunity charging integrates quick recharging events during working hours. As a consequence, driving range requirements switch from daily driving distance to distance between two locations of planned charging activity [50]. The charging opportunities' implementation forms vary from using public charging infrastructure to completely swapping the battery for a spare pack [51,52]. On the one hand, this decrease in range demand would result in less battery capacity and therefore smaller and lighter batteries. The savings in weight and space can be used to increase the vehicles' potential payload [53]. The savings in initial purchase costs can attract more logistic businesses to switch from combustion engine vehicles to electric vehicles. On the other hand, the dependency on charging infrastructure is enormous while the level of charging infrastructure remains one of the major concerns [54]. In addition to that, the time of charging within the working hours lead to higher personnel costs which lower the profit of logistic companies. In conclusion, the implementation of electric vehicles is not always suitable and should be discussed case-specific [55].

1.1.5. Data driven business models

Digitalization can enable new business models within an analogous field [56]. Platforms (Platform-as-a-Service, PaaS) are one breed of new business models driven by digitalization. They are variously defined but can be broken down into subsystems which are the basis for applications, processes and complementary technologies under development [57–59]. These platforms can take on four different tasks within the road freight transportation process: They can simplify transactions by matching the demand and supply for logistics operations. They can act as a long-term cooperation approach in the form of mutual investments. They can drive innovation by incorporating additional technologies and they can increase visibility by establishing end-to-end connectivity between business partners [22,57,60]. By performing one or more of these tasks, platforms affect the sustainability of freight transport. From an economic perspective, the use of capacity and loading space can be arranged more efficiently, less waste is produced (e.g., tires, well to tank) and time is saved. Fewer accidents and shorter time of deliveries lead to an improved social dimension of freight transport sustainability. Tackled environmental issues are the reduction of air pollution, reduction of noise and less congestion by decreasing the required number of simultaneous vehicles due to load optimization. In the context of road freight transportation, the most interesting start-ups based on investment sums are digital freight forwarders [61]. A digital freight forwarder is defined as a platform that acts as a market intermediary in freight transportation [62]. Mikl et al. [63] state that they differ from traditional freight forwarders regarding value proposition, value creation, value delivery and value capture, although traditional freight forwarders try to keep up with the fast-evolving start-ups. Value proposition implies the differentia of products or services to distinguish itself from competitors. Digital freight forwarders offer products, which are new to the logistics field such as online booking, standardized document management or live data. Taking a closer look at value creation, processes and resources of a firm, which create value, are discussed. Digital freight forwarders create value by selecting and contracting carriers and shippers like traditional freight forwarders. Additionally, promoting their platform is an important part of digital

freight forwarders' business strategy. Value delivery is targeting the customers of a firm and its communication systems. Traditional freight forwarders are often focused on specific customers or goods and communicate in traditional ways, mainly through in-person meetings or via phone and e-Mail. Their digital counterparts offer standard services to the mass market and communicate exclusively via digital channels. Digital freight forwarders use algorithms to calculate customized individual offers while traditional freight forwarders have generalized long-term contracts with limited customization options. In terms of cost structure, digital and traditional companies differ significantly. Most traditional forwarders own physical assets to fulfill the need of their customers whereas digital freight forwarders have almost zero physical assets. Due to major differences between business models, digital and traditional freight forwarders are not mandatory competitors. There are possibilities to collaborate and complement each other.

1.1.6. Business Intelligence

Business Intelligence (BI) is a very interesting technology because, compared to the aforementioned technologies, it is the only one considered to be essential to ensure competitiveness [64,65]. BI is defined as a collection of information systems to transform data into information and information into knowledge to support decision-makers [66–68]. Due to its importance in both practice and research as well as its implications for this thesis, the next sections will cover common applications of BI in more detail.

1.1.6.1. Route planning and optimization

The first and most commonly considered application of BI in road freight transportation is route planning and optimization. Real-time route optimization was previously mentioned while examining IoT but, as it mainly requires algorithms and data analysis to formulate optimal routes, this section exclusively focuses on route planning [69]. Vehicle Routing Problems (VRPs) can be defined in several ways depending on the environment and given constraints [70]. This thesis covers the general Vehicle Routing Problem without excluding or focusing on specific implementations.

Gayialis et al. [71] show the conceptual design of integrated web-based software to schedule deliveries under various conditions. To overcome traffic uncertainties and take care of time-dependent constraints, travel time predictions based on historical data were developed. This information allows for robust routing in advance, which is supported by real-time optimization.

A showcase in Spain shows that the VRP is solved much more efficiently when treated dynamically. Alvarez et al. [72] used the Savings algorithm as well as the Tabu Search algorithm to test four scenarios. Scenario 1 minimized Euclidean distance, scenario 2 minimized real distance, scenario 3 minimized travel time under consideration of static congestion and scenario 4 minimized travel time under consideration of dynamic congestion. By taking dynamic traffic information from Google Maps into account, time savings up to 11% can be achieved.

By solving a two-echelon VRP with a biased-randomized algorithm suited for parallel computing, do C. Martins et al. [73] achieve agile optimization to enable real-time decision-making. The proposed approach results in a runtime of milliseconds to compute results close to the best-known solutions. This enables computing in real-time after the integration of stochastic constraints without sacrificing the results' quality.

The VRP per se is considered NP-hard. In addition to that, incorporating (traffic) information to improve results' stability increases computational times even more. Sbai and Krichen [74] developed a parallel Spark Genetic algorithm to deal with big data in the context of Vehicle Routing Problems while remaining within bounds of acceptable computing times. On the one hand, the presented architecture delivers good results in terms of performance. On the other hand, it is only minimizing the total distance. This contradicts the aforementioned well-researched fact that it is necessary to incorporate travel time predictions to find the most efficient routes.

1.1.6.2. Travel time prediction

The most important enabler of robust route optimizing is travel time prediction. Because of this fact, it has gained a lot of attention in contemporary research. A survey analyzing the body of literature and interviews with 230 truckers found out that traffic congestion is by far the most important cause of delay. Other factors reported influencing travel times like weather conditions and accidents are mostly related to congestion as they are root causes of congestion [75]. Besides that, one of the main findings is the fact that arrival time or travel time is significantly influenced by the time of departure. Consequently, travel time predictions should always be time-specific.

Zhao et al. [76] present a gated recurrent unit model to predict truck-specific travel times. They imply that trucks are not allowed to travel on all streets in a network. Because of that, they gather GPS data from truck vehicles only, match them onto a network and predict future travel times. The results show predictions with Mean Absolute Percentage Errors (MAPEs) below 10% for most use cases. Travel times on days with accidents are much harder to predict and therefore produce MAPEs of 15% and above depending on the applied parameter optimization algorithm.

A deep learning approach with stacked auto encoders developed by Lv et al. [77] is supposed to deliver much better results. With the help of a greedy layer-wise unsupervised learning algorithm to pretrain the deep network, it is possible to predict traffic flow with an accuracy of over 93% within time intervals of 15 to 60 minutes. Traffic flow refers to the number of cars crossing a measuring-point within a given time interval. Data collection to train and test the network was done by 15,000 individual detectors, which are deployed state-wide in freeway systems across California. The big downside of this implementation is that the current flow must be known to predict the future flow. The current flow is not available in real-time in most cases as its underlying data tends to be derived from government-controlled devices.

Another way to predict travel times is proposed by van Lint [78]. He uses a state-space neural network to predict travel times directly from real-time traffic data collection systems. With a mean absolute relative error of 5.4% on a 13 kilometer highway section with 27 inductive loops to gather training data. The training set was totaling over 375,000 data sets distributed over 1,071 days. The test set contained over 41,000 data sets from 118 days. This thesis concludes that significant criteria for good travel time predictions are accuracy, robustness concerning data quality as well as adaptivity due to changing conditions.

Wang et al. [79] are using data from GPS sensors and dual-loop detectors to investigate the relation between speed and density measures. A k-means cluster analysis algorithm is designed to predict travel speeds dependent on given traffic densities in Washington State, USA. The measurements took place in a two- and three-mile highway section with MAPEs of 7.33% and 5.55 %. Although the results seem to be good at first, the methodology once again requires loop data to predict travel speeds, which are often not available in real-time.

1.1.6.3. Freight volume forecasting

Another widely researched topic within the field of BI in road freight is freight volume forecasting [80]. Knowing future demand lets carriers better utilize their human resources and physical assets. During fluctuations, they can react with short-term outsourcing or tender excessive capacity on freight platforms. To predict future freight volume, different methods can be found in the body of literature.

Mrowczynska et al. [81] implement Holt-Winters double exponential smoothing supported by an Artificial Immune System (AIS) and compare the results to predictions from a Bayesian network. They use yearly aggregated data to forecasts road freight volume in Poland. The MAPE on both models is 2.56%. While this appears as very good performance at first glance, the authors only used a set of 9 training data points and one test data point. These numbers seem too low to make reliable and generalizable statements. Another problem of this study is the forecasting interval of one year as road freight service providers must handle weekly or even daily fluctuations.

Other models to predict freight volume are simple linear regression, non-linear regression and multiple linear regression [82]. All methods can use the gross domestic product as independent variable. Researchers show that the simple linear regression is best fitted to predict the freight volume in Shanghai. With a fit (R^2) of 0.89 and an average MAPE of 5.29%, it delivers satisfactory results. Three problems can be identified when looking at the methodology. It is to be criticized that the number of data points is very low (10) as seen in the study of Mrowczynska et al. [81]. In addition to that, the forecasting interval of one year is too long for the application of road freight. The most remarkable problem is the independent variable the prediction is based on. The freight volume is predicted with the gross domestic product of the matching year. This means that to predict freight volume of the upcoming year the gross domestic product of exactly this upcoming year must be known.

To predict monthly freight volumes, Fite et al. [83] reference a combination of 107 different economic and industrial indices in addition to a 31-month data set of actual loads from one of the world's largest truckload carriers to formulate a multiple linear regression model. The authors state that changes in trucking volume would most likely follow changes of one or more indices. Based on this finding a correlation analysis is carried out to identify the best potential repressors among all indices. With the help of 7 indices the resulting multiple linear regression is able to predict volumes on a national level with a MAPE of 6.86%. The paper also shows models for specific market segments where MAPEs are a lot higher (varying from 3.88% to 54.82%) compared to the aggregated data on a national level.

By using a least-square Support Vector Machine (SVM), Yin et al. [84] predict highway freight volume in China. The authors use over 150 data points per province to train the model and predict another 20 data points to test their results. 31 different provinces are included which results in over 4,600 training points. This research focuses on monthly predictions which is a great advantage over the literature shown before. Because of the methodology, no additional data to predict future volumes is needed. The MAPE of the SVM predictions is 1.94%. As mentioned before, monthly predictions are still not accurate enough but can be used as a trend indicator [84].

1.1.6.4. Freight pricing

The trucking industries in Germany and USA have undergone substantial changes in regards to deregulations [85,86]. Consequently, tariffs are not regulated anymore which leads to negotiations about prices between carriers and consignors [87]. To elaborate contracts while taking financial health into consideration, carriers need to know the spot market prices. The spot market represents the set of transactions that lead to one-time transportation services between carriers and consignors [88].

When delivering freight to a recipient's location, many characteristics affect the costs and consequently the spot market price of the service. For example, the costs per shipment can be cut significantly by delivering several shipments to one location. The overhead of reaching the destination with its related costs like personnel cost, vehicle occupancy and driving occurs once for all shipments. With increasing shipments per stop, the price per shipment decreases due to its spread across multiple participants. This business strategy of adjusting the price of a product or service in a timely fashion to current circumstances is called dynamic pricing [89]. Lowering prices based on dynamic pricing is a method to gain an advantage over rivals and acquire more requests from consignors. If spot market contracts are seen as bidding for shipping requests, a carrier must offer the lowest price possible to convince a consignor to take advantage of its service. These bidding processes should be done concerning future requests. By predicting the totality of freight flow to each location, prices to bid for requests can be modified [90,91].

Figliozzi et al. [92] take the idea of dynamic pricing in road freight even further and implement the vehicle routing problem in a competitive environment (VRPCE). They extend the traveling salesman problem by adding dynamic requests with uncertain arrival times and characteristics. In addition, that profit per request is estimated by predicting the incremental costs of an accepted service request. This methodology allows for managerial decisions e.g., accept or decline requests, use private fleet or common carrier and whether or not to undercut rivals' prices.

To derive costs of future shipments without building routes and allow for a more robust cost estimation, Sun et al. [93] implemented regression models and Artificial Neural Networks (ANN). Robustness is needed as two similar shipments (in terms of distance to drive and weight to carry) can be priced differently based on inclusion in different tours at different times. While this difference can be intended in some cases, it will mostly decrease transparency for consignors and could be a barrier for a trustful cooperation. The problem of intransparency can be solved by calculating five geographic factors named single distance, neighborhood density, direction density, expected number of partners and expected isolation for every new location based on historical shipment data. Computational studies show that these attributes can effectively correlate with distribution costs. The constructed ANN performs shipment cost estimation with a MAPE of 13.7%.

Kellner et al. [94] brought infrastructure into the pricing of groupage freight by using data of navigation service providers. They constructed routes based on historical shipment data from the terminal to the first consignor within a tour, in between consignors of a tour, as well as from the last consignor of a roundtrip back to the terminal. These tours are transferred to the navigation service provider's Application Programming Interface (API) and include different timestamps to measure the temporal influence for any given route. After retrieving historical driving times and distances, the authors report significant cost differences for five terminal areas throughout Germany. The costs per kilometer driven vary from 1.06€/km in Ratisbon to 1.38€/km in Cologne. This spread of more than 30% can lead to significant differences in the financial performance of terminal areas' operations if the same price for the service is applied.

Based on the direct impact pricing has on operational margins, the following sections deal with the information needed to enable cost-based pricing in road freight networks. The focus lies on the utilization of available data sources and on how to derive cost-related information.

1.2. Leveraging data to quantify costs of transport networks' components

1.2.1. Understanding transport networks and their components

To understand the title of this thesis it is mandatory to understand the meaning of networks in the context of road freight transportation. In general, a graph is defined as a set of nodes that form pairwise connections, resulting in so-called edges [95]. A widely used graphical representation of a graph is a set of points (nodes) connected through lines (edges) [96]. A network is a special type of graph where the edges are characterized by a certain direction. In addition to that, weights or capacities are assigned to the edges and nodes act as origins or destinations [97]. In regards to the focus of road freight networks, nodes represent settlements and crossroads [98] whereas edges represent streets [99]. These edges are often enriched by information about street length, speed limits or traffic details [100].

1.2.2. About transport costs and related drivers

As important as the understanding about networks is the definition of road transport's costs. In the context of this thesis, we use a modified definition of Verhoef [101]: Road transport's costs are negative internal and external effects that arise through actual transport activities. These costs can be structured by looking at the three dimensions of sustainability: social, ecological, economic [102].

Social costs are mainly referred to as health problems that are caused by noise and accidents [103–108].

Ecological costs are embodied by climate change. The main contribution of road transport to climate change is pollution [109–113].

Financial expenses represent economic costs. Financial expenses which exceed the expectations of stakeholders are the consequence of delay and detour [114–120][1].

Figure 2 derives an overview of network costs and their related drivers. Going upstream on these relations, the costs' extent is directly determined by the transport activities. The extent of these activities – also referred to as intensity - is characterized by volume and velocity of the flow [121] as well as the length of the affected edge [100]. To measure the intensity of a transport activity, the underlying real-world circumstances impacting volume, velocity and length are determined in the next section.

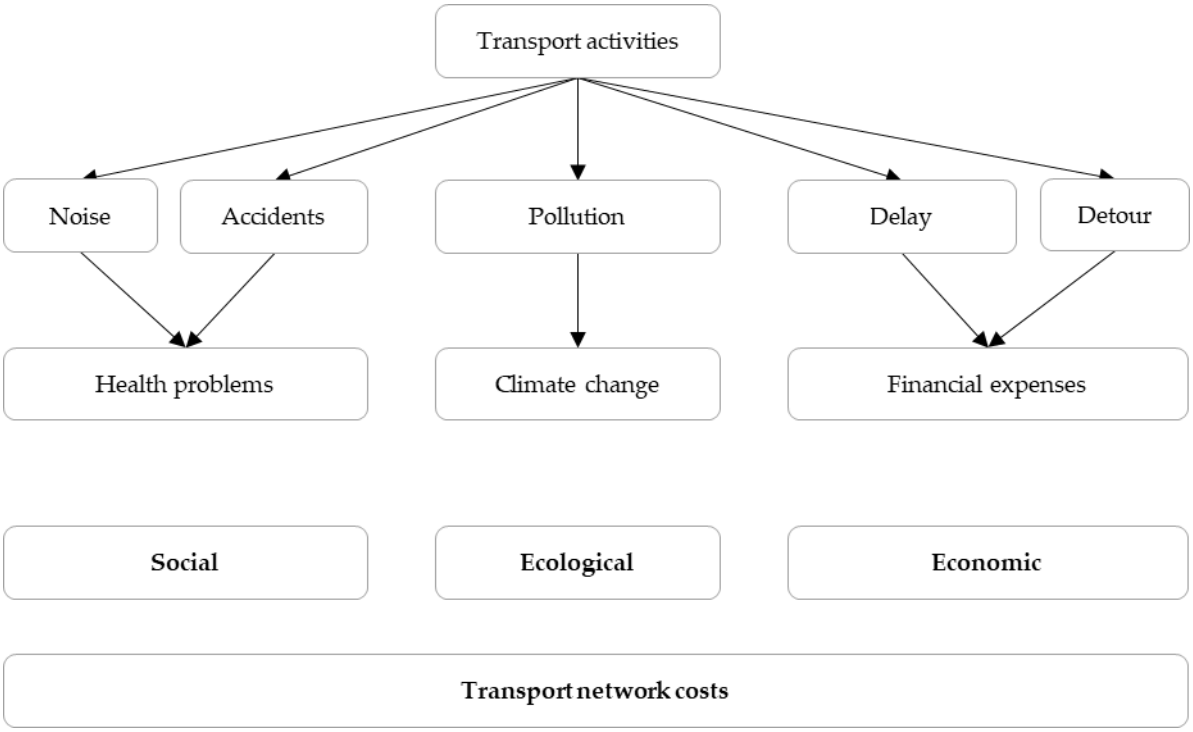

Figure 2 Relations between network costs and their respective drivers

1.2.3. How to determine transport activity's intensity

Volume, velocity and length are general expressions to describe the intensity of transport activities. To search for matching data sources, it is necessary to identify real-world characteristics linked to the above-mentioned phrases.

Volume is generally referred to as the number of shipments transported on a specific edge. Since bundling is a key competence of logistics service providers, the volume on edges is influenced by multiple factors. The type of vehicle, boundaries of working time and shipments per stop dictate the building of appropriate routes. These routes connect locations within the given shipment structure. In a practical sense, the volume is embodied by the number of vehicles traveling on a specific edge within a specific timeframe.

The allowable and realizable speed of movement on a specific edge is called velocity. When thinking about road velocities, three factors restrict the maximum possible speed. We assume that drivers follow official speed restrictions. These restrictions are present in most, except some special streets like

[1] The terminology „which exceed the expectations of stakeholders" is used in the context of economic costs as this dimension of costs cannot be removed entirely. As long as teleportation without the need for energy is not invented, financial expenses will occur while moving freight. Consequently, the goal is to cut the excessive or avoidable portion of these expenses. In contrast to that, social costs and ecological costs can be cut to almost zero by strictly avoiding accidents and operating electric vehicles.

parts of the German autobahn. Even if a road section is not officially restricted, the vehicle used has its own limitations in terms of maximum speed. The last restriction comes in the form of traffic. Congestion leads to a decrease in overall speed and might be unavoidable at times.

The length of the edge is the distance from start- to endpoint. It is important to note that travel distance is different from air distance between these points. To get the exact length of an edge it is mandatory to look at the infrastructure and the associated detour factor. The detour factor is defined as an indicator that measures the ratio between the traversed road distance and respective air distance of a specific set of edges. Since the shortest distance between two points is always a straight line, which corresponds to air distance, the smallest possible value of the detour factor is determined at a ratio of 1.0. As the detour factor increases, so does the deviation of actual road shapes from straight-line connections. While most highway networks tend to follow a rather straight path on overland connections, corresponding to low detour factors, they increase rapidly when investigating inner-city traffic networks. The most noteworthy example to be considered when thinking about large detour factors is the so-called taxicab geometry in Manhattan, New York.

After linking real-world characteristics to volume, velocity and length, a few different data sources can be utilized to determine the characteristics' values.

1.2.4. Classifying available data sources to determine a transport activity's intensity

In the wake of continuously growing numbers of sensors and technical devices to measure data in the context of road transportation, more opportunities to refine cost calculations arise [122]. Putting the best-suited data to use requires an overview of available sources and their characteristics. This section explores interfaces and repositories to support the process of choosing a set of adequate databases[2].

1.2.4.1. Shipment structure

When talking about volume, respectively the number of distribution vehicles traversing a specific edge, the only data source to retrieve information from is a historic shipment structure. The shipment structure is a list of locations to be served within a specific time interval. Tour IDs, coordinates, volumes/weights and intra-tour orders derived from timestamps can enrich this list. Depending on the available information, routes must be built or locations geocoded, to leverage the full potential of shipment data.

1.2.4.2. Geocoding

To geocode data, which means retrieving the exact address for a latitude/longitude coordinate pair, several sources are available. A selection of providers is described below. All mentioned providers use Representational State Transfer (REST) APIs with JavaScript Object Notation (JSON) responses to deliver results. As input variables, every API requires latitude and longitude coordinate pairs.

[2] The latest information on service providers' APIs can be found on their related websites:
- HERE Technologies: https://developer.here.com/ [123]
- TomTom: https://developer.tomtom.com/ [124]
- Google Maps: https://developers.google.com/maps [125]
- Mapbox: https://docs.mapbox.com/ [126]
- Bing Maps: https://www.bingmapsportal.com/ [127]
- Nominatim: https://nominatim.org/release-docs/develop/ [128]
- ArcGIS: https://developers.arcgis.com/ [129]
- MapQuest: https://developer.mapquest.com/ [130]
- geocode.xyz: https://geocode.xyz/api [131]
- INRIX: https://inrix.com/developers/ [132]
- OpenStreetMap: https://www.openstreetmap.org/ [133]
- OSMnx: https://osmnx.readthedocs.io/ [134].

HERE Technologies is a company located in the Netherlands owned by several German car manufacturers (BMW, Audi and Daimler), Mitsubishi, Intel and other shareholders. Its database where geocodes are retrieved from is generated via navigational systems integrated into vehicles as well as a fleet of cars equipped with sensors and cameras.

Another Netherlands-based navigation service provider offering geocoding is TomTom. TomTom delivers data, which is gathered analogous to HERE Technologies. They also operate a car fleet equipped with sensors and cameras. In addition to that, users share their positional data via mobile apps to generate real-time information.

One of the most dominant providers of location data is Google. Operating under the Alphabet Inc. company in California, Google gathers data by processing user information from their location service Google Maps as well as with their own fleet of sensor-equipped cars.

A provider without self-owned hardware and no processing of user data is Mapbox. The database is a combination of open-source data such as OpenStreetMap and commercial data from other mapping services.

The Microsoft-owned map service Bing Maps is based on TomTom data as Microsoft and TomTom are closely collaborating with each other. This means that the usage of Bing Maps and TomTom results in a response with the same content, supposing the user-generated call contains the same information.

The only open-source geocoding service to mention is Nominatim. Its database is built from OpenStreetMap. The main purpose of this API is to enable the search bar implemented on OpenStreetMap, but it is also externally usable. In contrast to the other providers, OpenStreetMap relies on community-mapped data that is non-commercial and open source.

Last to mention is the ArcGIS platform powered by the mapping software company ESRI from California. ESRI's database is a mix of open-source data, official data from authorities, user-gathered data and data that has been generated directly by ESRI.

Several less popular geocoders such as MapQuest or geocode.xyz can be found on the internet but it is worth mentioning that these providers utilize data from the above-mentioned sources. This means that the results will not differ from what the above-mentioned APIs deliver.

Dependent on the use case, the API's coverage and costing should be considered. Coverage can be evaluated via testing for the specific demand area and pricing is listed on the providers' websites. In general, it can be stated that geocode information quality is rather consistent throughout all providers.

1.2.4.3. Routing

Speed restrictions can be induced either by official limitations or via usage-induced traffic congestion. To ensure the correctness of the information, official limitations should be retrieved from official websites whenever this is possible. If official information is not available, tools such as OpenStreetMap can be used to retrieve speed limits. While official websites are country-specific, OpenStreetMap has been covering the world's road network by 83% in 2017 according to the project's official wiki. OpenStreetMap data can be accessed via several sources which are implemented in two different ways. Instant API calls supply the user with the area information limited by a call-specific bounding box. Compressed files of predefined areas (e.g., countries, administrative districts) can be downloaded and extracted. This results in the same data format that the API calls deliver. The advantage of API calls is the possibility to define the bounding box as per needs with the downside of longer processing times in contrast to downloading compressed files. This is especially noticeable when working with large areas.

Speed reductions caused by traffic congestion and infrastructure can be measured by retrieving travel speeds on edges. A set of companies provide these travel speeds recorded by road users in different forms. A selection of available APIs to determine travel speeds is given below.

HERE Technologies offers the routing service. This service is split into two independent APIs. The first one is a simple routing between a set of two (origin and destination) or more waypoints. The maximum length of a website call (around 2000 characters) determines the maximum number of waypoints per call (approximately 150 points). The result indicates the travel distance and travel time between the single pairs of waypoints. The second API is called "Isoline Routing". This comes from the fact that, given a certain start point combined with a restriction in travel time or travel distance, the API delivers an isoline around the start point. This isoline marks the area, which includes every reachable destination from the start point in respect to the restriction. Both APIs consider certain parameters such as departure time, type of car and area avoidance.

Like HERE Technologies, TomTom offers a "Calculate Route" and "Reachable Range" API. Calculate route takes a route of at least two and up to 150 waypoints and calculates the travel times and travel distances between sequential pairs of waypoints. The reachable range API calculates isolines to indicate reachable destinations the same way HERE Technologies does. Even the configurable input parameters are congruent for the most part. The big difference is the accuracy as HERE Technologies delivers an isoline in the shape of the exact reachable area whereas TomTom's isolines consist of a maximum of 50 connected points. This can result in HERE Technologies' API being more accurate than TomTom's.

The "Directions API" offered by Google is very similar to HERE Technologies' simple routing and TomTom's "Calculate Route" API. The user defines a REST call with a maximum of 25 waypoints and many additional available input variables. The returned JSON file contains the same information as the results from HERE Technologies and TomTom do.

Based on TomTom's data, Bing operates the same routing and isoline APIs under different names. The routing API takes a maximum of 25 waypoints and features the same input variables as TomTom . In terms of isoline calculations, Bing uses the expression "isochrones" and slightly differs from the TomTom reachable range API. Bing's result does not only contain a maximum of 50 points but is as precise as the isoline delivered by HERE Technologies.

The last provider of routing services is INRIX. INRIX is a company based in the United States that aggregates data from road users, vehicles, officials and sensors along the roadside to deliver a broad variety of analyses. Their routing API consist of three different steps: "FindRoute", "GetRoute" and "GetRouteTravelTimes". "FindRoute" allows for up to 10 waypoints and results in an INRIX-compatible route. "GetRoute" delivers the general route attributes like length and street type for any given route defined via "FindRoute". "GetRouteTravelTimes" results in travel times based on "FindRoute" for current and future traffic conditions. This information is only delivered in an averaged form for the whole route, not per waypoint pair as the other providers do. INRIX also offers isoline calculations called "Drive time polygons". This API works like the "Isoline Routing" or "Reachable Range" but only takes time-specific restrictions excluding the maximum drivable distance parameter. Isoline calculation based on travel distance restrictions is not possible. The resulting accuracy falls in between TomTom and HERE Technologies/Bing. The maximum count of isoline borders it not restricted but the polygon defining points must be lying on the street network.

To determine the travel distance instead of the travel time between a pair of locations, either information from the above-mentioned routing APIs or offline maps such as OpenStreetMap can be referenced. When using routing APIs, the process of data retrieval does not change. The difference to retrieve speed information is to extract a different value from the generated JSON file. As a result, all the above-mentioned providers' APIs provide information about travel distance. If offline processing is desired, preparing a street network via files from OpenStreetMap enables the performance of operations on local machines. The most common library to load, modify and analyze street networks based on OpenStreetMap data is OSMnx. It is a toolset written in Python by urban planning professor Geoff Boeing [135,136]. It features simple routing, isochrones calculation, graph simplification and many more algorithms [137,138]. After discussing data sources available and corresponding characteristics, the next section will dive deep into research and applications based on this data.

1.3. Literature Review on the usage of routing APIs and OpenStreetMap

To allow for an overview of possible use cases regarding the available data sources described above, recent literature in the context of logistics referring to a minimum of one data source or library is analyzed.

1.3.1. Routing

TomTom data has been used to show that the three-phase traffic theory (free flow, synchronized flow, wide moving jam) can also be found in urban road networks. Vehicle speed data in combination with road detector flow rate measurements enable the comparison of microscopic traffic simulation in Düsseldorf and real-world data. The results show synchronized traffic flow in oversaturated city traffic which leads to the acceptance of the three-phase traffic theory [139]. Up to this publication, synchronized flow has only been observed in highway traffic scenarios.

Stanojevic et al. [140] use the Google Directions API to implement their so-called MapReuse system. To use traffic data of routing APIs offline, they query a relatively small number of routes within a network to estimate travel time on each individual edge. Therefore, edges are weighted by their usage frequency and road characteristics as well as supplementing them with physical constraints. As a result, a travel time prediction for every edge within the network can be given. Case studies in Doha, NYC and Rome prove the system's accuracy in comparison to other prediction methods.

Google's routing service is also incorporated into the Vehicle Routing Problem with time windows [141]. Given information on truck capacity, costs per time unit and distance as well as breaks and customer service times, the genetic algorithm can be applied to solve the underlying problem. The algorithm aims for minimized total costs which are influenced by the APIs results regarding travel times and distances. The case study is carried out for one day of distribution in Sofia, Bulgaria.

Similar to the work of Dimitrov Berov [141], Google's API is also used to solve the dynamic Vehicle Routing Problem. Li et al. [142] implement a decision support system based on the Google Maps service to offer the user geocoding, map display and solving of routing problems. In contrast to most other authors, they especially emphasize the possibility of visualization delivered by several navigation service providers (Google, HERE, TomTom, Bing, INRIX).

Pearce et al. [143] use HERE Technologies' 250,000 free-to-use API calls per month to collect traffic data within the region of Birmingham, UK. This speed information can be combined with vehicle counts from officials to generate a vehicle emissions map. These results were obtained before policy implementations to enable the measurement of policies' efficiency.

With electric vehicles rising in share among all types of vehicles, battery consumption and locations of charging stations increasingly become part of several routing problems. Nunzio et al. [144] use HERE's routing API to optimize trips in regard to power consumption and charging locations. The authors divide possible routes from source to destination into two categories. The first route is considered the fastest in terms of driving speed; the second route is considered the fastest in terms of overall trip time including charging.

Google's Directions API enables a web spatial decision support system for urban trash collection in Coimbra, Portugal. Optimized vehicle routes for multiple VRPs are generated via a combination of an improved path-scanning heuristic and an ant-colony meta-heuristic approach. This methodology allows for what-if analysis in terms of shift limits or vehicle capacities. Even optimization goals can be changed to derive ad hoc analysis of different use case scenarios [145].

Levermore et al. [146] use HERE's routing API to retrieve real-time information about the traffic in upcoming sections. They use the data within dynamic programming to calculate the optimum choice of gear and speed. Equipped with an onboard device, it is possible to save energy in form of fuel and consequently produce less emission. In fact, 8% less fuel is needed to complete trips while remaining trip duration as without optimization.

1.3.2. OpenStreetMap

Luxen and Vetter [147] use OpenStreetMap data to implement a server and a handheld device-based application to imitate the functionality of Google Maps. They enable real-time routing, visualization of routes and features like drag and drop to choose alternative routes. The project named OSRM is deployed on a publicly available webserver to give general access to the open-source application.

In addition to that, OpenStreetMap is used to enable localization, path planning, path following and lightning control. An autonomous mobile robot based on an off-the-shelf vehicle is designed to conduct real-world experiments in different spots in Hannover, Germany. The vehicle was able to localize itself on OpenStreetMap Edges. It planned paths given a start point and a destination as well as following these paths. The last feature was turn signal control as the turn signals of the vehicle automatically activated if a turn of a minimum of 45 degrees lies ahead and the upcoming change of direction takes place at a junction of two or more ways [148].

Bischoff et al. [149] simulate electric vehicle trips in Sweden with the combination of MATSim and OpenStreetMap. They evaluate the impact of electrification on long-distance trips. Therefore, an agent-based long-distance microscopic transport model is enriched by a detailed model of energy consumption and charging schemes. Based on this information the energy demand can be spatially allocated to deliver information about optimized charging locations.

As described before, OpenStreetMap data was used to imitate Google Maps features. This idea is carried even further by Chen et al. [150] who implement an API to offer isochrone calculation for free. Their system is based on a sub-graph extracted from a wide-scope OpenStreetMap dataset. In the next steps, isolated links are removed and a parallelized non-recursive breadth-first algorithm builds isochrones based on given input parameters. The API works like TomTom reachable range and HERE's isoline calculations. The difference lies in traffic information which is not available for the OpenStreetMap network.

Extensive analysis of OpenStreetMap data is easy to do with the python library OSMnx. When talking about literature regarding OSMnx, the best source available is the library's author itself. Goeff Boeing has described and demonstrated the potential of his library in several publications [135–138].

Besides the author himself, OSMnx is also referenced by other researchers. Alattar et al. [151] combined data from Strava with OSMnx to elaborate the dependencies of cyclist routes and street layouts in the city of Glasgow, Scotland. Strava is a fitness app to track activities. In the case of cycling, routes are tracked via GPS. These routes were mapped on the OpenStreetMap data. Based on the OpenStreetMap network, several centrality measures were calculated using OSMnx, which leads to the possibility of analyzing the connection between street network characteristics and cyclist route choice.

OSMnx can also be used to retrieve and transform street network data. SUMO is a well-known microscopic traffic simulation tool which requires certain input file types to be operated. To convert OpenStreetMap data into one of these file types, Dingil et al. [152] developed a road network extraction process based on OSMnx and SUMOPy (another python library). This process enables a seamless OpenStreetMap to SUMO import.

Based upon these existing use cases, this thesis presents novel methods and research questions to be answered in separate sections. The upcoming chapter gives an overview of the structure of the following topics.

1.4. General Outline

1.4.1. Overview of the three published manuscripts

As shown in the previous section, a lot of research utilizes available data sources to answer relevant questions. In contrast to that, some data sources remain open for research. The goal of this thesis is to

search for unanswered questions in the field of road freight transportation costing and solve their underlying problems with the help of data, algorithms and network visualization. An important focus is to present use cases relevant in theory and practice, which demonstrate the application of different data sources in combinations as well as standalone.

This thesis is organized as follows: Every research question is answered in an independent peer-reviewed manuscript. Every one of these manuscripts is published open access in a scientifically recognized journal and represents one chapter in this thesis. Table 1, Table 2 and Table 3 derive an overview of the incorporated manuscripts.

Table 1 Overview of manuscript 1 [153]

Title	**Bringing economies of integration into the pricing of groupage freight**
Research Question	How should a freight forwarder calculate the impact of a new consignor's shipments on the costs per shipment?
Authors	Christian Brabänder, Maximilian Braun
Journal	Journal of Pricing and Revenue Management
Data Source/Library	Shipment structure
Network focus	Nodes
Date	14.03.2020
DOI	https://doi.org/10.1057/s41272-020-00237-3

Table 2 Overview of manuscript 2 [154]

Title	**Towards Sustainable Cities: Utilizing Floating Car Data to Support Location-Based Road Network Performance Measurements**
Research Question	How can relevant data be collected programmatically to measure road network performance?
Authors	Maximilian Braun, Jan Kunkler, Florian Kellner
Journal	Sustainability
Data Source/Library	TomTom reachable range[3]
Network focus	Nodes and edges
Date	02.10.2020
DOI	https://doi.org/10.3390/su12198145

[3] Based on previous sections, TomTom Reachable Range may not look like the best alternative. By the time the paper was written, other APIs were not available or pricing was too demanding for self-funded research.

Table 3 Overview of manuscript 3 [155]

Title	**Speed Limit Induced CO_2 Reduction on Motorways: Enhancing Discussion Transparency through Data Enrichment of Road Networks**
Research Question	How can road networks be enriched by publicly available real-world data to enable CO_2 emission calculations?
Authors	Jan Kunkler, Maximilian Braun, Florian Kellner
Journal	Sustainability
Data Source/Library	OpenStreetMap, TomTom Routing
Network focus	Edges
Date	04.01.2021
DOI	https://doi.org/10.3390/su13010395

1.4.2. Focus of manuscript 1

The purpose of this paper is to develop a novel calculation scheme for the costs of distribution per shipment according to a cost-by-cause principle. An estimation of the full costs of distribution routes excluding and including a new consignor is proposed. Then the marginal costs per shipment and per consignor are estimated. This is done to answer the following research question:

How should a freight forwarder calculate the impact of a new consignor's shipments on the costs per shipment?

The methodology is based on the historical shipment structure of a German Transportation Service Provider (TSP). In terms of network components, it focuses on the analysis of nodes. The contributions of this paper are (1) a comprehensive list of drivers of Economies of Integration and (2) a calculation scheme on how to estimate true marginal cost of new consignors. Practitioners may deploy the method and insights of this paper for tariff design, negotiations, consignor acquisition and demarketing.

1.4.3. Focus of manuscript 2

Road network performance (RNP) is a key element for urban sustainability as it has a significant impact on economy, environment and society. Poor RNP can lead to traffic congestion, which can lead to higher transportation costs, more pollution and health issues regarding the urban population. To evaluate the effects of RNP, the involved stakeholders need a real-world data base to work with. This paper develops a data collection approach to enable location-based RNP analysis using publicly available traffic information. Therefore, we use reachable range requests implemented by navigation service providers to retrieve travel times, travel speeds and traffic conditions. According to the methodology, the following research question is to be answered:

How can relevant data be collected programmatically to measure road network performance?

Incorporated network components are nodes and edges. To demonstrate the practicability of the proposed methodology, a comparison of four German cities is made, considering the network characteristics with respect to detour factor, infrastructure and traffic congestion. The results are combined with cost rates to compare the economical dimension of sustainability of the chosen cities. Our results

show that digitalization eases the assessment of traffic data and that a combination of several indicators must be considered depending on the relevant sustainability dimension decisions are made from.

1.4.4. Focus of manuscript 3

Considering climate change, recent political debates often focus on measures to reduce CO_2 emissions. One key component is the reduction of emissions produced by motorized vehicles. Since the amount of emission directly correlates to the velocity of a vehicle via energy consumption factors, a general speed limit is often proposed. This article presents a methodology to combine openly available topology data of road networks from OpenStreetMap with pay-per-use API traffic data from TomTom to evaluate such measures transparently by analyzing historical real-world circumstances. This leads to the answer to the question:

How can road networks be enriched by publicly available real-world data to enable CO_2 emission calculations?

The focus of this analysis lies on the node-connecting edges of the network. From our exemplary case study of the German motorway network, we derive that most parts of the motorway network on average do not reach their maximum allowed speed throughout the day due to traffic, construction sites and general road utilization by network participants. Nonetheless, our findings prove that the introduction of a speed limit of 120 kilometers per hour (kph) on the German autobahn would restrict 50.74% of network flow kilometers for a CO_2 reduction of 7.43% compared to the unrestricted state. It is worth to mention that this manuscript is based on private fleet data. Therefore, it focuses not on freight transportation. With the underlying methodology being split into several independent steps, data can easily be exchanged to shift the focus towards freight transportation.

2. Bringing Economies of Integration into the Costing of Groupage Freight

2.1. Introduction to pricing in groupage freight

All freight forwarders face the recurring same problem of integrating new consignors into their distribution. A prospective new consignor who plans to outsource distribution of shipments always negotiates about discounts off the standard tariff [156,157]. The standard tariff is either build on historical and regulatory tariffs, the forwarders cost structure or a modified version of the competitors' tariffs. The pivotal argument of consignors is that more volume (ton-kilometers) results in better economies of scale as the large, fixed costs decrease on a per shipment basis. The distribution tour is viewed as a service production process, in which joint deliveries of many consignors are produced and thus the costs of that process are allocated to ever more shipments. Nevertheless, this is only one side of the coin. Every new consignor adds new shipments onto an incumbent shipment structure which is distributed within an incumbent distribution network using incumbent vehicles, subcontractors and tariffs. As a result, on the one hand, new consignors might complement the incumbent shipment structure smoothly, but on the other hand, they might disrupt optimized routes, increase the number of tours and add far-off stops to the distribution. Therefore, whenever a freight forwarder acquires a new consignor, he must evaluate the fit of the new consignor's shipments and the incumbent distribution network's shipment structure to calculate a tariff which covers the new (combined) shipment structure's costs. The difference between the calculated tariff and the standard tariff is the negotiating range. From collaborations with practitioners, we learn that negotiation ranges are based historic rates, competition and gut instinct. This may lead to unprofitable long-term deals because once contracted, the newly acquired shipments change the forwarder's distribution costs and thus the profitability.

2.1.1. The groupage freight forwarding process

The transportation network of freight forwarders is usually a three-echelon system. The process and the structure of that system is visualized in Figure 3.

Collection

The first echelon is the collection. Typically, the number of shipments per ship-from (elsewhere pick-up) location is already dense. Corporate shippers ship a large number of shipments to many destinations. Therefore, collection tours collect many shipments from a few consignors which are ultimately addressed to many different recipients. As a result, groupage freight networks are essentially few-to-many transportation networks.

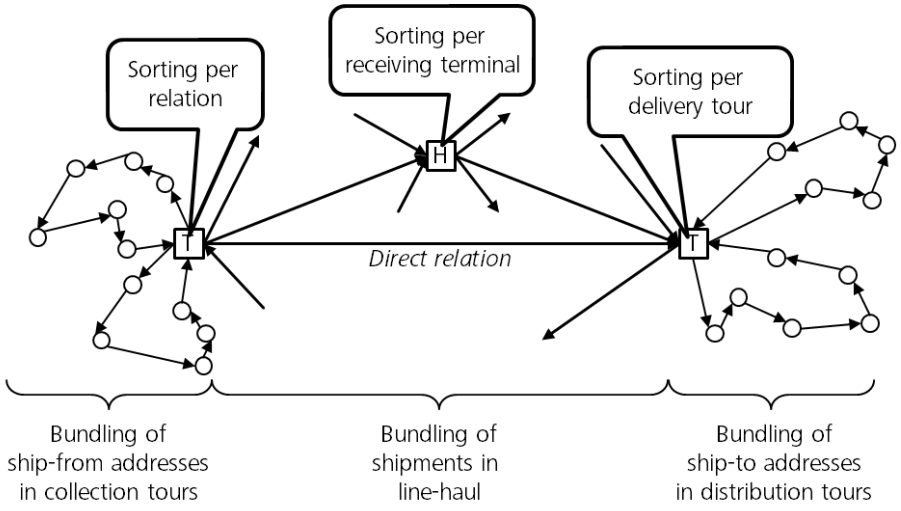

Figure 3 Process and structure of freight forwarding systems [158; modified and translated by the author]

Line-Haul

The second echelon is line-hauling. At this stage, full truckloads (FTL) of bulk shipments are transported to a central hub or directly to a receiving terminal. The function of the central hub is sorting and consolidation of bulks of shipments from different origins towards the same receiving terminal.

Distribution

The third echelon is the distribution. The receiving terminal acts as a break-bulk-terminal [159] where the FTL bulks of shipments are broken up and sorted into daily distribution tours. Typically, the density of shipments per destination (stop factor) is slightly greater than 1. As a result, the distribution accounts for the major share, often more than 50%, of the total cost per shipment [160,161].

2.1.2. Problem definition

In this paper, we investigate the problem of a groupage freight forwarder (GFF) who wants to evaluate a new consignor. This evaluation problem is herein called the "New consignor integration problem" (NCIP). The NCIP occurs in the sales department of any logistics service provider (LSP), such as GFFs, daily. Despite its practical relevance, the NCIP is not well-researched, yet.

The situation of a new consignor is the following:

In the past, shipments have been shipped via in-house fleet or by some LSP. For some reason, the consignor decided to move forward and now plans to outsource distribution or to replace the outsourcing partner. Therefore, the consignor, who outsources distribution, requests a proposal for a long-term shipping contract. In order to obtain a great discount on the tariff as a result of negotiation, the consignor provides a history of past shipments to the prospective GFF [162].

The situation of the GFF is the following:

There are many incumbent consignors feeding shipments into the GFF's distribution network. The incumbent shipment structure has some distinct, well-known properties and the operational tours are optimized for this shipment structure. As a result, distribution costs in the past have had a certain level. Tariffs are calculated based on these costs [163]. Now, as the prospective new consignor wants to feed more shipments into the incumbent network, the shipment structure changes and so does the cost structure. The GFF wants to analyze the provided shipment history with respect to the change in cost per shipment. Good consignors decrease the cost per shipment, neutral consignors do not change the cost per shipment and bad consignors increase the cost per shipment compared to the previous shipment structure.

Research question

This paper addresses the NCIP and investigates the following research question:

How should a freight forwarder calculate the impact of a new consignor's shipments on the costs per shipment?

2.1.3. Use cases for measuring a new consignor's impact on distribution

There are plenty of use cases for measuring a new consignor's impact on the distribution cost per shipment.

1. Most important, negotiations with prospective consignors benefit from better reasoning. First, reasonable hard facts in line with the cost structure replace arbitrary volume-based discounts. Second, the freight forwarder is protected against self-deceiving sales practices that try to gain revenue instead of profit.
2. A second use case is the transfer pricing within horizontal freight forwarding alliances. The forwarder who acquires a new customer is involved in the negotiations but is not responsible for the distribution of the new shipments. As a result, the acquiring forwarder grants a discount on the basis of fixed transfer prices (The receiving forwarder invoices the transfer price of a shipment to the acquiring forwarder). However, this might be a bad idea, as the transfer pricing may be outdated, ignore major drivers of distribution costs [160] or assume symmetrical and homogeneous shipment structure and volume. As a result, the acquiring forwarder and the receiving forwarder should exchange information and cooperate in the acquisition and integration of a new consignor with respect to its impact on the distribution costs.
3. A third use case is subcontracting. Freight forwarders outsource freight in order to fulfil their transportation requirements. Subcontractors are often self-employed carriers driving on behalf of the freight forwarder on a daily basis. Subcontracting tours, standard tours or distribution districts is a common outsourcing practice in CEP (courier, express, parcel) and groupage industries. Forwarders and their subcontractors are interested in productivity, especially the over- or underutilization of tours and districts. Measuring a new consignor's impact on a tour or district is helpful for evaluating a subcontractor's expected workload and the fairness of wages among different subcontractors. Furthermore, such a measure is an early warning of overutilization and all its consequences such as delays, penalties, overtime hours and idle time of additional capacities.

2.1.4. Outline

The next section reviews the body of literature on cost and revenue accounting in GFF starting from the period of deregulation in the early 90's. There is a research gap identified with respect to an identification procedure for the new consignor's impact on costs per shipment. Section 3 defines, explains and dismantles the pivotal term "economies of integration" from the perspective of a GFF. Based on the insights from sections 2 and 3, section 4 lays out a procedure on how to calculate the marginal cost per shipment of a new consignor as a function of the shipment structure. In section 5, we demonstrate a computational case study using real-world data from a disguised GFF. The final section concludes this paper by discussing both theoretical and practical implications and outlining further research.

2.2. Literature review

The transportation industry has been subject to very strict regulations in Germany until 1994 [86] and in the U.S. until 1980 [85]. Among others, these regulations were about the governmental prescription of freight transportation tariffs. With the abolition of the so-called Güterfernverkehrstarif in Germany and the Motor Carrier Act in the U.S., previously existing regulations have been removed completely. Because of this deregulation, freight forwarders are permitted to deploy their own tariffs. This new process of pricing transportation services often uses the freight-specific attributes distance and tonnage to determine the price of an individual shipment [164]. In this context, distance is measured as the length of a one-way trip from pickup location to delivery location. Tonnage describes the overall payload of a specific shipment. As a result, the LSP calculates so-called base rates, which are mainly cost-driven [163]. The reason is obvious: in order to make profits the price per shipment has to include the

marginal costs per shipment and a reasonable surcharge of overhead costs such as back-office processes, IT and real estate. Consequently, cost-based pricing of shipments requires two pivotal cost information: the cost structure of distribution operations itself and the overhead cost. In literature, many contributions towards the topic of cost calculation in freight forwarding can be found.

Bø and Hammervoll [165] calculate transportation costs with an extensive Microsoft Excel Tool. They categorize costs by dividing them into fixed costs and variable costs. Fixed costs are independent with regard to time and distance travelled. Variable costs are either depending on the round tours' distance or travel time. An interesting aspect of their categorization is the handling of wages. They assume that the driver gets paid per minute. As a result, a driver who works for only six hours due to underutilization is only paid for six hours. In reality, the drivers are getting paid fixed wages per tour or day.

Boone and Quisbrock [161] categorize all costs as variable costs considering different cost drivers except the costs for the company/network containing central management, scheduling and maintenance of IT-systems. An allocation algorithm is used to allocate those fixed costs among all shipments. The authors' main contribution is the conclusion that costs increase progressively as a function of the drop distance.

A very similar approach is used by Bokor [166]. He uses performance costs and performance units (e.g. the number of shipments, driven kilometers) to calculate the costs of one performance unit. The resulting rates per unit can be used to calculate the different costs of a transportation service.

Sun et al. [93] present a novel approach on how to estimate the long term costs of a new delivery destination. The authors used multiple geographic factors of an incumbent network structure as input data for a neural network which estimates the costs of every possible delivery location. The difference between their previous analysis and our current method lies in the selection of input features used. We assume to know the exact shipment structure of a potential consignor as proposed by Harrington [162]. Sun et al. [93] do not deploy data on the new consignor and his new delivery destinations. Another difference is the incorporation of payload as a driver of cost. We propose to account for payload because heavier shipments consume more capacity and more loading time.

In this paper, the NCIP is solved using a modular methodology. The cost calculation scheme is adapted from Wittenbrink [167]. This calculation scheme accounts for four main cost types. First, the variable cost of kilometers driven is calculated. The second type is personnel cost. The third type are time-dependent fixed costs of asset usage. Finally, the last type are fixed overhead costs that cannot be allocated directly to a specific performance unit. Wittenbrink [167] uses the same calculation process as Bokor [166]. He calculates the sum of every cost type (e.g. purchase price of truck, tires, maintenance and fuel). The next step is to estimate the average used performance units in the considered period. Thereafter, the costs per performance unit is calculated. The same principle of cost-accounting is also found in Kaplan and Anderson [168] where the authors describe the usage of unit costs that correspond to costs per performance unit. The so-called "time-driven activity-based costing" is exclusively described with the usage of time units as performance units. In our work we are not only using time units as a calculation base. We adapt the principle to "unit-driven activity-based costing". Our performance units are driven kilometers and working time. The overhead costs that cannot be allocated by distance or time are allocated by the number of shipments. In Table 4 the main cost types, performance unit dependencies and several exemplary components are illustrated.

Table 4 Main cost types regarding transportation service. Translated and modified from Wittenbrink [167]

Cost type	Distance-dependent costs	Time-dependent (fixed) human resource costs	Time-dependent (fixed) truck costs	Overhead costs
Description	Costs arise for driving a certain distance	Costs arise mostly independent to the utilization of employees	Costs arise independent to the intensity of truck usage	Costs arise for disposition and administration
Examples	Fuel, tires, maintenance	Wages, social insurances, travel expenses	Taxes, insurance, interests, depreciation	Scheduling, IT, staffing

2.3. Economies of integration

Economies of integration (EOI) are introduced by Keeler [169]. He defines EOI as follows: "[…] economies of integration, […] relate to all forms a large trucking firm can be more efficient than a small one. [...] economies of integration include more than scale economies in the strictest sense. Economies of large-route networks can be thought of as economies of density combined with economies of vertical integration." Fleischmann [170] calls a similar phenomenon "transport economies of scale". This leads to the supposition that freight forwarders do not only gain competitive advantage in the form of cost reductions by distributing more overall volume. Therefore, EOI are of major importance when a GFF evaluates the effect of new consignors. We consider the following characteristics to determine the extent of EOI.

2.3.1. Overall shipment structure

Shipments are the revenue and cost objects in accounting of freight forwarding companies.

Lin et al. [171] show an example of a consignor's shipment structure being the weight-demand per day. In that example, the average weight per shipment is 120kg, which is a typical example of groupage freight. However, the majority of shipments have below-average weight and only few outliers are heavier, weighing up to 450kg.

2.3.2. Volume of shipments

Giordano [172] states that there is persistence of continuous economies of scale in the transportation industry. He refers to the total ton-miles per firm as a measurement for volume. An increase in ton-miles can be achieved by acquiring more shipments, heavier shipments or shipments with greater length of haul.

2.3.3. Average payload of shipment

McMullen and Tanaka [173] find that increasing average load and size per shipment is associated with significant economies of scale. Higher average payload of shipments increases the probability of better-utilized trucks. The costs per truck, driver and driven kilometer can be split among a greater number of cost objects, thus decrease the costs per object. On routes with lower densification this effect has an even higher impact.

2.3.4. Drop factor: The average shipments per stop

The drop factor is an indicator of stop productivity and is defined as the average number of shipments that are delivered to the same destination. As Shah and Ward [174] stated, an important part of

lean production is the reduction of production downtime between product changeovers. In transportation, the production process is moving shipments from one location to another. Following that, the time when no shipment is moved is considered as production downtime. Whenever the driver stops at a delivery location, he loses some time for parking and taxi. In the case of delivering more than one shipment to the same destination, this stopping time can be split up between these shipments. The production downtime per shipment decreases and so do the costs.

2.3.5. Densification: The average distance between stops

Decreasing costs per shipment also result from better tour densification [173]. Higher density directly leads to more shipments being distributed due to less driving time between stops. Keeler [169] calls this "economies of density" due to "more traffic on one route". Less driving time stems from less average distance between subsequent stops. Densification means to decrease the average stop-to-stop distance of any tour.

Another indicator of densification is area density: it is defined as the average number of stops per area unit. Area density can be improved through the acquisition of more shipments into the same area or district. The two indicators area density and tour density correlate positively.

2.3.6. Approach distance: The average distance from terminal to stops

The length of one tour is limited by the truck's capacity and the driver's maximum allowed working time per day[4]. We assume that every tour has fixed costs because of loading and scheduling before the start. The goal should be to utilize drivers to full capacity with one tour per day to save as many fixed costs as possible. Accordingly, the tours should be planned to reach the time restriction. Meeting the time restriction gets more probable with a rising average length of haul. McMullen and Tanaka [173] also find that a greater average of haul is associated with lower costs per output (ton-miles). A significant increase in the average of haul can be achieved with larger approach distances. The approach distance can be seen as an overhead of the tour length. It is the sum of the distance between the terminal and the first stop as well as the detour from the last stop to the terminal.

2.4. Methodology: A data-driven approach

We propose to apply a data-driven modular approach in order to compare the costs per shipment. Shipments are characterized by their distance and weight. The most important advantage of this characterization is the practical applicability in tariff building and sales negotiations. Our approach to quantify the impact of a single new consignor is the following function: input data are both the GFF's shipment history and a history of the new consignor's shipments. The output data are costs per shipment. The marginal costs of the new consignor are the difference between the distribution costs per shipment with and without the additional shipments (Figure 4).

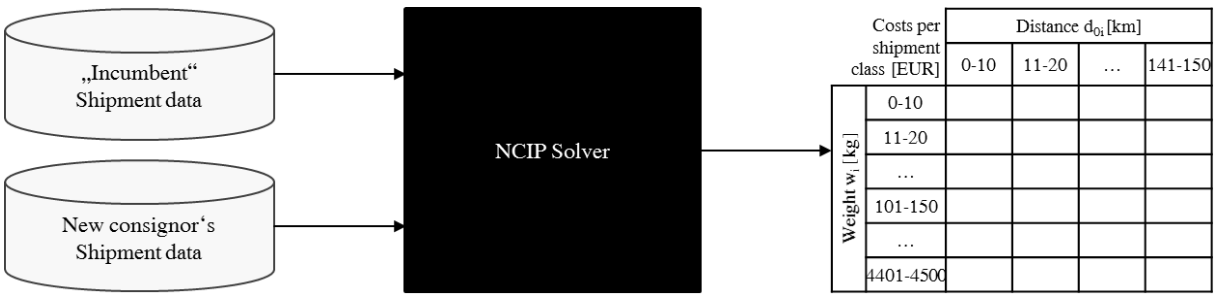

Figure 4 Functional relation of inputs and outputs

[4] In context of electrification, the vehicle range due to limited battery charge is another constraint besides capacity and working hours.

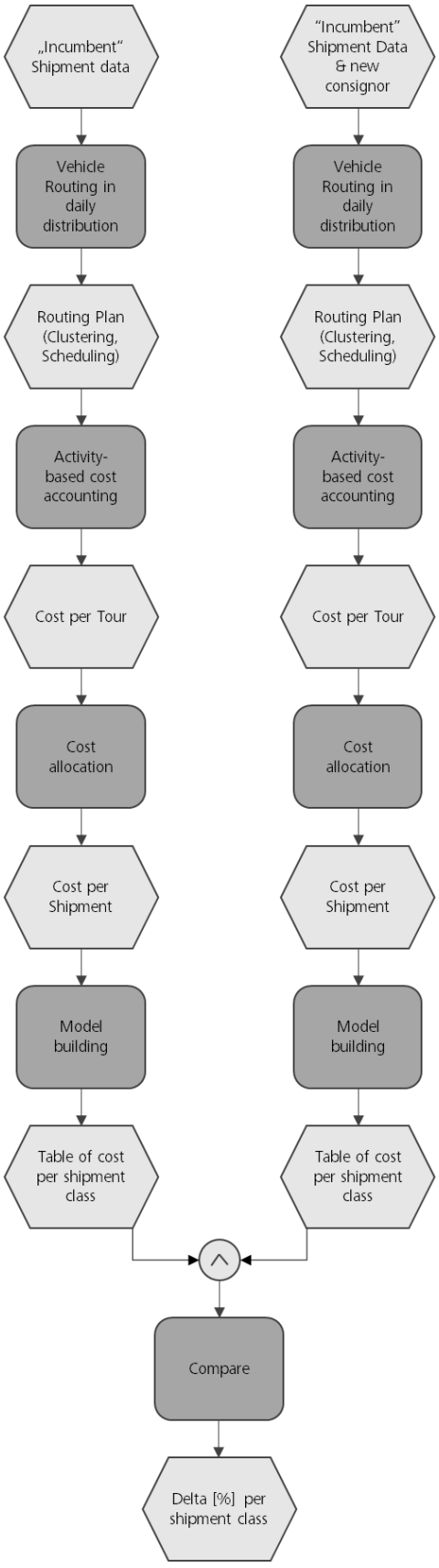

Figure 5 Calculation procedure

The "NCIP Solver"-function from Figure 4 is the core of our proposed methodology and further outlined in Figure 5. There are four modular, sequential steps in the computation procedure: (1) vehicle routing, (2) cost accounting, (3) cost allocation and (4) model building. Every module can be modified by the user in order to improve the suitability of its outputs. The idea here is to walk through the same process twice, first with the incumbent shipment history and second with the combined shipments including the new consignor. In the second walk-through, the new shipments are incorporated into the routes of the GFF, as if they were integrated already without making any difference between incumbent and new shipments. Applying the same modules twice enables comparability.

In the following subsections, we present our proposed methodology that is developed over many experimental setups and runs. In the description of our procedure, we use the following set of variables:

Sets and Indices

I'	Set of all incumbent shipments
I''	Set of the new consignor's shipments
I	Set of all shipments $i, j \in I$ where $I' \cup I'' = I$
$i = 0$	Terminal-node of the GFF, used for routing
T	Set of tours, with $T = \{T_1, T_2, \dots, T_t, \dots, T_N\}$
T_t	Tour with $T_t \in T$ which includes a scheduled disjoint subset of shipments from I: $T_t = \{0, \dots, k, \dots, 0\}$ and starts and ends at the terminal $i = 0$
$T_t(k)$	The k -th shipment of tour T_t where $T_t(0) = T_t(\lvert T_t \rvert) = 0$ is the terminal

Coefficients

lat_i	Latitude of destination for shipment i
lng_i	Longitude of destination for shipment i
d_{ij}	Direct one-way distance from the location of i to the location of j in km
t_{ij}	Direct one-way driving time from the location of i to the location of j in h
kg_i	Payload (tonnage) of shipment i in kg
ct	Costs per truck per hour in EUR: $ct = 7.5€$
cd	Costs per driver per hour in EUR: $cd = 20.5€$
ckm	Costs per driven kilometer in EUR: $ckm = 0.7€$
se	Time for scheduling and loading before a tour in hours: $se = 1h$
tx	Time for parking and taxi at drop off location in hours: $tx = 0{,}1\overline{3}h$
ul	Time for unloading one kilogram in hours: $ul = 0{,}000\overline{3}h$
W	Upper bound for tonnage capacity of the homogeneous vehicles in kg: $W = 7000$
D	Upper bound for duration of tours in h including se: $D = 8$
$Len(T_t)$	Length of driving distance of tour T_t in km: $Len(T_t) = \sum_{i=T_t(0)}^{T_t(\lvert T_t \rvert - 1)} d_{i,i+1}$
$Ton(T_t)$	Tonnage of tour T_t in kg:

	$Ton(T_t) = \sum_{i \in T_t} kg_i \leq W$
$Dur(T_t)$	Duration of tour T_t in h: $$Dur(T_t) = \sum_{i=T_t(0)}^{T_t(\lvert T_t \rvert - 1)} t_{i,i+1} \leq D$$
$DrF(T_t)$	Drop factor of tour T_t, which is the average number of deliveries per stop: $$DrF(T_t) = \frac{\lvert T_t \rvert}{\sum_{i \in T_t : lat_i \neq lat_{i-1} \wedge lng_i \neq lng_{i-1}} 1}$$
$CV(T_t)$	Variable driving costs of tour T_t including personnel, fuel and truck in EUR: $$CV(T_t) = Len(T_t) \cdot ckm + Dur(T_t) \cdot (ct + cd)$$
CV	Overall variable driving cost of tours in EUR: $CV = \sum_{t=1}^{N} CV(T_t)$
$ICC(T_t)$	Idle capacity cost of tour T_t in EUR: $$ICC(T_t) = (D - se - \lvert T_t \rvert \cdot tx - Dur(T_t) - Ton(T_t) \cdot ul) \cdot (ct + cd)$$
ICC	Overall idle capacity costs for all tours in EUR: $$ICC = \sum_{i=1}^{N} ICC(T_i)$$
w_{kg}	Allocation weight of payload in relation to weight of distance $w_{kg} \in [0,1]$
cv_i	Allocated variable costs per shipment i in EUR: $$cv_i = CV \cdot \left(w_{kg} \cdot \frac{norm(kg_i)}{\sum_{j \in I} norm(kg_j)} + (1 - w_{kg}) \cdot \frac{norm(d_{0i})^2}{\sum_{j \in I} norm(d_{0j})^2} \right)$$
sr	Idle capacity cost surcharge rate per shipment: $$sr = \frac{ICC}{CV}$$
$CF(T_t)$	Fixed costs per Tour T_t in EUR: $$CF(T_t) = (se + \lvert T_t \rvert \cdot tx) \cdot (ct + cd)$$
cf	Fixed cost surcharge per shipment for scheduling/loading in the morning and taxi at drop off location in EUR: $$CF = \frac{(\lvert T \rvert \cdot se + \lvert I \rvert \cdot tx) \cdot (ct + cd)}{\lvert I \rvert}$$
$cl(kgi)$	Unloading cost surcharge per shipment $i$in EUR: $$cl(kg_i) = ul \cdot kg_i \cdot (ct + cd)$$
ci	Full costs per shipment i: $$ci = cvi \cdot (1 + sr) + cf + cl(kgi)$$

$\beta_1,\ \beta_2$	OLS coefficients of the costing model per shipment
ce_i	Estimated variable costs of shipment i with characteristic d_{0i} and kg_i in EUR: $ce_i = \beta_1 \cdot norm(d_{i0})^2 + \beta_2 \cdot norm(kg_i)$

2.4.1. Vehicle Routing

The vehicle routing module applies operations research methodology to cluster and route daily distribution tours. The objective function is a minimum function that optimizes either mileage, duration or costs. In general, this module permits the incorporation of manifold formulation variants from literature on the vehicle routing problem (VRP). Mandziuk [175] reviews different modern problem formulations and solution methods for variants of the VRP. From a practitioner's view, the problem formulation in the routing module has to ensure the applicability and thus validity of the tours to compare. For example, an LSP who offers time windows to his consignors needs to account for these time windows in vehicle routing.

We propose to use a VRP formulation with a homogeneous capacitated fleet and to apply well-known local search heuristics in the solution. Local search heuristics provide an acceptable trade-off between objective quality, computational speed, flexibility and simplicity [176]. For our purpose, an acceptable objective quality is sufficient, since we are interested in the effect of different inputs rather than different solution methods. Therefore, as long as the same methods are applied to both inputs I' and I, the solution quality is comparable with respect to these inputs.

Figure 6 visualizes our procedure: we initially apply the well-known savings algorithm by Clarke and Wright [177]. The results are then improved by a 2-opt intra-route search heuristic [178]. Then, the 2-optimal routes are further improved by an inter-route 2-opt* heuristic [179].

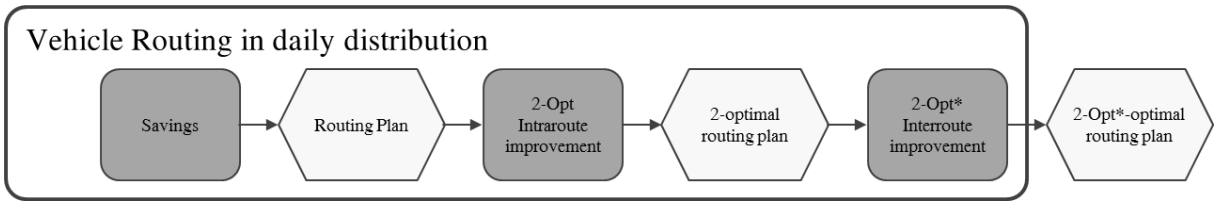

Figure 6 Proposed procedure for the vehicle routing module

2.4.2. Cost Accounting

This module isolates idle and fixed costs from variable costs per tour. Inputs for the costing module are:

- tours from the vehicle routing module,
- cost coefficients $ckm,\ ct$ and cd,
- and estimates of parameters $se,\ tx$ and ul.

Idle costs arise by underutilization of drivers and trucks. Fixed costs arise through loading and scheduling before starting the distribution and whenever the driver stops (parking and taxi) at a drop off location to deliver one or more shipments. Costs for unloading are also calculated separately because they are charged directly to distinct shipments.

Variable tour costs include the costs per kilometer multiplied with the mileage travelled as well as the costs per hour (truck costs per hour + personnel costs per hour) multiplied with the tour duration.

$$CV(T_t) = Len(T_t) \cdot ckm + Dur(T_t) \cdot (ct + cd) \quad (1)$$

These variable costs per tour are summed up and are called overall variable costs.

$$CV = \sum_{t=1}^{N} CV(T_t) \tag{2}$$

The overall variable costs are allocated to shipments in subsection 4.3.

In addition to variable costs, the idle capacity costs per tour arise. We assume the costs of employing a driver and using a truck to be fixed per day. This means the driver gets paid to work 8 hours a day. The truck's planned time-dependent depreciation is also calculated on 8 hours of daily usage. Following this, idle capacity costs per tour are the result of unused time per tour multiplied with the costs per hour considering the driver and the truck. For example, a tour having a total duration of 7 hours, leaves one hour of idle time during which truck and driver inflict costs that cannot be charged directly on any shipment.

$$ICC(T_t) = (D - se - |T_t| \cdot tx - Dur(T_t) - Ton(T_t) \cdot ul) \cdot (ct + cd) \tag{3}$$

The sum of all idle capacity costs is called the overall idle capacity costs.

$$ICC = \sum_{t=1}^{N} ICC(T_t) \tag{4}$$

The overall idle capacity costs are surcharged onto the variable costs. This surcharge rate is calculated by the ratio of overall idle capacity costs and overall variable costs.

$$sr = \frac{ICC}{CV} \tag{5}$$

To calculate full costs, the fixed costs are added. We assume the sum of all fixed tour costs and fixed stop costs to be distributed evenly among all shipments. The fixed tour costs are calculated by multiplying the costs per hour and the vehicle loading time se. The fixed costs of stopping are the product of parking/taxi time tx and the costs per hour.

$$CF(T_t) = (se + \frac{|T_t|}{DrF(T_t)} \cdot tx) \cdot (ct + cd) \tag{6}$$

All fixed costs are summed up to the overall fixed costs. Dividing the overall fixed costs by the number of shipments results in fixed costs per shipment.

$$cf = \frac{\left(N \cdot se + \sum_{t=1}^{N} \frac{|T_t|}{DrF(T_t)} \cdot tx\right) \cdot (ct + cd)}{|I|} \tag{7}$$

The full costs of distribution per shipment are consequently the sum of allocated costs cv_i including idle costs and the fixed costs per shipment and the arising costs of unloading the shipment.

$$ci = cvi \cdot (1 + sr) + cf + cl(kgi) \tag{8}$$

2.4.3. Cost Allocation

The cost allocation module is meant to allocate the variable cost per tour onto the shipments $i \in T_t$ of that tour. The idle and fixed costs are then surcharged on top of the allocated variable tour costs. The input to this module is the resulting cost vector $CV(T_t)$ from the cost accounting module and the output of the allocation is a cost vector cv_i. In literature, there exist many proposals for different allocation methods (AM). The incorrigible problem with the selection of an AM is how to evaluate its outputs. Since there is no observable and well-known correct benchmark result, any AM is to some degree arbitrary and not completely defensible [180,181]. As different AM produce different outputs, economic consequences and incentives, any AM can be more or less preferable over others in various circumstances. However, several criteria are proposed in the relevant literature [182–185]. AMs may be classified as [cf. 185]:

- Shipment-focused: Allocation weights are a function of individual shipments' characteristics.
- Marginal cost-focused: Allocation weights are a function of the marginal cost a that single shipment (consignor, recipient) inflicts upon the coalition of shipments/consignors.
- Stability focused: Allocation weights are dimensioned in a way that minimizes the incentive for any subset of individuals to leave the game/network/GFF.

In the context of distribution cost allocation, all three classes of AMs may be applicable, depending on the overall use case. For example, in a tariff-building use case, a shipment-focused AM seems appropriate, in a negotiation context a marginal cost-focused AM may provide a lower bound in pricing or for transfer pricing within horizontal groupage freight alliance the stability focused AM is more suitable.

Selection of the AM

Herein, we propose to reference literature for recommendations and evaluate these literature-based recommendations with respect to applicability in the distribution case.

The suitable AM must generate a vector of the costs per shipment class cv_i, which enables the classification of shipments in a two-dimensional table by weight kg_i and distance d_{0i} (rhs of Figure 4). The cost vector must be a progressive function of the distance d_{0i} [161]. That effect has been demonstrated by Boone and Quisbrock using a ring-radial model, but it is intuitively explicable (Figure 7): As the distance increases, the number of shipments that fit onto a tour decreases due to the time restriction and the costs are allocated to less and less shipments, causing progressive costs per shipment. For example, within a 2-stop tour, two equal-weight, equal-distance shipments are delivered to their destinations, which are both 50km away from the terminal. The driver returns to the depot just in time without violating the allowed driving duration. Therefore, both shipments have equal halves of the tour's variable cost allocated to them:$cv_1 = cv_2 = \frac{CV(T_0)}{2}$. If one of these shipments were not 50 but 51km away from the terminal, the driver would inevitably violate the allowed driving duration and the vehicle routing module would not allow that 2-stop tour. Instead, the now farther away shipment has double the costs allocated to it. This marginal cost is much smaller for less distant stops on tours with higher volume.

With respect to payload, we expect the AM to tend to allocate more costs to heavier shipments in a linear manner. The reason is obvious: if the marginal costs per kg were increasing, the consignor has a monetary incentive to split up his shipments.

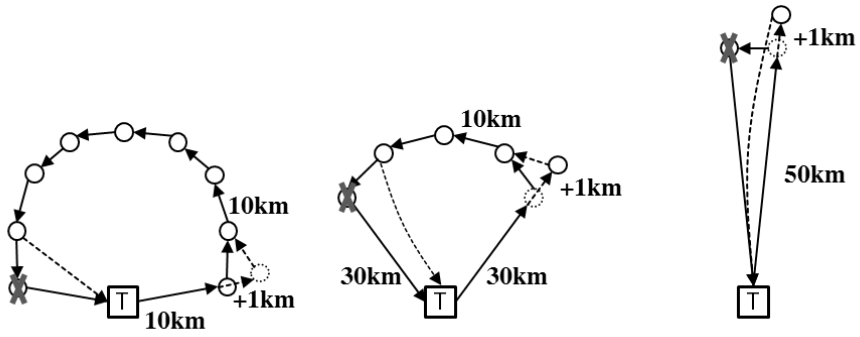

#Stops before	8	5	2
#Stops after	7	4	1
Cost per stop before	12.5	20	50
Cost per stop after	14.29	25	100
Marginal cost	1.79	5	50

Figure 7 The cost per shipment grow progressively as the distance increases

Experimental implementation of recommended AM

Kellner and Otto [184] experiment with 15 different AM with respect to a broad set of criteria including robustness, coalition stability and ease of application. In their paper, the authors consider the allocation of greenhouse gas emissions in one-to-many distribution networks. As they collect AM from literature on cost allocation, we consider their comparison relevant for this paper. They recommend three AM:

AM1: Proportional willingness-to-pay (PWTP) from Fishburn and Pollak [182].

AM2: KM and Tons-KM Allocation (KTA), which the authors proposed themselves

AM3: Savings cost proportional allocation (SCPA), which we identified as a generalization from Fishburn and Pollak [182].

Furthermore, in another paper on tooling cost allocation Kellner et al. [185] recommend a similar AM:

AM4: Louderback-Moriarity Allocation (LMA) from Balachandran and Ramakrishnan [186]

Since none of the mentioned contributions comments on the relationship between costs and distance per shipment in distribution, we implemented all four and experimented with shipment data from a German GFF. In the case of KTA, we test several weights w_{kg} of payload. For the allocation in Figure 8, $w_{kg} = 0.3$ is set.

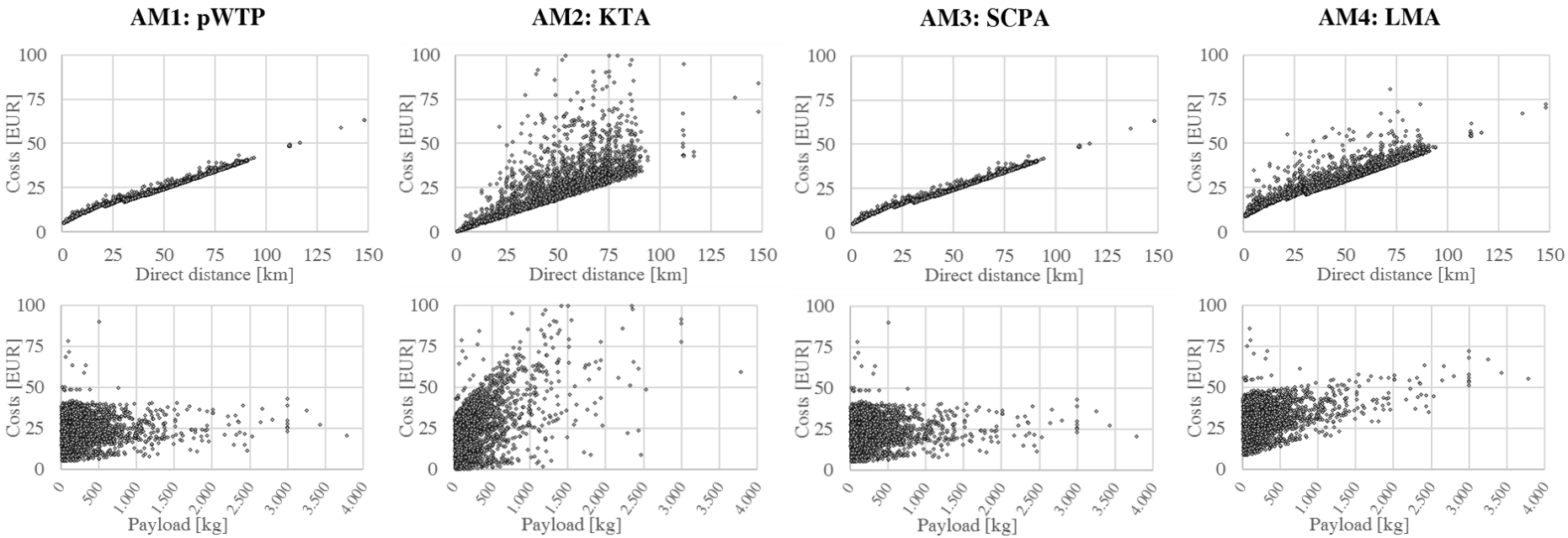

Figure 8 Experimental results of four recommended AM

Figure 8 visualizes some of our experimental results. We apply all AMs for inter-tour cost allocation, which means we allocated the total variable costs onto all shipments[5]. Visually, one can identify that the relation between costs and distance is not progressive for any of the AMs. pWTP and SCPA from Fishburn and Pollak [182] performed identically and thus confirm that SCPA is a generalization of pWTP. However, both neglect payload. Indeed, the Pearson correlation of allocated costs and payload is 0.07 for both AM1 and AM3. This relation is better captured by KTA and LMA.

AM design

As all of the recommended AM fail to account for the progressive relation between costs and direct distance, we propose to design a new shipment-focused AM. We acknowledge the suitability of marginal cost and stability focused AM for respective use cases. Nevertheless, this paper investigates the true cost of a new consignor's shipments and thus, we focus on those shipments' characteristics and how they perform in daily routing.

The following shipment-focused AMs are designed in order to produce the expected behavior.

AM5: proportional normalized tons-km (pnTKM)

The KTA accounts for a combination of tons-km and km. The problem of using tons-km is the scale of payload and distance in distribution. While the distance usually scales from 0.4 to 90km (with some outliers up to 150km), the payload ranges from 1 to 4,500kg and thus outweighs the distance. Therefore, we normalize both payload and distance on a scale from 1 to 100. Therefore, every shipment has characteristics, normalized tons-km $ntkm_i$.

$$ntkm_i = norm(kg_i) \cdot norm(d_{0i}),\ norm(kg_i) \in [1{,}100] \text{ and } norm(d_{0i}) \in [1{,}100] \tag{9}$$

AM5 pnTKM allocates the variable costs CV of all tours onto the shipments proportional to the normalized tons-km:

$$cv_i = CV \cdot \frac{ntkm_i}{\sum_{j \in I} ntkm_j} \ \forall i \in I \tag{10}$$

AM6: proportional normalized tons-km squared (pnTKM²)

In order to stress the progressive impact of the direct distance on costs, we experiment with the idea to square the distance and thus weigh it even more. AM6 pnTKM² allocates the variable costs CV onto the shipments of all tours proportionally to the normalized tons-km²:

$$cv_i = CV \cdot \frac{norm(kg_i) \cdot norm(d_{0i})^2}{\sum_{j \in I} norm(kg_i) \cdot norm(d_{0i})^2} \ \forall i \in I \tag{11}$$

AM7: normalized payload and normalized (distance)^a allocation (nPnD^{a}A)

AM7 is inspired by KTA from Kellner and Otto [184]. We propose three modifications: first, we account for payload instead of tons-km in order to not include distance twice. Second, we normalize both terms in order to adapt the scale of payload and distance. Third, we exponentiate distance after that normalization. AM7 nPnD^{a}A allocates the variable costs CV onto the shipments of all tours proportionally to a weighted combination of normalized payload and normalized distance to the power of a:

[5] We also experiment with intra-tour allocation, which means we apply the four AMs to allocate the variable costs per tour onto the shipments of that tour. The results of intra-tour allocation cause excessive variability in the allocated costs among comparable shipments. For example, repetitive homogeneous shipments that are addressed to the same destination on multiple days are routed in different tours. As a result, these homogeneous shipments receive different costs. Therefore, we recommend to allocate variable distribution costs on an aggregated level, e. g. across multiple tours.

$$cv_i = CV \cdot \left(w_{kg} \cdot \frac{norm(kg_i)}{\sum_{j \in I} norm(kg_j)} + (1 - w_{kg}) \cdot \frac{norm(d_{0i})^a}{\sum_{j \in I} norm(d_{0j})^a} \right) \quad (12)$$

The exponent a should be some number $a \geq 1$. However, the fitting of a is not completely defensible, just as any other parameter of any AM.

The three designed AM 5-7 are implemented and tested with the same GFF data set. In case of nPnD^{a}A, the weighting factor is set to $w_{kg} = 0.3$ and the exponent is set to $a = 1.5$. The results are visualized in the scatter plots of Figure 9.

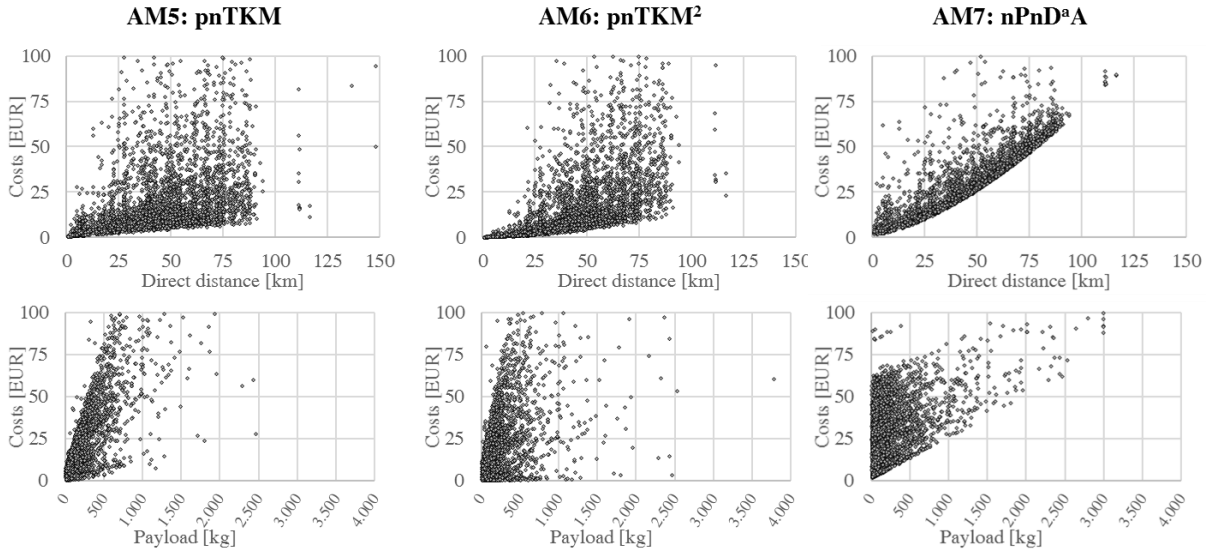

Figure 9 Experimental results of the designed AM

In the case of pnTKM and pnTKM², costs depend on both direct distance and payload. The visual effect is a large scatter in both uni-variable plots. In pnTKM², one can observe the progressive trend in the scatter plot (AM6 top). However, the visually most appealing results are achieved by nPnD^{a}A. There is both a clear progressive trend in the cost per km and a supposedly linear trend in the cost per kg. This linear trend gets steeper with increasing weight w_{kg} and vice versa. The more weight is set on distance, the less dispersion can be observed in the costs per km.

Herein, it is not intended to make the case for criteria of fairness, robustness or neutrality. Therefore, we propose to apply the nPnD^{a}A in the cost allocation module in order to determine the costs per shipment.[6]

2.4.4. Model building

To evaluate the shipment specific cost differences between the incumbent structure and the structure including the new consignor we build a cost table with the dimensions distance and payload. Every cell in that table represents a class of shipments with similar characteristics regarding distance and payload. The sizing of the classes is done in incremental steps of 10 kilometers and 10 kilograms. The scales reach until 200 kilometers or 5000 kilograms. At this point, the costs of every single shipment are calculated, but there are large gaps in the cost table. In practice, this is a problem when new shipments need costing. To fill every cell of the table with appropriate costs, the cost function of distance and payload is approximated.

To build the model a multiple linear regression is performed as follows:

$$y = X \cdot \beta + \varepsilon \text{ with } \varepsilon \sim (0, \sigma^2 I_T) \quad (13)$$

[6] In our case we set $w_{kg} = 0.1$ and $a = 2$.

The output vector y is the vector of allocated costs including idle costs per shipment[7]. The matrix X contains the exponentiated normalized distances and the normalized payloads. As a result, the vector of coefficients for exponential normalized distance and the normalized weightβ is estimated. Based on that calculation, variable costs per class of shipment characteristics can be estimated with the following equation:

$$\hat{y}_i = \beta_1 \cdot norm(d_{i0})^2 + \beta_2 \cdot norm(kg_i) + \beta_0 \quad (14)$$

As a result of the model building, we get the following costs shown in Table 5 (reduced due to clarity):

Table 5 Modelled costs in EUR

	20km	**40km**	**60km**	**80km**	**100km**	**120km**	**140km**	**160km**	**180km**	**200km**
25kg	7,23	13,96	27,06	46,53	72,37	104,58	143,17	188,13	239,46	297,16
50kg	7,55	14,28	27,38	46,85	72,69	104,90	143,49	188,45	239,78	297,48
75kg	7,87	14,60	27,69	47,16	73,01	105,22	143,81	188,76	240,09	297,80
100kg	8,19	14,91	28,01	47,48	73,32	105,54	144,12	189,08	240,41	298,12
200kg	8,98	15,71	28,81	48,28	74,12	106,33	144,92	189,88	241,21	298,91
300kg	10,25	16,98	30,08	49,55	75,39	107,61	146,19	191,15	242,48	300,18
400kg	11,53	18,25	31,35	50,82	76,66	108,88	147,46	192,42	243,75	301,45
500kg	12,80	19,52	32,62	52,09	77,94	110,15	148,74	193,69	245,02	302,73
750kg	15,02	21,75	34,85	54,32	80,16	112,38	150,96	195,92	247,25	304,95
1000kg	18,20	24,93	38,03	57,50	83,34	115,56	154,14	199,10	250,43	308,13
2000kg	26,15	32,88	45,98	65,45	91,29	123,51	162,09	207,05	258,38	316,08
3000kg	38,87	45,60	58,70	78,17	104,01	136,22	174,81	219,77	271,10	328,80
4000kg	51,59	58,32	71,42	90,89	116,73	148,94	187,53	232,49	283,82	341,52
5000kg	64,31	71,04	84,14	103,61	129,45	161,66	200,25	245,21	296,54	354,24

2.4.5. Costing comparison

To compare the costs per shipment with and without the new consignor two cost estimating models are built. With these two models, a detailed comprehension of every shipment's cost with and without the new consignor can be calculated. We search for correlations between the changes regarding the costs and changes in the network. Therefore, we calculate relative changes in the network's characteristics and the change in the costs per shipment. Performing multiple correlation tests helps us understand the interdependencies between all the calculated changes.

[7] Not including fixed costs.

2.5. Computational analysis

In this section, we introduce the structure of our given data and the assumptions of the computational analysis. After that, our presented methodology is applied to the data of an anonymous German GFF. We analyze the results of our study in order to gain practical insights into the effect of a new consignor within a distribution network.

2.5.1. Data

Our data represent shipments of the distribution structure from a random terminal of a German GFF. The given time period is a recent month. As of confidentiality agreements, the identity of the GFF, the consignors and the recipients are anonymous. After data cleansing, the data sample includes 3,742 shipments with the following attributes listed in Table 6.

Table 6 Data attributes of raw shipment data

Attribute	Description
Date	The date of the delivery
Consignor No.	The consignor's number
Consignor Street	The pickup street
Consignor Zip-Code	The pickup Zip-Code
Consignor City	The pickup city
Consignor Country	The pickup country
Recipient No.	The recipient's number
Recipient Street	The drop-off street
Recipient Zip-Code	The drop-off Zip-Code
Recipient City	The drop-off city
Recipient Country	The drop-off country
Payload	The shipments payload in kilograms

In addition to the raw data from Table 6, we compute the following attributes per shipment (Table 7).

Table 7 Computed attributes for shipment data

Attribute	Description
Recipient Latitude	Latitude of the drop-off location
Recipient Longitude	Longitude of the drop-off location[8]
Recipient Distance	One-way distance from the terminal to the drop off location in kilometers[9]

2.5.2. Assumptions

In order to estimate the costs per shipment, we calculated different cost rates. Truck costs per hour, truck costs per kilometer driven and drivers' hourly wages are calculated with schemes described by Wittenbrink [167] and Hartmann [187]. The results are $ct = 7.5€$ per hour per truck, $ctkm = 0.7€$ per kilometer driven and $cd = 20.5€$ per hour per driver. Our calculations on cost rates are shown in the appendix. Furthermore, we estimated the loading and scheduling time at the beginning of a tour to be $se = 1h$. The time for parking and taxi is $tx = 0.1\bar{3}h$ and the time for unloading is $ul = 0.000\bar{3}h$ per kg. These values are estimates from past projects with other GFFs and are thus not characteristic for this specific GFF in our computational study.

2.5.3. Computational result

In order to answer the research question, we implement the proposed methodology from section 4. Thereafter, we perform multiple runs for the largest consignors in the data sample. A consignor is considered large if his number of shipments or tonnage ranks among the top 25 consignors. After sorting out the two list's duplicates 31 consignors remain.

From a practitioner's view, it is interesting to investigate the most valid predictors of cost differences. Therefore, correlation tests between the changes in the shipment structure and the cost differences are performed. The results are shown in Table 8.

Correlations' significance

As we are interested in the shipments structure's impact on costs we are focusing on the correlations between the structural changes and the delta in costs per shipment which are represented in the last column of Table 9. Before interpreting the data, we check the p-values of our correlations to sort out non-significant results. Our maximum significance level is $p <= 0.05$. Discarded correlations are marked by crossed-out values.

Strong predictors (p-Value <= 0.05, Correlation >= 0.8)

The set of characteristics which induce the strongest absolute correlation to the change of costs per shipment consists of:

- Number of shipments (-0.88)
- shipments per tour (-0.93)
- stops per tour (-0.92) and
- stop-stop distance (0.82)

[8] The drop-off location's longitude and latitude are calculated using MapBox's Place Search API via https://www.mapbox.com/search/.

[9] The distance is calculated as the great circle distance from the terminal's geolocation to the drop-off geolocation with a detour factor of 1.25.

A plausible explanation could be the following logical approach: Less stop-stop distance comes from higher density tours. This means that more stops are performed within the same or a smaller number of kilometers driven which is limited by the maximum driving time. To achieve this setting more shipments overall have to be distributed via the network.

Multicollinearity

As there is a correlation of 1.0 between the characteristics shipments per tour and stops per tour, we can state multicollinearity and view them as an identical feature when it comes to interpretation. In general, there are pretty high correlations between the most important characteristics named above. All of the correlations are in an interval ranging from 0.66 to 0.88 which leads to the guess that one single effect is described by a set of characteristics.

Table 8 Structural changes in the GFF's shipment structure due to the integration of a new consignors

Consignor	Delta shipments	Delta payload	Delta shipments per tour	Delta stops per tour	Delta drop-factor	Delta payload per shipment	Delta Stop-Stop Distance	Delta approach distance	Delta time utilization	Delta capacity utilization	Delta costs per shipment
1	0.51%	3.27%	-0.14%	-0.12%	0.03%	2.75%	-0.76%	1.56%	0.41%	1.06%	-0.21%
2	0.38%	1.15%	0.05%	0.04%	0.00%	0.77%	-1.08%	1.36%	0.18%	0.34%	-0.15%
3	0.24%	1.11%	0.24%	0.06%	0.26%	0.87%	-0.23%	0.49%	0.27%	0.46%	-0.18%
4	0.78%	1.11%	0.45%	0.49%	0.14%	0.32%	-0.42%	0.89%	0.42%	0.32%	-0.52%
5	0.54%	1.04%	-0.12%	-0.18%	0.08%	0.50%	-1.52%	0.59%	0.01%	0.16%	0.06%
6	0.19%	0.94%	-0.47%	-0.46%	0.11%	0.75%	-0.56%	0.91%	-0.30%	0.12%	0.28%
7	0.27%	0.74%	-0.39%	-0.37%	0.09%	0.47%	-0.30%	-0.51%	-0.31%	0.03%	0.29%
8	1.14%	0.73%	0.48%	0.45%	0.06%	-0.40%	-0.07%	-0.63%	0.12%	0.03%	-0.36%
9	18.01%	13.10%	4.17%	3.96%	0.21%	-4.17%	-10.19%	3.13%	0.55%	-0.07%	-4.78%
10	8.34%	1.86%	3.05%	2.85%	0.33%	-5.98%	-4.25%	-0.27%	0.20%	-1.35%	-2.30%
11	7.22%	1.38%	2.33%	2.05%	0.39%	-5.45%	-4.25%	0.13%	-0.24%	-1.41%	-1.66%
12	4.61%	14.24%	-1.52%	-1.64%	0.30%	9.20%	-3.53%	-0.73%	-1.31%	2.94%	-0.02%
13	3.97%	4.42%	-0.77%	-0.86%	0.24%	0.43%	0.97%	-1.58%	-1.42%	-0.15%	0.39%
14	2.32%	4.16%	-1.34%	-1.31%	0.22%	1.79%	-1.77%	1.29%	-0.74%	0.18%	0.56%

15	2.27%	2.09%	-0.06%	-0.04%	-0.14%	-0.17%	-0.80%	1.05%	-0.13%	-0.10%	-0.24%
16	1.91%	1.22%	0.91%	0.83%	-0.06%	-0.68%	-0.95%	0.79%	0.14%	0.10%	-0.95%
17	1.63%	4.46%	0.31%	0.13%	0.31%	2.78%	-0.58%	0.03%	0.27%	1.26%	-0.80%
18	1.52%	0.94%	0.53%	0.55%	0.23%	-0.57%	-0.61%	0.13%	0.12%	-0.02%	-0.53%
19	1.41%	0.86%	0.42%	0.37%	0.19%	-0.55%	0.58%	-1.33%	-0.02%	-0.05%	-0.46%
20	1.30%	1.60%	0.31%	0.06%	0.22%	0.30%	-0.60%	1.30%	0.12%	0.25%	-0.23%
21	1.11%	0.99%	0.45%	0.45%	-0.07%	-0.12%	-0.52%	1.74%	0.36%	0.14%	-0.45%
22	1.03%	0.99%	-0.29%	-0.24%	-0.02%	-0.04%	1.57%	0.18%	-0.07%	-0.14%	0.02%
23	1.00%	0.58%	0.34%	0.36%	0.08%	-0.41%	0.44%	-0.86%	0.17%	-0.03%	0.14%
24	0.92%	2.02%	-0.40%	-0.35%	0.05%	1.09%	-0.95%	0.37%	-0.18%	0.29%	0.29%
25	0.84%	1.63%	0.84%	0.88%	-0.20%	0.79%	-1.58%	2.97%	0.68%	0.67%	-0.67%
26	0.81%	0.51%	0.15%	-0.01%	0.16%	-0.30%	-0.08%	0.53%	-0.08%	-0.06%	-0.33%
27	0.81%	0.46%	0.48%	0.52%	0.04%	-0.35%	-0.71%	-0.54%	0.02%	0.05%	-0.60%
28	0.81%	0.66%	0.81%	0.79%	0.06%	-0.14%	-0.81%	0.27%	0.39%	0.28%	-0.42%
29	0.78%	0.24%	0.45%	0.35%	0.22%	-0.54%	0.27%	0.52%	0.30%	-0.04%	-0.26%
30	0.75%	0.10%	0.10%	0.05%	0.02%	-0.65%	-2.85%	-0.06%	-0.26%	-0.23%	-0.02%
31	0.67%	0.78%	0.34%	0.38%	-0.12%	0.10%	-0.16%	0.54%	0.23%	0.19%	-0.50%

Table 9 Correlation between shipment structure changes and cost differences [10]

Pearson Correlation coefficients	Overall Payload	Shipments per tour	Stops per tour	Drop factor	Payload per shipment	Stop-Stop Distance	Approach distance	Time utilization	Capacity utilization	Costs per shipment
Overall shipments	0.68	0.73	0.71	0.40	-0.44	-0.88	0.25	-0.01	-0.22	-0.88
Overall Payload		0.11	0.09	0.34	0.35	-0.65	0.17	-0.34	0.53	-0.44
Shipments per tour			1.00	0.18	-0.80	-0.68	0.32	0.56	-0.53	-0.93
Stops per tour				0.12	-0.80	-0.66	0.33	0.58	-0.54	-0.92
Drop factor					-0.09	-0.28	-0.36	-0.33	-0.06	-0.23
Payload per shipment						0.32	-0.10	-0.40	0.94	0.58
Stop-Stop Distance							-0.42	-0.08	0.08	0.82
Approach Distance								0.54	0.07	-0.39
Time utilization									-0.19	-0.41
Capacity utilization										0.28

[10] Numbers that show a p-value greater than $p = 0.05$ in Table 10 are not part of further analysis.

Table 10 p-Values of pearson correlation coefficients

p-value	Overall Payload	Shipments per tour	Stops per tour	Drop factor	Payload per shipment	Stop-Stop Distance	Approach distance	Time utilization	Capacity utilization	Costs per shipment
Overall shipments	0.0000	0.0000	0.0000	0.0040	0.0013	0.0000	0.0828	0.9327	0.1320	0.0000
Overall Payload		0.4312	0.5378	0.0150	0.0120	0.0000	0.2412	0.0147	0.0001	0.0013
Shipments per tour			0.0000	0.2090	0.0000	0.0000	0.0251	0.0000	0.0001	0.0000
Stops per tour				0.3918	0.0000	0.0000	0.0189	0.0000	0.0001	0.0000
Drop factor					0.5155	0.0456	0.0114	0.0182	0.6878	0.1110
Payload per shipment						0.0217	0.4865	0.0044	0.0000	0.0000
Stop-Stop Distance							0.0021	0.5603	0.5728	0.0000
Approach Distance								0.0001	0.6486	0.0050
Time utilization									0.1801	0.0030
Capacity utilization										0.0484

2.6. Discussion

The present paper contributes both to the theory and practice of distribution. However, there are also some limitations to our results and plenty of room for further research.

2.6.1. Theoretical implications

Economies of Integration

Keeler [169] introduces the term EOI. This is a major contribution to transportation theory because EOI clearly deviate from Economies of scale. A major contribution of the presented paper is the comprehensive list of indicators that drive EOI in distribution. In section 3, we identify shipments, payload, certainty, drop factor, tour and area density as well as approach distance. Furthermore, the correlation matrix of Table 9 highlights the importance of different characteristics of distribution with respect to their impact on costs. For example, it turns out that the overall number of shipments has a greater impact than the overall tonnage.

Relation between costs per shipment and distribution structure

The computational analysis of section 5 reveals several insights about the relationship between the costs per shipment and other characteristics of the distribution shipment structure. Our analysis shows that the number of stops and shipments per tour decreases the costs per shipment as the coefficient of correlation is smaller than -0.8. Furthermore, the average stop-to-stop distance and the overall number of shipments in the distribution significantly decrease costs per shipment. We could not show that the drop factor decreases costs significantly, however, this may be the result of an overall low level of drop factors for all consignors in our sample.

Summarizing the results from the computational study, we conclude, that (1) without a great volume, consignors have only limited impact on the overall cost structure and (2) consignors with a great volume usually reduce the average costs per shipment for all consignors, but (3) the exact level of cost reductions depends on the densification of tours and thus needs meticulous investigation.

Development of a new AM based on recommendations from the literature

In subsection 2.4.3, we identify recommended AM from relevant literature. However, none of the recommendations succeed in providing a progressive functional relation between distance and costs according to Boone and Quisbrock [161]. The identification of this insufficiency is a contribution itself. Furthermore, based on those recommendations, we propose further development of the recommendations from Kellner and Otto [184], which incorporates a normalization to overcome different scales and a potential or exponential term to overcome the degressive relation.

2.6.2. Practical implications

Distribution costing and cost-based tariff design

The proposed methodology is of great practical use. Due to its modular design, it is easily adaptable to specific use cases and it may be integrated into an existing IT landscape. Calculations of cost rates (appendix) and estimates of durations need to be adapted, however, we present a valid starting point for practical usage. The output of our methodology is the well-known structure of transportation tariffs with the dimensions of distance and payload. Therefore, the methodology can be applied for tariff design.

Individual consignor rates and discounts

Table 8 shows the changes in costs per shipment for different consignors. As it turns out, the EOI of a single consignor often decrease the costs per shipment, but not without exceptions. Take for example consignor 14 from Table 8: this consignor adds 2.3% of new shipments to the incumbent shipments. However, the average costs per shipment increase. Reviewing the EOI indicators, we assume that the

increase in the average payload per shipment causes an increase in costs. As a result, the 14th consignor is not eligible for a discount, although he accounts for a large volume.

Due to our results, we make the following general recommendations for tariff negotiations:

- Calculate the relative number of shipments added by the new consignor
- A consignor who adds less than 1% of shipments to the incumbent shipments, should always pay the standard tariff.
- For large consignors, who add more than 1%, a new tariff based on the combined shipment structure should be calculated and the negotiating range should be derived using the proposed methodology.
- Discounts should not exceed the reduction of costs per shipment.
- New consignors who do not present their shipment structure should always pay the standard tariff and after some period their shipments should be analyzed in order to determine their EOI.

2.6.3. Limitations and further research

Allocation method

It is worthwhile to investigate new AMs which are aligned with the progressive relation that is described by Boone and Quisbrock [161]. We propose a new AM, developed from recommendations from the literature. Cost allocation within the calculated tariff table is heavily dependent on the chosen AM. Modifications in the AM module will modify the outputs and thus the negotiation rates. With that in mind, the costs of a new consignor can be modified by choosing an AM that attaches more or less weight to either distance or payload. For example, choosing an AM which stresses payload is going to increase the allocated costs of a new consignor adding only high payloads to the system. The investigation of AM that account for the progressive relation of cost and distance is an interesting research gap.

Drop factors

As our analysis could not find significant results for the relation between drop factor and costs, this relation is subject to further research deploying data with much higher drop factors. In our sample, no single consignor has a significant impact on the overall drop factor and thus no cost reductions could be observed. From a practitioner's view, we would expect that dedicated GFFs, who serve only consignors from selected industries, e. g. automotive parts, pharmaceuticals, fresh groceries, achieve greater drop factors, as the recipients are often times identical.

Collection and line-Haul

The present paper investigates the distribution of groupage freight. As distribution often accounts for more than 50% of the total costs per shipment, this last mile is the most important part. Nevertheless, a GFF should also investigate the costs per shipment using a similar methodology. Our proposed methodology is easily applicable to the collection in groupage freight. From a costing perspective, line-hauling is the easiest part. Due to this limitation on distribution, we consider a comprehensive model that comprises all of the three legs to be a worthwhile practical contribution.

Hidden consignor clusters

Our analysis looked into the question of the effect of a single new consignor. However, the shipments from different consignors collude: stops and tours are clusters of shipments from many different consignors. It may be the case that some subsets of consignors have great EOI in combination. For example, a producer of paints and a producer of ironmongery always send shipments to the same hardware and DIY stores. Therefore, both consignors have great EOI in combination with each other, even though both consignors neither cooperate nor know about this relation. Further research may extend our work to complementary hidden consignor clusters. From a GFF's perspective, it may be valuable to

unveil such hidden clusters in order to (1) make sure none has an incentive to leave the network and (2) acquire new consignors who integrate smoothly with incumbent hidden clusters.

Stochastic inputs and robustness

We consider our given dataset including shipments over one month to be representative in terms of the long-term shipment structure. However, there may be consignors whose data cannot be considered deterministic. The new consignor's shipment structure is constantly changing or - in the worst case - the consignor deceives the GFF with modified shipment data to blend in smoothly into the incumbent structure. Therefore, incorporating robustness against stochasticity or changes in the shipment structure is an important issue in tariff design. One starting point could be an additional safety premium. This safety premium should account for uncertainty in the number and the location of shipments.

Multiple consignor strategy

In case of two or more consignors entering the system at the same time, sequential calculation of the consignor specific negotiating range would always lead to different results depending on the sequence of calculation. This emerges from the fact that adding one consignor's shipments will change the shipment structure and leads to a different baseline for the second consignor. There is no fixed rule that implies whether the second consignor will benefit from the first one and vice versa. An extreme example are two consignors which are not very suitable for the incumbent shipment structure in terms of density. Let's assume their drop off locations are outside of the LSP's incumbent service area but relatively close to one another. As a result, the first of the two consignors will always decrease density and increase costs per stop. The second consignor will benefit from the first consignor's added stops and increase density as they are very close to each other. As a result, the costs per stop will decrease compared to the shipment structure including stops from the first consignor. Therefore, there are two options to solve this problem.

Option 1: Aggregation of the new consignors' shipments to one structure and then use our methodology to calculate one single negotiating range.

Option 2: Parallel calculation of every consignor's shipment separately based on the incumbent shipment structure.

Our recommendation is to use option 2 with respect to the following aspects:

1. If the two consignors are treated as one they might influence each other. Let's assume we add a large consignor with a huge positive impact on costs and a small consignor with minor negative impact on costs. The negotiation range for the small one itself is 0, but with the aggregation in mind the small consignor gets a huge discount because of the large consignor's shipment structure. Aggregation would thus counter the cause-by-cause principle.
2. In a real-world situation one of the two consignors could cancel negotiations at some point. The negotiating range has to be calculated before the negotiation starts. In the case of the large and the small consignor, this could lead to the situation where the small consignor benefits from the aggregated negotiation range, although the cause of this discount (the large consignor) has cancelled the negotiation and will not be part of the future shipment structure. This could lead to a tariff which is not even covering the costs of the small consignor's shipments.

2.7. Appendix

Calculations according to a combination of the costing schemes from Wittenbrink [167] and Hartmann [187].

Table 11 Personnel cost calculation

Costs	Based on	%	EUR/h	EUR/Day	h per day	h per week	Weeks per month	h per month	Days per month	Costs per month in EUR
Standard wage			12.00		8	40	4.33	173.33		2079.96
Holiday pay	Days per month			14.0					2.5	35
Christmas bonus	Standard wage	8.33%								172.64
Standard wage incl. allowances										2287.6
Pension insurance	Standard wage incl. allowances	9.35%								213.89
Health insurance	Standard wage incl. allowances	7.30%								166.99
Nursing care insurance	Standard wage incl. allowances	1.18%								26.88
Unemployment insurance	Standard wage incl. allowances	1.50%								34.31
Trade association	Standard wage incl. allowances	3.66%								83.73
Insolvency allocable	Standard wage incl. allowances	0.15%								3.43
Continued payment	Standard wage incl. allowances	0.38%								8.69
Costs per month										2825.53

Output	p.a.	%	h/Month
Working time			174
Days of vacation	30		-21,75
Illness rate		4,5%	-7,83
Public holidays	10		-6,69
Hours worked			137,73
Hours worked per month			15,30

	Month	Day	Hour
Costs per unit in EUR	2825,53	164,12	20,5

Table 12 Truck cost calculation

	MAN TGL 12.220 BL Koffer	Units	Value
Technical data	Maximum weight allowed	kg	12000.00
	Maximum payload	kg	6400.00
Usage	Days of usage	Days p.a.	240.00
	Hours of usage per day	h	8.00
	Mileage per year	km	25000.00
	Expected life cycle	Years	5.00
	Mile within expected lifecycle	km	125000.00
Fixed costs	Buying costs (excl. Value-added tax)	EUR	65400.00
	Vehicle tax (Germany)	EUR p.a.	534.00
	Insurance	EUR p.a.	5080.00
	Depreciation (50% time-based)	EUR p.a.	6540.00
	Mobile devices	EUR p.a.	600.00
	Capital charge	EUR p.a.	1635.00
	Sum fixed costs	EUR p.a.	14389.00

	... per hour	EUR/h	7.5
Variable costs	Fuel consumption (diesel)	L/100km	19.80
	Fuel price (excl. Value-added tax)	EUR/L	1.09
	Fuel price per km	EUR/km	0.22
	Maintenance costs	EUR/km	0.19
	Depreciation (50% mileage-based)	EUR/km	0.26
	Toll	EUR/km	0.09
	Toll-quote (% of mileage on toll roads)	%	0.40
	Toll per km	EUR/km	0.04
	Sum variable costs	EUR/km	0.70

3. Towards sustainable cities: Utilizing floating car data to support location-based road network performance measurements

3.1. Introduction

Rising urbanization around the globe leads to high requirements in terms of urban sustainability [188]. Therefore, indicators to measure urban sustainability are an extensively discussed topic in literature [189–192]. These indicators often contain terms like "mobility" [193], "efficient transportation" or "transportation and roads" [194]. When dealing with the sustainability of transportation and the efficient movement of people and goods, beside topics like railways [195] and public transportation [196–200] the urban road network is a major research area [201–207]. This stems from the fact that road network performance (RNP) can lead to significant negative impacts on all three dimensions of urban sustainability:

Economic sustainability can suffer in several ways. Many authors found that poor RNP in terms of traffic congestion is a reason for higher costs and reduces efficiency significantly [114–116,118–120]. In addition to that, traffic congestion intensified in the past [208,209], causing as much as 23 percent of all truck transportation delays [117].

Environmental sustainability is mainly focused on pollution and greenhouse gas emissions. A lot of literature proves the relation between traffic congestion and air pollution [109–111,113,210]. Longer travel distances and congestion lead to more pollution and a lower level of sustainability.

Social sustainability focuses on the well-being of the population. Poor RNP can lead to several health issues: Traffic congestion implies a higher number of vehicles polluting engine noises on road. The generated noise has a significant health impact [105,107] like sleep disturbance and anxiety [104]. In addition to that, the number of accidents happening can depend on the road network [103,106,108].

RNP in general has been studied extensively over the years employing different methods and geared towards different purposes [211–215]. Especially the relation between the three-dimensional urban sustainability (economy, environment and society) and the road network have been addressed:

An extensive body of literature discusses the reduction of traffic congestion [216–218]. Russo and Comi [219] analyze the effects of logistics measures on the economy of the city, Baghestani et al., Armah et al., Borza et al. and Zhang et al. [110,220–222] deal with on road emissions and Kleiziené et al., Ohiduzzaman et al. and Sirin [104,107,223] discuss vehicle noise reduction and the development of quieter pavements.

To carry out these analyzes, all stakeholders who are dealing with road networks and urban sustainability must gather a real-world data base to work with. Therefore, the research hypothesis of this paper can be formulated as follows:

How can relevant data be collected programmatically to measure road network performance?

The long-term trend towards digitizing the environment, including the logistical infrastructure like road networks and vehicles, fundamentally eases the programmatical assessment of information and gives way to study new data collection methods [224–227]. Due to this, the purpose of this paper is to develop a new methodological approach to gather relevant RNP data on an area wide scale. An exemplary application of the gathered data on the economic dimension is demonstrated on four selected cities in Germany to prove the usability of the proposed methodology. Thus, the paper deals with what Sun et al. [228] call the physical issues of RNP, i.e. we are concerned with the determination of travel times, travel speed and traffic conditions.

The paper is organized as follows: Section 2 provides theoretical information on RNP measurement and the underlying data collection procedure. In section 3, a data collection method for measuring RNP is presented by providing an exemplary use case. In section 4, this methodology is applied to four German cities and a comparison of these cities is carried out. In section 5, theoretical and practical implications are discussed. An outlook for further research is provided in section 6, followed by a short conclusion highlighting the main takeaways of this paper.

3.2. Literature Review

3.2.1. Fundamentals on road network performance measurements

The assessment of RNP has been widely researched. We start by introducing our definition and will then give reference to the extant body of research. We suggest defining RNP generally as the network driven impact on sustainability. In the context of this paper, we exemplary focus on the economic dimension, which leads to the refined definition of RNP as being the network driven economical costs of moving a vehicle from a specified origin to a specified destination using the road network. Although the definition is open, we confine our analysis to urban transportation, i.e. short distance traffic, sometimes called the last mile or urban cargo traffic [40,229]. The road network is defined as the set of roads that can be used by vehicles. Thus, our definition of RNP is geared towards the structural properties of the network that shapes the flows within the network and affects operational performance [230,231]. The definition acknowledges but excludes the analysis of further notions or indicators of network performance like levels of service, capacity, safety, smoothness of flow, reliability, vulnerability, accessibility, resource constraints or travel time reliability [232] that respectively represent the functionality of the network for particular research goals. As our analysis is restricted to network driven costs only it is confined to a share of the total cost only. The cost of moving a vehicle is determined by many factors like vehicle type [233], toll [234] or fuel [235]. We restrict the analysis to those factors that are related to the road network. The definition of RNP borrows in part from Santosa and Joewono [236] who measure RNP by speed and vehicle cost.

We suggest measuring RNP by detour and travel speed. Detour is defined as "road distance from origin to destination" over "aerial distance from origin to destination" [237]. Thus, detour represents widely discussed network attributes like density [231] or connectivity [238]. Travel speed is defined as the average speed that can be driven from origin to destination considering vehicle and road constraints. Thus, travel speed summarizes road network attributes like speed limits, traffic lights or the level of congestion within the network [239–241]. Travel speed can be easily converted into travel time [242]. Thoen et al. [243] demonstrate that longer travel times lead to higher transportation costs, emphasizing the importance of determining travel times objectively.

Road distance is defined as the distance of a tour. A tour is defined as the network path a rational decision maker would choose to minimize the travel time from origin to destination. Thus, we assume an efficient use of existing road infrastructure and available traffic status information [244]. We suggest measuring RNP with reference to two factors only and thus depart from earlier approaches that suggest multi-criteria measurements like Fancello et al. [212].

RNP results vary by tour since characteristics of the road network vary across space. Ciscal-Terry et al. [245] called this the origin-destination-distribution problem. Thus, a meaningful RNP statement must be specific on how to select the locations that enter the analysis.

Fundamentally, RNP can be measured via three origin-destination settings. One is to measure across the complete network, i.e., from anywhere to anywhere. A second setting measures from defined origins to defined destinations [94], i.e. from somewhere to somewhere. We suggest following a third setting: Given an origin, we do not specify a destination and then measure detour and travel speed for the origin-destination pair but specify the origin only and list all destinations that can be reached within a given range or time frame.

Since we focus on studying RNP for general cargo moving purposes, typical logistics service providers' locations like freight transport centers, logistic zones or urban consolidation centers represent meaningful origins. For a case-specific analysis, Alho A.R. et al. [246] find that declared data regarding bases might not be as accurate as inferred data, suggesting the identification of central network nodes via algorithms instead of relying on survey data to determine meaningful points of origin. Referring to Saedi et al. [232] our approach does not report RNP across the complete road network but well-defined partitions.

3.2.2. Road network data collection: Developing a new method

Data sources to compute RNP have been mentioned in recent literature but have never been an explicit focus of the research community. Some papers model the variability of RNP via a stochastic framework and compute journey time estimators [247]. Figliozzi [115] uses tour data reported in the literature to perform a sensitivity analysis on changes in travel time and tour characteristics. The problem with this procedure is the availability of data as the current literature does not provide suitable or publicly available tour data for most areas around the world. Another way to gather road data is the usage of equipped single cars [248,249]. These cars are equipped with a range of sensors to record road data while driving. The extensive needed manpower and machinery of this solution gets multiplied as global coverage is attempted. Urban areas could be analyzed under consideration of induction loops, cameras and sensors measuring current road traffic [250,251]. Data accessibility as well as processing data from a lot of different sources drive complexity of this data collection method. Mondschein and Taylor [119] interviewed people about personal trip data and corresponding travel times. Two major concerns arise when we take a closer look at this procedure. Global coverage is very weak as a lot of interviews must be conducted to gather enough data for one specific area. An additional problem are people's privacy concerns when sharing their driving data [115]. A "digital version" of interviewing people is the usage of navigation service providers' Application Programming Interfaces (APIs) as these providers gather and compress anonymized data from all their users [252]. The anonymization of data also overcomes the privacy concerns mentioned before. Kellner et al. [94] used navigation service providers' data to build distance matrices with customers' locations and requested travel times at different times throughout the day. To generalize the approach by Kellner et al. [94] and bypass any problems related to trip generation on basis of personal preference, as for example experienced by Sun et al. [253], we use real-world floating car data (FCD) with compressed information collected over time.

The use of FCD to evaluate traffic status has been studied intensively [254–260]. However, there is no research that exploits FCD, especially FCD processed into reachable ranges, to assess RNP. That is what we suggest doing.

Processing FCD to measure RNP is challenging as traffic data can be considered big data due to its complexity and heterogeneity [246,261,262]. However navigation service providers can produce the needed data efficiently [252]. Because of that, we suggest using navigation service providers APIs, especially retrieving so-called "reachable ranges".

A "reachable range" is defined as an area that can be reached by a specific vehicle under certain constraints such as maximum travel time or maximum travel distance starting at a specified location. The use of reachable ranges to assess networks has gained only limited attention so far. Hirako et al. [263] analyze reachable areas to understand the travel behavior of elderly citizens to medical facilities. Referring to Phan et al. [264] calculating a reachable range is one part of the algorithm for maximizing range sum queries turned inside out.

In our case, we retrieve a reachable set K^c that consists of 50 nodes that can be reached from origin node v_0 by the end of constraint c [265]. As a result, we obtain a subgraph showing only one origin and 50 reachable destinations. Assuming a completely paved environment, the reachable range would resemble a circle. In a real-world scenario, it will be a snowflake-shaped object with some locations

being closer to the origin (areas with poor RPN) and some locations further from the origin (areas with good RNP).

Combining this information with the need for multi-time measurements we obtain time-dependent graphs. By varying the defined timeframe, the RNP measurement can be suited to different goals of the analysis.

Our approach is considered efficient as wide areas can be analyzed by a few API calls. This allows measuring RNP on a large scale for defined origins without the need for second best solutions like regional aggregation as suggested by Casadei et al. [266], for instance.

3.3. Methodology

3.3.1. Basic idea

To measure RNP and make regional comparisons using speed information, the following data is required: Free flow and congested speeds, which can be derived from travel times and travel distances. Air distances, which in relation to previously determined actual road travel distances, enable a detour calculation.

To investigate the relation between the time of day and congestion-induced delays, exemplary trips are simulated leading from the city center outwards (to the east, west, north and south) for every city considered in the comparison below (Section 4). The results generated via the TomTom routing API are shown in Figure 10.

From 03:40 o'clock to 21:50 delays are occurring in every city. Two rush hours can be identified: The first one can be classified as the morning rush hour where large parts of employees commute to work and more than 75 Percent of commercial distribution tours depart from their origin as observed by Nuzzolo et. al. [267]. It peaks at about 08:00 o'clock, in accordance with the observations made in Italy. The second rush hour peaks at 17:00 o'clock when most people are heading home from work. In between these rush hours the congestion-induced delays settle in Hamburg, Munich and Stuttgart whereas Berlin shows a rise in level of delay until peak rush hour is reached. The interval from 22:00 to 03:30 o'clock the next day can be considered as free flow state as there are no congestion-induced delays measured.

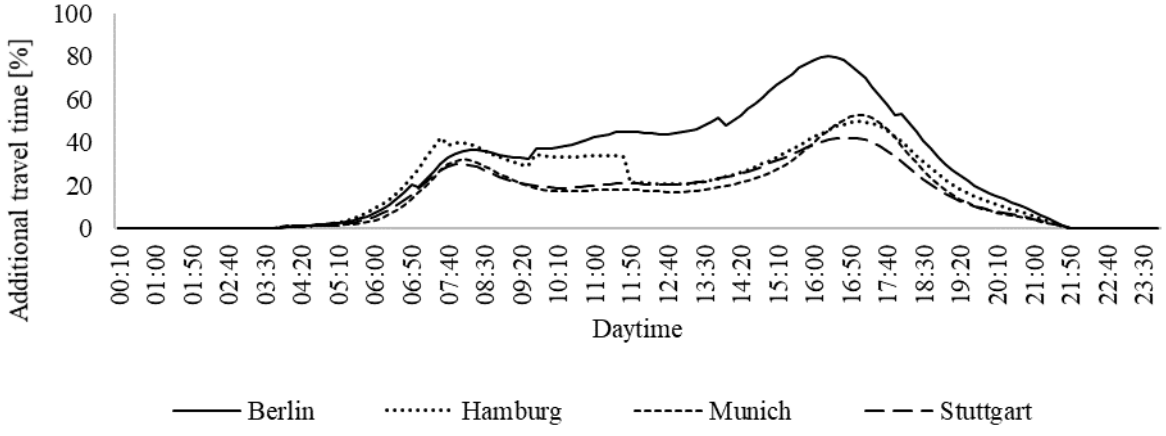

Figure 10 Time-delay dependency

Table 13 TomTom Reachable Range API Parameters

Parameter	Unit / Format	Description
Origin	Latitude, Longitude	Origin describes the starting point of the request.
Time Budget	Seconds	Time restriction that limits the maximum travel time.
Distance Budget	Meters	Distance restriction that restricts the maximum travel distance.
Route Type	Fastest; Shortest; Eco	Describes the routing mode. Fastest optimizes travel times, shortest travel distance, eco finds a compromise.
Depart At	Date in the RFC 3339 Format	Start time of all fictitious routes. Must be in the future.
Travel Mode	Van / Truck / Car	Historical speed profiles that are used depending on the vehicle type.

The data collection process uses the TomTom Reachable Range API. It returns the reachable area in form of reachable destinations from a certain starting point in the form of a polygon. The restrictions for the reachability analysis can be as follows: Maximum travel distance = "distance budget", maximum travel time = "time budget" or maximum fuel consumption = "fuel budget".

This API has become more and more interesting, especially during the electrification of vehicles, because it is possible to determine which locations can be reached with a given battery capacity and a corresponding consumption.

In the context presented in this paper, the API is used to determine all locations that can be reached within a time or distance restriction. Many parameters can be specified as input variables. The most important parameters in this context are shown below in Table 13.

As a result, the API always provides a polygon with a maximum of 50 corner points (see Figure 11), regardless of the selected input parameters. The area described by the polygon includes all geolocations that can be reached considering the specified restrictions. For each corner point of the polygon the corresponding air distance can be estimated using the great circle distance formula [268]. Consequently, the air distance can be used as a common base to compare queries for different restriction parameters.

The data collection methodology to determine the attributes Detour Factor, Infrastructure and Traffic Congestion is explained below. The parameters *Origin, Travel Mode* and *Route Type* are identical for all queries. In case of the following example, the starting point "Schäftlarnstraße 10, 81371 Munich, Germany" with the coordinates of 48.116431 degrees latitude and 11.556811 degrees longitude is selected. The parameter *Travel Mode* is set "truck", the *Route Type* requested is "fastest".

To summarize the data collection methodology, all three calculation steps are presented in Table 15 and explained in depth in the following sections. The used variables are defined as follows in Table 14.

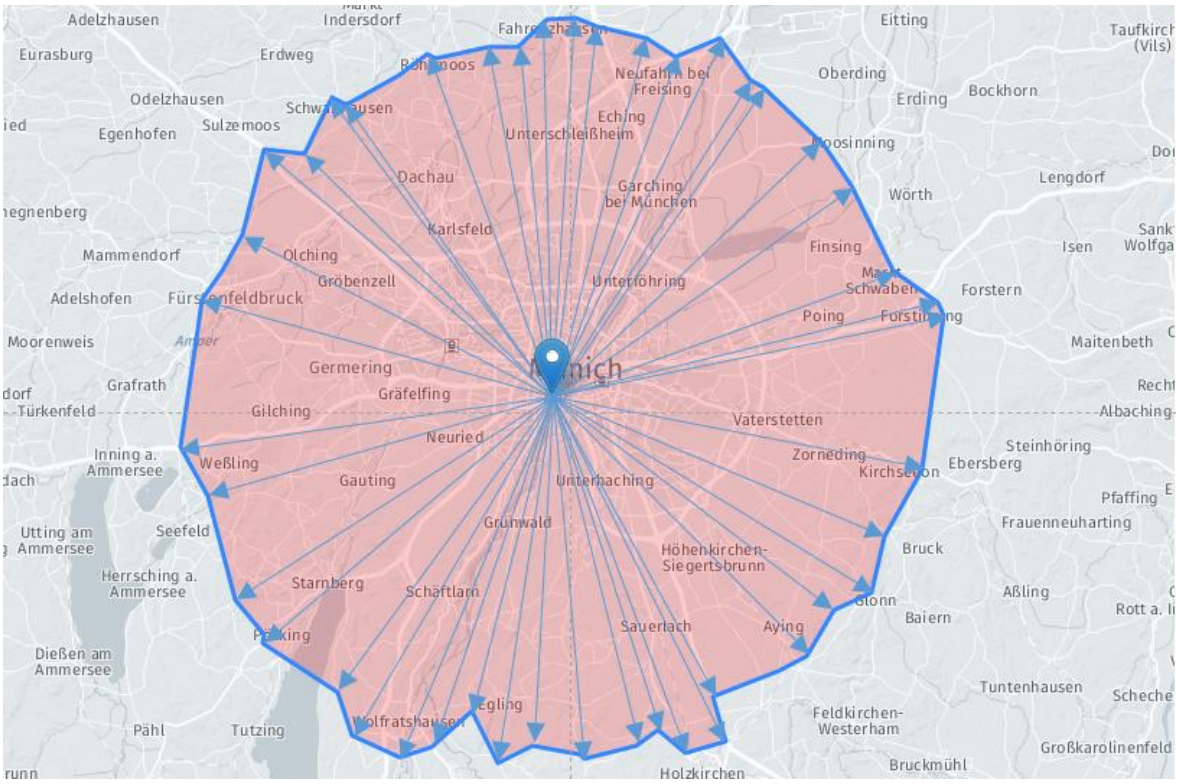

Figure 11 Result of a TomTom Reachable Range request with a 30km travel distance restriction

Table 14 Variables and descriptions

Variable	Description	Explanation
d_t	Travel distance	The road distance from a start point to an end point
d_a	Air distance	Air distance with $d_a = \frac{1}{n} \cdot \sum_{i=1}^{n} d_i$ where d_i is the air distance between the polygon's corner point i and the request's origin and n is the number of polygon corner points (in our case 50).
t_t	Travel time	The time needed to travel from a start point to an end point
$df(d_a)$	Detour Factor regression	Continuous Detour Factor regression based on discrete measures
$v_f(d_a)$	Free flow velocity regression	Continuous free flow velocity regression based on discrete measures
$v_c(d_a)$	Congested velocity regression	Continuous congested velocity regression based on discrete measures

Table 15 Data Collection Overview

Calculation Step	**1: Detour Factor**	**2: Infrastructure / Free flow**	**3: Traffic congestion**
API Restriction	d_t	t_t	t_t
API Result	Polygon to estimate average reachable d_a		
Deduced information	$\frac{d_t}{d_a} = df(d_a)$ Polynomial regression $df(d_a)$	$d_a \cdot df(d_a) = d_t$ $\frac{d_t}{t_t} = v_f(d_a)$ Power Regression $v_f(d_a)$	$d_a \cdot df(d_a) = d_t$ $\frac{d_t}{t_t} = v_c(d_a)$ Power Regression $v_c(d_a)$

The next subsections focus on an in-depth explanation of the collection methodology to understand the requirements and results of every step. Besides, the generated data is visualized by individual charts. Connections between marks within one chart indicate that the gradients are results of continuous regressions based on discrete measures.

3.3.2. Detour

Detour in general is defined as the difference between travel distance via road and the corresponding air distance. The detour factor is defined as the quotient of travel distance and calculated air distance between two points. It will always be greater-than or equal to 1.0, because the shortest travel distance is always a straight line and thus equals the air distance. The detour factor changes with the length of the travel distance/air distance (with increasing air distance, straight routes such as highways can be used, which reduces the detour factor). However, the API query only accepts one maximum travel distance value as a restriction at a time. Consequently, one query for each value between 1km and 30km travel distance (= distance budget) with a step size of 1km is requested and the returned polygons analyzed. The parameter *Depart At* is not relevant here as the polygon is calculated via a traffic-independent shortest path algorithm.

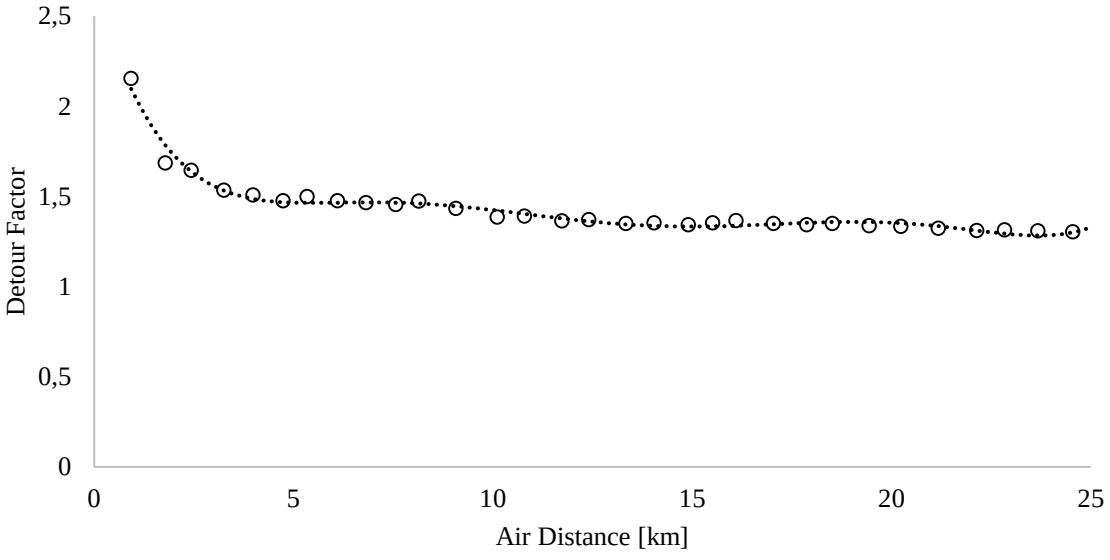

Figure 12 Detour factor for Munich, Germany

In the last step, the query's restriction (= travel distance) can be related to the average value of the calculated air distances. Thus, for each travel distance a corresponding air distance and a detour factor is calculated. The relationship between air distance and detour factor can be displayed using a polynomial regression. In our example, this results in the chart shown in Figure 12.

One can clearly see that the detour factor decreases with increasing air distance, which is due to the possibility of using relatively straight routes (e.g., access to inner-city highways or the German motorway network), until it reaches a nearly stable value (in this case about 1.5).

3.3.3. Infrastructure

After determining the detour factor regression, the API can be used to determine the average speed during free-flow state. The free-flow state describes the traffic flow without congestion exceeding an agreed upon norm [269]. This means that delays due to infrastructural influences such as speed limits or traffic light changes are considered part of the free flow. Consequently, the average free-flow speed provides a quantification of the existing infrastructure. In order to determine this average speed, queries are formulated sequentially to retrieve points that can be reached for a certain journey duration. For this purpose, the queries are restricted by applying a time budget restriction. To ensure free-flow conditions, the parameter *Depart At* is set to 00:00:00. This time is derived from Figure 12 as there is no delay measured in any of the investigated regions. Using the returned polygon, the average air distance between all polygon corners and the starting point can be calculated per iteration step. The time steps and their corresponding free flow distances are shown in Figure 13. However, the magnitude of the travel distance is dependent on the air distance and implicitly manipulated via the detour factor. For this reason, a travel distance is estimated using air distance averages and the corresponding detour factor, as is shown by the formula in Table 15. The ratio of travel distance to travel time returns the average free flow travel speed.

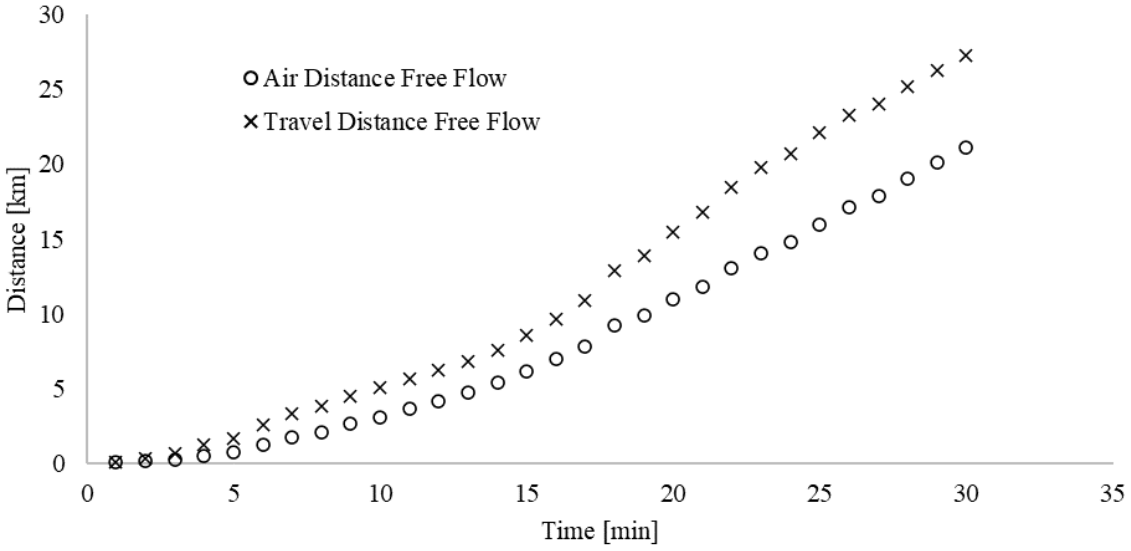

Figure 13 Distance covered during free flow for Munich, Germany

3.3.4. Traffic congestion

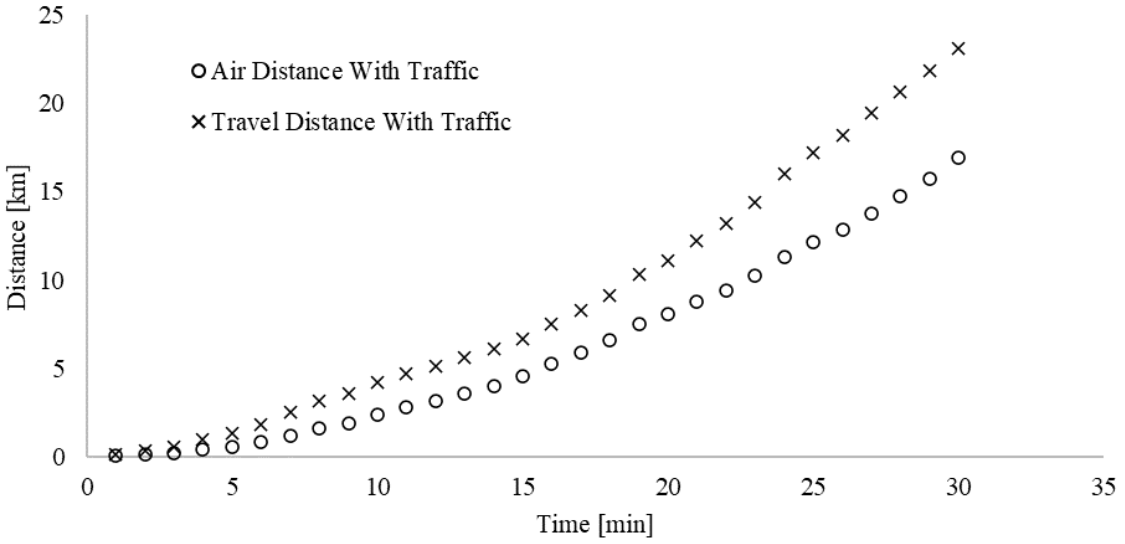

Figure 14 Distance covered including traffic for Munich, Germany

With the given definition of free-flow state in mind, the effect of traffic congestion can be measured by the difference between free-flow speed and congested speed. The travel speed in congested state can be determined by repeating the procedure for calculating the free-flow speed, setting the *Depart At* parameter at a time suitable for the analyzed scenario. In the context of this research, we set the *Depart At* parameter of the API query to 07:00:00. The results are shown in Figure 14. The ratio of travel distance (estimated by using the detour factor regression) to travel time again gives the average travel speed.

3.3.5. Speed comparison

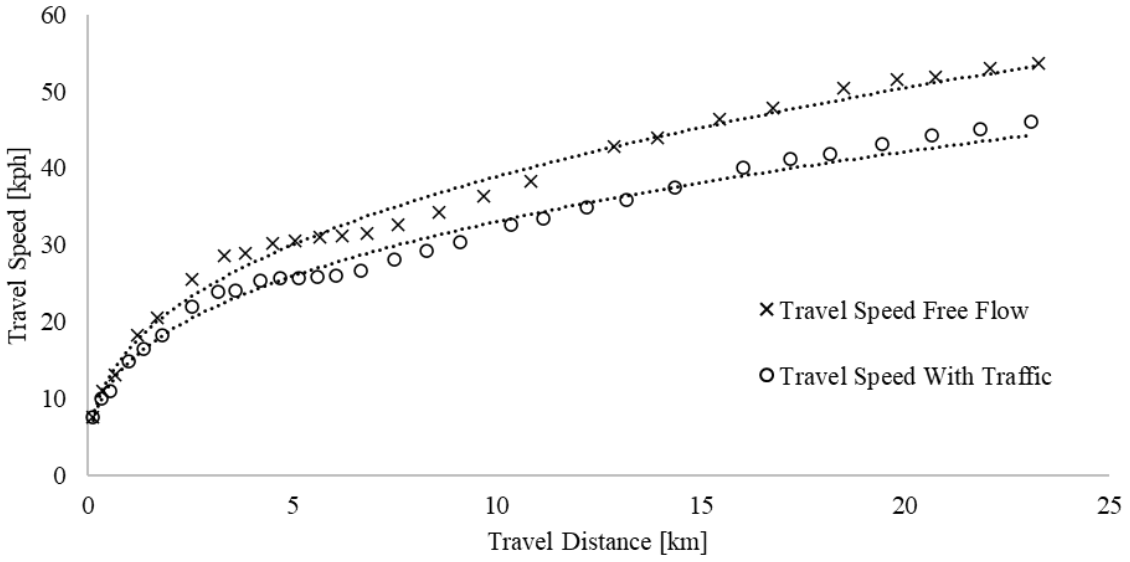

Figure 15 Speed profile comparison for Munich, Germany

To compare free flow and congested state more clearly, Figure 15 shows the average travel speed as a function of the travel distance for both states of the road network. By using a power regression model of the free flow and congested speeds, the speed difference can be determined continuously throughout the analyzed travel distance interval.

Both speed profile curves displayed in Figure 15 clearly show a degressive course. When reaching beyond the localized, urban space, both slopes approach a common value. The convergence of these curves can be explained as follows: As the travel distance increases, the traffic density usually decreases outside the inner-city boundaries and traffic volume considered with the API-calls corresponds more and more to the free flow state. The actual value that both graphs converge towards can be explained by referring to the route type, which is defined as fastest for all calls. This means that roads with the highest possible travel speed (usually motorways) are favored for the analysis. Consequently, the asymptote of the two speed graphs corresponds to the average speed at which the vehicle type defined in travel mode moves on motorways.

3.3.6. Area comparison

Travel times needed to reach an end point from a start point are the result of travel distance and travel speed of the specific route. To compare different areas, a combination of detour based on the street layout and delays based on traffic influences must be considered. This means that both the detour and traffic factor for different areas must be calculated based on a comparable variable. Since in practice, the determination of air distances with the help of the great circle formula is easy to implement and free of location specific influences, the air distance is chosen as the comparable variable. The goal of this area comparison is to derive a travel distance and travel time for free and congested state depending on the covered air distance. The travel distance on the one hand can already be determined by the air distance multiplied with the detour factor: $d_t = d_a \cdot df(d_a)$. On the other hand, the travel time is calculated as follows: $t_t = d_a \cdot df(d_a) \cdot v\ (d_a)$. The travel time comparison is shown in Figure 16.

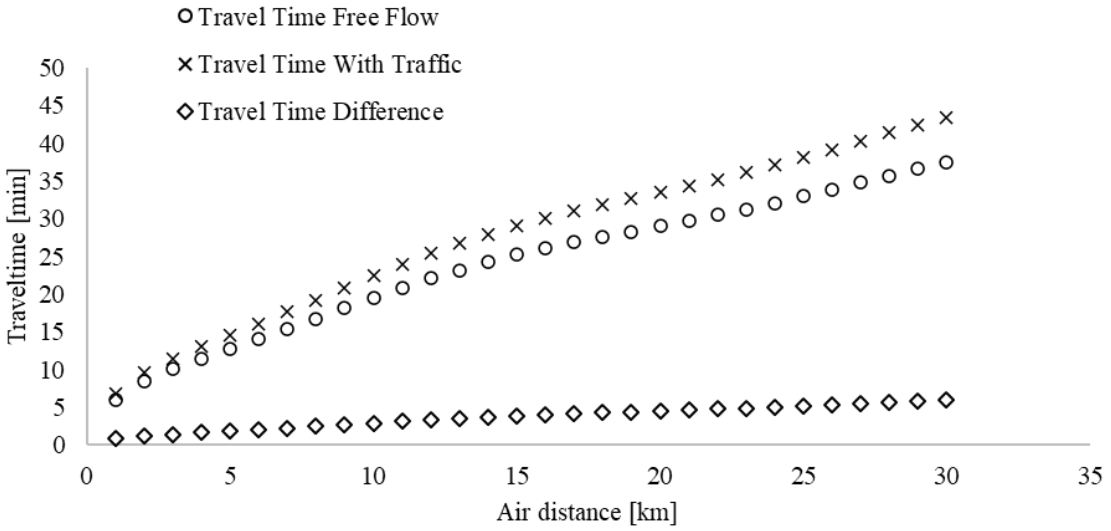

Figure 16 Travel time comparison for Munich, Germany

The combination of travel distance per air distance and travel time per air distance allows us to assess the considered area based on sustainability aspects. To show the applicability of our measures in the context of sustainability we analyze exemplary one sustainability dimension: The economical sustainability is measured by costs per air distance. Therefore we assume 0.7€ per kilometer driving costs, an hourly wage of 20.5€ as driver costs and 7.5€ per hour of vehicle occupation costs, which is in line with other literature [153]. Continuing, the costs per air distance kilometer for Munich are shown individually and in total in Figure 17.

All curves are degressive. The costs during free flow (dashed lines) are always slightly below the congested graphs, although they become more and more similar over time due to the aforementioned

reason of motorway access when the air distance increases. The relationship between driving costs and driver + vehicle occupation costs is particularly noteworthy. With increasing distance, the driver + vehicle occupation costs are dominated by the driving costs. In this example, the driving costs exceed the driver + vehicle occupation costs in free flow / in the congested state from 8 / 12 air kilometers. On average, the congested mode results in higher costs of about 12 cents per air distance kilometer compared to free flow, which corresponds to additional costs of about 6.7%.

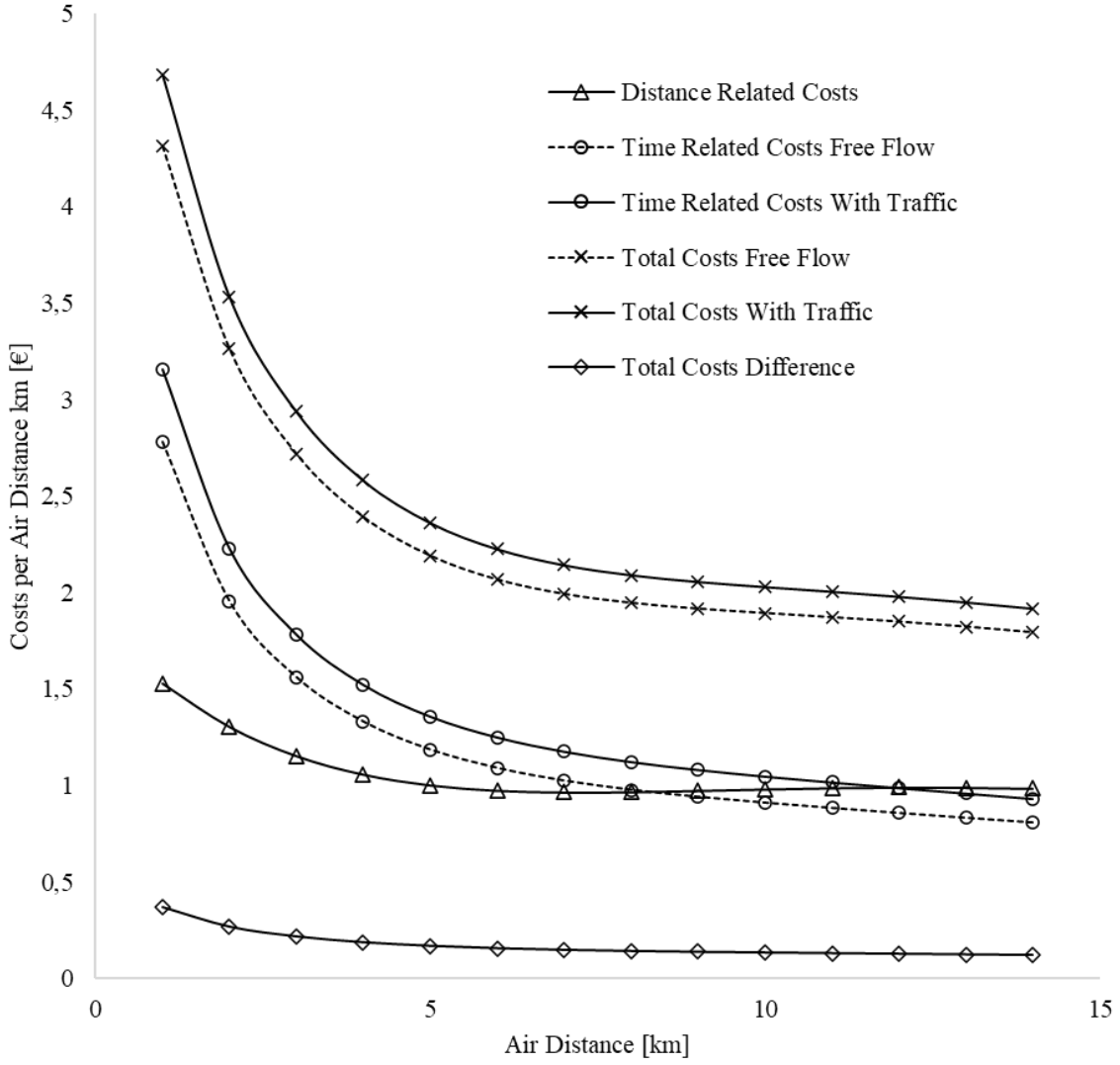

Figure 17 Costs per air distance for Munich, Germany

3.4. Case Study: Comparison of four German cities by detour, infrastructure and traffic congestion indices and their impact on road network performance

In order to compare four different cities, data on detour factor, travel speed and costs are determined in free flow and congested state for each city using the previously described methodology. The four selected cities are Berlin, Hamburg, Munich and Stuttgart as they are ranked among the top 6 German cities within the 2019 TomTom traffic index ranking. The central starting locations in Table 16, mainly based on existing depots by local transportation service providers, were used in this case study:

Table 16 Selected cities' starting locations

City	Latitude	Longitude	Street-Level Address
Berlin	52.519051	13.408583	Berliner Innenstadt, 10178 Berlin
Hamburg	53.551181	9.992416	Alter Wall, 20095 Hamburg
Munich	48.116363	11.556560	Schäftlarnstraße, 81371 Munich
Stuttgart	48.776248	9.180116	Dorotheenstraße, 70173 Stuttgart

In the following paragraphs, all results are plotted and interpreted. In the descriptions of the diagrams, the keyword "collected" indicates that the data shown is displayed as it has been retrieved and has not been smoothed or modified in any way. "Calculated" means that the data was estimated by regression and therefore smoothing can occur. The curves of the different cities are always marked identically to allow for easy comparison as shown in Figure 18:

Figure 18 General graph legend

3.4.1. Detour, Travel Time and Costs Charts

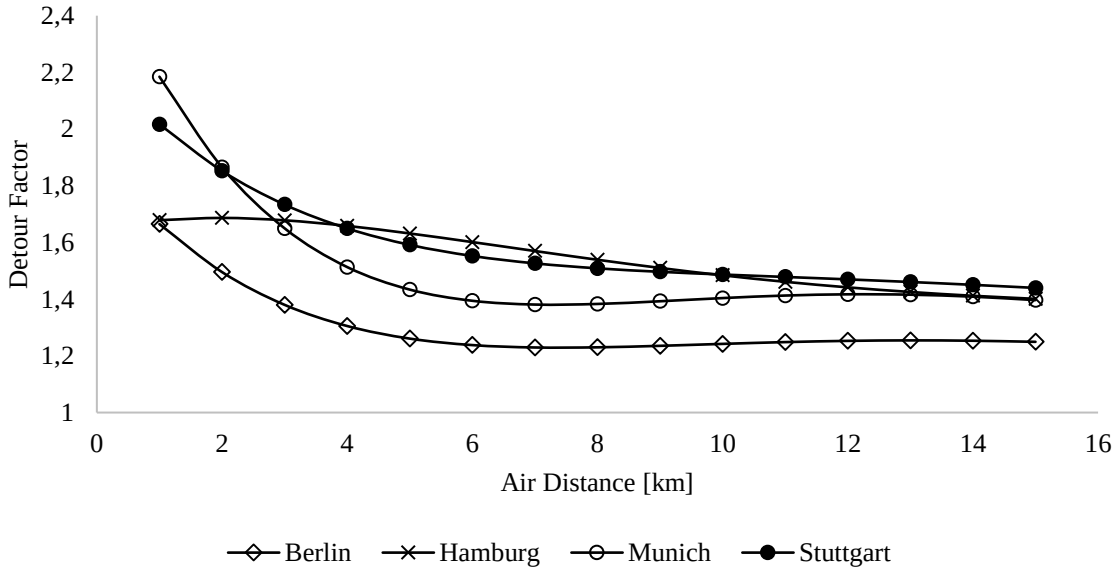

Figure 19 City comparison: Detour factors (collected)

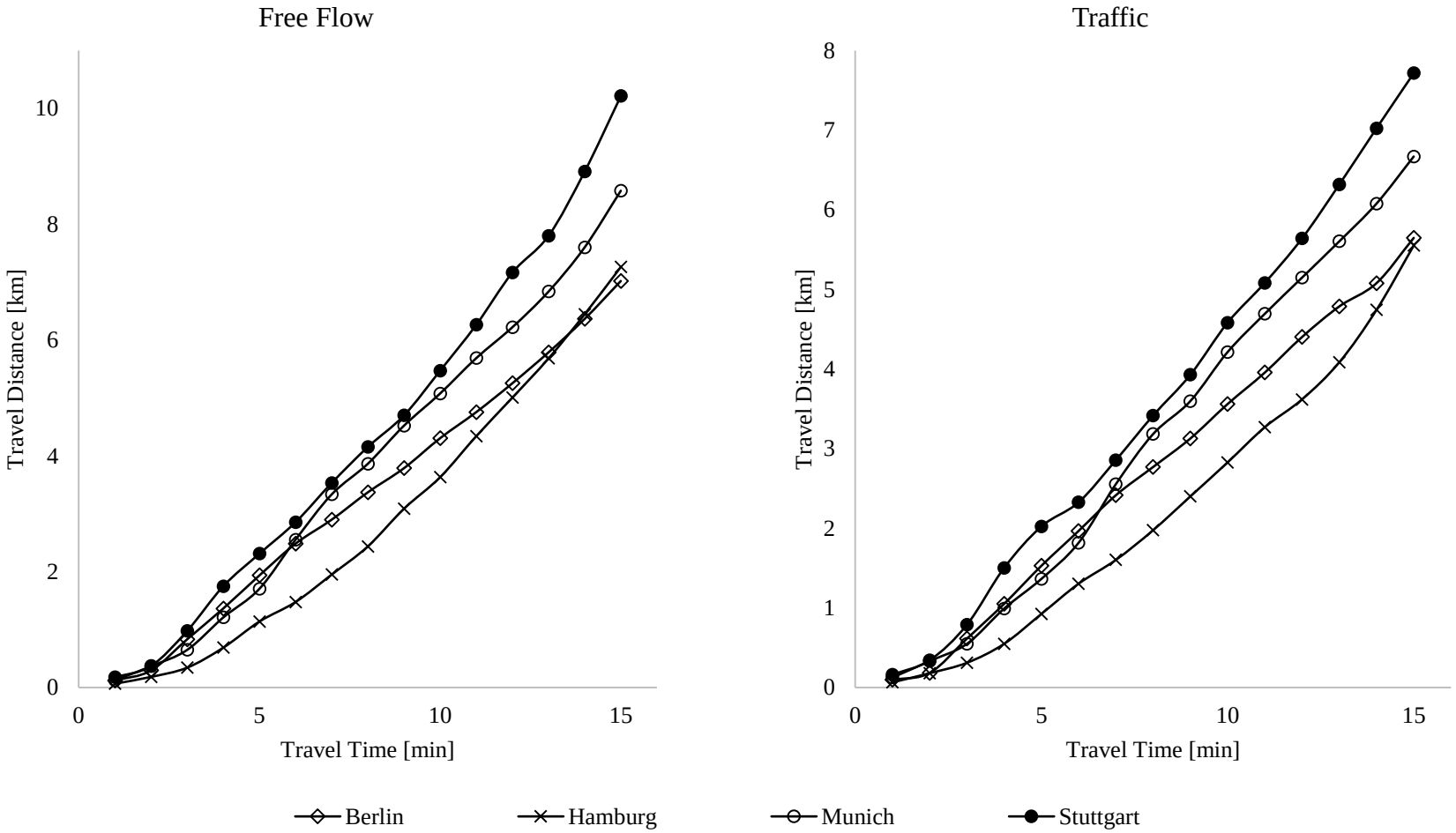

Figure 20 City comparison: Travel distances (collected)

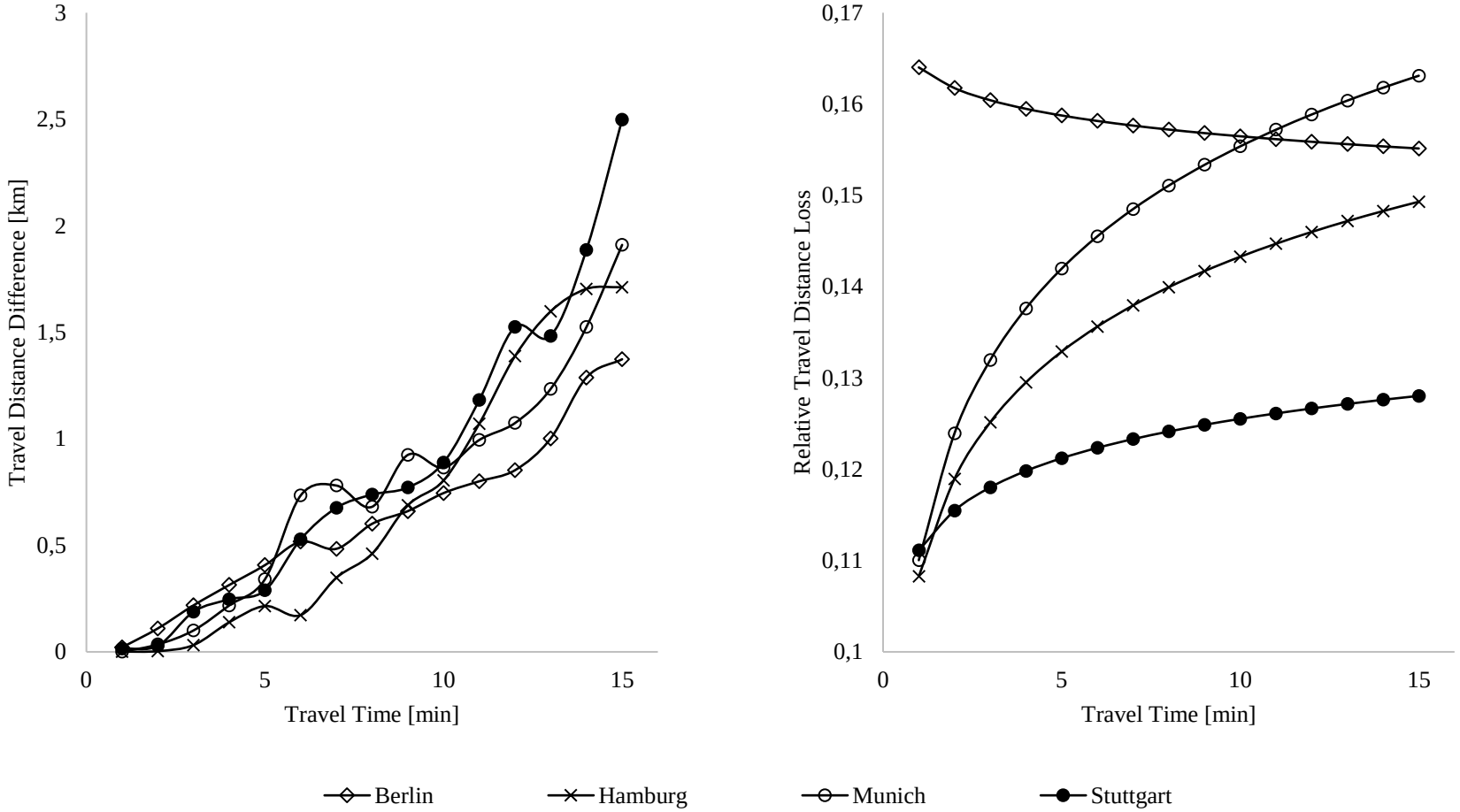

Figure 21 City comparison: Absolute travel distance difference (collected) and relative travel distance loss (calculated)

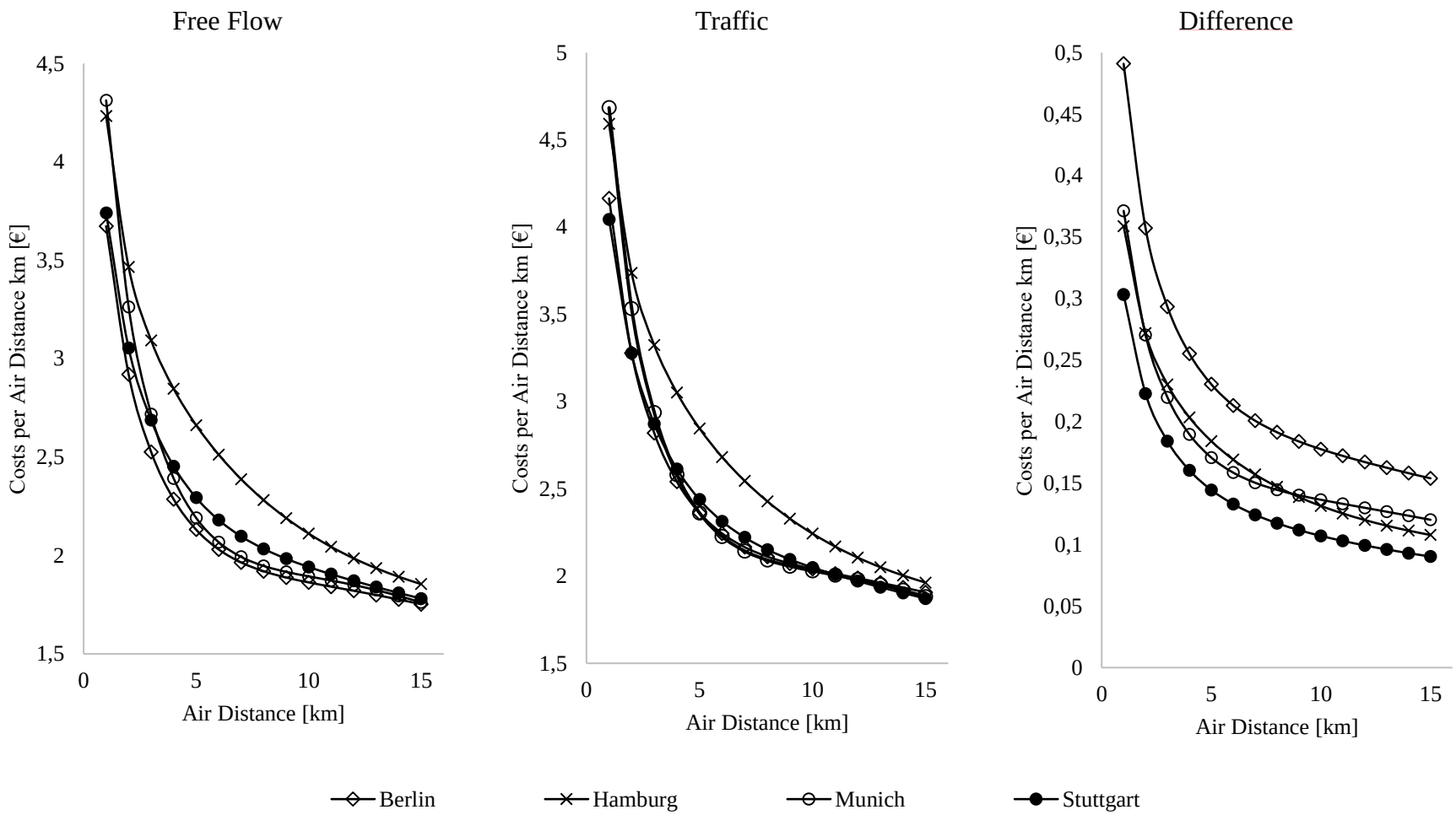

Figure 22 City comparison: Costs per air distance km (calculated)

3.4.2. Detour Factor

The detour factors in Figure 19 describe the interaction between air distance, street network density and straightforwardness of existing connections. By taking a closer look at the curves of the detour factors, it is noticeable that the detour factors of the three cities Hamburg, Munich and Stuttgart develop nearly identical starting at about 11 kilometers air distance and approach a value of 1.4. In addition, the course of the curve for Hamburg is noteworthy, as it is rather constant at the beginning in contrast to the other curves. This indicates a strong deviation from a road network made up from straight connections around the centralized starting point, which is the case in Hamburg due to the river Elbe and its many waterways inside the inner-city area. Only after exiting the inner-city area and gaining motorway access, the detour factor decreases as more direct connections become available. Lastly, Berlin's detour factor is consistently lower than all other detour factors, which indicates a well-developed road network.

3.4.3. Travel Times

The travel time curves provide information on how cities position in terms of infrastructure and congestion measurement. Four different charts are generated. The two charts in Figure 20 show the travel distance in relation to the travel time both in free flow and congested state. The next two charts in Figure 21 focus on travel distance loss: The left chart in Figure 21 shows the absolute difference between these curves. The right chart shows the relative loss of travel distance from free flow to congested status.

It is apparent that Stuttgart has the highest travel distances compared to the given travel times in both free flow and congested state. When looking at the relative loss curve for Stuttgart, we notice that it is relatively low compared to the other curves. This means that Stuttgart does not have a major congestion problem and the city has a very good infrastructure.

The counterexample to this is Hamburg. The speed of movement tends to be lowest in Hamburg in free flow and congested state. The relative loss curve for Hamburg is above average. This suggests a poor infrastructure, as the possible travel distances without traffic are already relatively low. The congested state in Hamburg can be classified as slightly above average in comparison.

The most congested cities are Munich and Berlin, with Berlin showing a relatively constant relative loss of around 16 percent (0.16) compared to free flow. Munich, on the other hand, is characterized by an increasing level of relative loss, which is approaching 17 percent (0.17).

Depending on the observation interval, Berlin (up to 10 minutes of travel time) or Munich (from 10 minutes of travel time) can be classified as the most congested city in the comparison at 07:00:00 departure time.

3.4.4. Transportation Costs

The economical sustainability of infrastructure, congestion and detour factor is reflected in total costs of transport. The cost rates from Chapter 3 were used for this calculation. The first two curves from left to right shown in Figure 22 represent costs per air distance kilometer for free flow and congested condition. The right curve in Figure 22 shows the cost difference between congested and free flow.

The costs per kilometer are highest in both free flow and congested conditions in Hamburg. This can be explained by the fact that Hamburg has an average detour factor, a poor infrastructure and a moderate traffic congestion level. Due to the average detour factor, the driving costs per air distance are also average, whereas the driver and vehicle occupation costs are far above average due to the low absolute speeds.

The graphs for Stuttgart in free flow and congested state are slightly above the curves of Munich and Berlin, which describe a comparable course. The absolute speeds are highest in Stuttgart, which

means that the higher costs can only be explained by the higher detour factor of Stuttgart. Stuttgart's detour curve is always above average and to a large extent the highest amongst all cities.

Munich and Berlin share the lowest costs per air distance kilometer. In Munich, the absolute speed is higher than in Berlin, both in free flow and congested state, with Berlin having a significantly lower detour factor. These two facts cancel each other out, resulting in both cities having an almost identical level of transport cost.

The cost difference curves allow conclusions to be drawn as to how much additional cost per air distance kilometer is incurred depending on the choice of departure time. In Berlin, different departure times cause the highest difference, Stuttgart the least and Hamburg and Munich show almost identical cost difference curves. In addition, the costs induced by congestion can vary between 0.07€ and 0.5€ per air distance kilometer, depending on the distance and city, which results in a considerable total cost difference for a high number of kilometers travelled.

3.4.5. City comparison

When approaching a comparison of two or more regions from a RNP standpoint it is essential to define the scope of comparison. As we can derive from the subsections above it is not enough to know detour/travel speeds to conclude a transport cost related order of different regions. To order regions within the context of RNP a clear perspective to interpret the data must be set. This perspective consists of the following three characteristics: (1) Performance indicator, (2) daytime and (3) air distance. To begin analyzing our four regions, one of the suggested (1) performance indicators must be chosen. This stems from the fact that analyzing only one regional performance indicator indicates high costs per kilometer but at the same time another performance indicator's values compensate the first one and lead to lower costs per kilometer as we would have expected. For example, Stuttgart has a high detour factor which - considered isolated - would lead to the expectation of high costs per kilometer. Stuttgart's high travel speeds in contrast lead to low travel times and therefore result in transportation costs per kilometer only slightly above average. Because of that, the interpretation of the level of different performance indicators must not be mixed up. Following that, a (2) daytime to compare regions must be set. This is of course necessary due the fact that the level of traffic congestion and thus congested speeds/costs in congested state are highly time dependent as shown in Figure 10. As the peak congestion times are slightly different for specific regions the decision must be made whether different regions are analyzed at different times or one daytime for all regions is set. Individual daytimes for every region would allow comparison of peak congestion states whereas an identical starting time for every region increases comparability in cases where departure times are fixed (e.g. due to business and delivery hours/time windows). Last aspect to take care of is the air distance (3). Performance indicator values are dependent on the travelled air distance. Therefore, specific air distance intervals or fixed air distance values should be set to ensure context specific analysis. To remotely compare regions without any knowledge about locations to be approached from the starting point, an average air distance of potential trips should be estimated. If precise information about locations to be approached is available, the distances between these locations and the starting point should be calculated and used for further analysis.

3.5. Discussion

The collection method presented in this paper assumes that the free flow condition in a traffic area occurs at midnight. This means that the time of departure influences the volume of traffic and thus the transportation costs incurred. To minimize these costs, the additional costs caused by the traffic volume must be included in scheduling algorithms. These are often offset by penalty costs for delayed deliveries. Scheduling algorithms should therefore not solely minimize the penalty costs but consider the addition of congestion costs and penalty costs.

As previously described in literature [250,269], free flow is characterized by an accepted delay. This means that even in free flow, the maximum speeds allowed will mostly not be reached. On the

one hand, this is due to a certain number of road users that are considered acceptable, on the other hand, parts of the infrastructure such as road conditions, traffic lights and traffic routing considerably influence the maximum speed any road user can be expected to reach. Traffic congestion therefore is not defined by a speed lower than the maximum speed, but as the excessive delay above an agreed upon norm.

So far in literature, little attention has been paid to the explanation of the detour factor, its determination and the investigation of its influencing factors. It has a direct influence on the cost per air distance kilometer. Driving costs are influenced because travel distance is dependent on the air distance and the detour factor. In addition, driver and vehicle occupation costs are influenced, since longer travel distances also increase travel times.

As shown in Chapter 3, the cost factors detour factor, infrastructure and traffic change with increasing air distance. This means that describing regions by using only a single value for detour, infrastructure and traffic would be very imprecise. Therefore, when considering the individual performance indicators, a progressive function should be modelled to ensure accuracy. In addition, when comparing different regions, observation intervals must always be defined (here 15min travel distance or 15km air distance) and kept constant across all observations, since the arrangement of the curves can change relative to one another for increasing distances.

The detour factor decreases with increasing air distance in urban areas. This means that the greater the air distance to be covered, the less detour is required. As previously explained, this stems mainly from the fact that motorways or inner-city highways which usually follow a comparably straight or direct course, can be accessed as air distances increase. Consequently, when calculating costs, transportation companies must take a closer look at short distances, as the costs per kilometer can be many times higher than for longer distances. These short distances occur mainly in distribution between customer locations.

The conducted studies show that the arrangement of the curves can differ considerably from detour, travel speed and cost per kilometer. The transportation costs per kilometer are always the product of the factors detour, free flow speed and delay by congestion. A consideration of individual cost drivers such as detour or traffic makes sense from certain interpretation points of view, but to estimate or even compare the transportation costs, an isolated consideration is not enough.

Chapter 4 shows that significant cost differences can arise between different geographical regions. As transport companies mostly charge prices for distribution regardless of the region, the contribution margin of a single shipment will vary between regions. It is therefore advantageous to carry out the analysis presented prior to choosing a location for a terminal or depot. This will allow managers to compare all available locations and make a final choice dependent on future transportation costs. In addition, single customer locations could be evaluated by selecting a customer's delivery address as the starting point for the analysis. The results obtained can be used to model or adjust customer-specific tariffs.

3.6. Limitations and further research

The results of our analysis are directly dependent on the choice of starting locations. This means that when comparing regions, care should be taken to ensure that the characteristics of the different starting locations are comparable. During the exemplary case study presented in this paper we have decided on terminals or depots of local transportation service providers. For a comparison that is not dependent on the distribution context, we recommend that the centrality of the location should be considered. Consequently, the most accessible and central point within the region to be investigated should be chosen. However, this is only a rule of thumb. Future research could focus even more intensively on the correct choice of starting location.

Large areas, where no passable infrastructure is available, can influence the result of the analyzes. All corner points of the retrieved polygons always form accessible points and are therefore

located directly on existing roads. In case of areas without (accessible) roads, the polygon points directly at the edge of the area and remains constant until a road can be reached. This distorts the result of the detour factor. In most cases, this leads to a higher detour factor since the points bordering the road free area produce small air distances in relation to the increasing API query's restriction. After overcoming the road free area by sufficiently large travel distances (=API restriction), the air distances which have been constant before increase dramatically and the error of the detour factor is corrected.

Currently, all polygon corner points are included in equal parts in the air distance's mean value calculation. However, if there are areas within the region to be investigated which are irrelevant for the analysis or which should not be considered, certain corner points could be excluded from the air distance calculation. The key points could also be weighted in relation to the customer locations. The modification of the point weights to individual business cases offers more room for further research.

The TomTom API always returns a polygon with a maximum of 50 corner points. This means that regardless of the size of the accessible area, a maximum of 50 accessible points relates to straight lines and this polygon is used for further evaluation. However, depending on the restrictions of the query, this number of points may be too low. 50 points are too few if the result of a query with high restrictions (e.g., 120 minutes of travel time) is retrieved. In this case many roads could be accessible, i.e., the polygon would have to show many more corner points. TomTom reduces this large number of accessible points to exactly 50 polygon points and thus distorts the average air distance. The methodology on when and especially how this reduction occurs is a black box as TomTom is not providing any details on the algorithm in use. A remedy could be the usage of the HERE Maps API, because the maximum number of corner points is unlimited for this service and grows with the number of reachable points. However, the quality of the traffic data currently does not allow the use of HERE's API. In the future, researchers could try to combine the two APIs, i.e., the accuracy of HERE's presentation and the accuracy of TomTom's traffic data.

To estimate the environmental impact of RNP our presented method can help to estimate pollution per air distance based on speed and detour. Therefore, we must combine our results with vehicle data such as power and fuel type. This information combined with speed values can be used as input variables to calculate energy consumption per kilometer via COPERT regression functions [270,271]. With the information derived by DIN Deutsches Institut für Normung e.V. [272] the energy consumption can easily be converted into pollution per driven kilometer. Based on aerial distance and the offset with detour factors travel distances can be derived. The combination of vehicle data, COPERT regressions, travel distance and speed leads to overall emissions produced by certain road users [273,274]. Following that, our method can be used to analyze the impact of the RNP on emissions of specific user groups and areas.

One impact of RNP on social urban sustainability can be expressed by road noise emissions. A widely used calculation model for road noise is CORTN [275] which was originally designed by the Great Britain Department of Transport [276] and adapted by different researchers for several regions like Tehran and the whole European Union [277,278]. Beside the travel speed measurements this model processes information like traffic flow and road characteristics which must be gathered from other resources. Combining all the needed information to implement the CORTN model our method can help to quantify the impact of RNP on urban social sustainability.

3.7. Conclusion

The contribution of this paper is an efficient methodology of programmatical data retrieval, supplementation and analysis for RNP measurements utilizing publicly available traffic information. We base our methodology on the scarcely researched reachable range concept. Reachable range APIs allow for time and resource-efficient retrieval of area-wide results by outsourcing data processing. Due to this, the problem of defining the sum of all relevant sinks can be overcome by defining a centralized starting location and analyzing the retrieved polygons encompassing all possible, by definition reachable, destinations within a road network.

We have quantified and shown that when examining the impact of road network performance on the economic dimension of sustainability, it is mandatory to consider two types of costs in tandem: distance based as well as time-based costs. These cost factors are driven by the specific network performance characteristics of detour and travel speed as presented in this paper. Evaluating any of these two factors in isolation, in example by referencing the publicly available TomTom Traffic Index Ranking, does therefore not allow for reliable inference of total costs and might lead to wrong business decisions.

Future studies could head into different directions. Considering our methodology, the accuracy can be increased by combining technology from different navigation service providers. Considering the three dimensions of sustainability, our methodology can be used to evaluate the RNP's environmental and social impacts on urban sustainability with the combination of the retrieved data and a framework like COPERT or CORTN.

4. Speed Limit Induced CO_2 Reduction on Motorways: Enhancing Discussion Transparency through Data Enrichment of Road Networks

4.1. Introduction

Greenhouse gas emissions, especially carbon dioxide emissions, are a significant driver of climate change [279]. Therefore, political discussions and ecological debates have focused on reducing CO_2 emissions to slow down the impact of man-made climate change for more than 25 years [280].

According to the European Environment Agency (EEA), the energy supply and transport sectors are main contributors to this problem by producing the largest amounts of CO_2 emissions. More specifically, one major factor is road transport, which accounted for 18% of European CO_2 emissions in 2018. Road transportation can generally be divided into the commercial and private transportation sectors. The European Commission stated that commercial road transportation accounts for about 38% of all CO_2 emissions produced via road transportation, whereas private road transportation represented by passenger vehicles contributes the remaining 62% of CO_2 emissions. Extensive literature can be found on the topic of dealing with the connection between the public road transport sector and greenhouse gas emission as well as potential actions to achieve certain reductions [271,281–287]. While examining the literature, two major proposals to reduce greenhouse gas emissions within the private road transport sector are identified: (1) a global change of fleet to electric vehicles powered by renewable energy sources instead of fossil fuels, as well as (2) the introduction of general speed limits to reduce higher amounts of emission produced at increased velocities.

The proposal of switching to electric vehicles has one significant disadvantage: It is considered a long-term strategy and therefore has no significant instant impact on CO_2 emissions [288]. Research on electric vehicle sales forecasting provides evidence that the first country to achieve a targeted market penetration of electric vehicles of 50% will be Norway by the year 2026. Germany is considered to reach the 50% mark of electric vehicle market penetration by 2032 [289]. This slow diffusion stems from two sub-problems: The first and rather obvious problem lies in the fact that people are required to swap their combustion engine vehicles for electric vehicles. In most cases, this means buying a new car. Buying a new car leads to an additional financial burden, which results in people not daring to take the step without need or necessity [290]. The financial burden can be lowered by governmental support in the form of subsidies or tax discounts [291]. In addition to that, the willingness to adopt this new technology is highly dependent on the available charging infrastructure, which must be improved to make using an electric vehicle over long distances a viable alternative [292,293]. Therefore, the problem of conversion time from conventional vehicles to electric vehicles is dependent on the life cycle of current conventional fleets, the financial support provided by the government and the willingness of consumers to adopt and accept this new technology. Secondly, a more severe problem inhibiting a short-term change of fleet is the required power supply to support large fleets of battery-powered vehicles. Electric vehicles do not rely on fossil fuels during operation, which results in reduced operating CO_2 emissions. Nonetheless, one key fact that is easily forgotten is the heavily increased CO_2 emission as a result of generating large amounts of electric energy via conventional means of power generation. Therefore, electric vehicles can realistically only help reduce road-transport-induced CO_2 emissions under the assumption that electricity output is generated in a decarbonized way [294,295]. Inspecting the G20 states, Brazil and Canada lead the comparison with shares over 70% of renewable power generation capacities. Indonesia, Republic of Korea and South Africa are considered negative examples with shares of renewable power generation capacities under 20%. Trailing far behind in terms of renewable power generation is Saudi Arabia with zero renewable power generation capacity [296]. Generating most of the electricity demand via renewable resources like wind and sunlight is part of most governmental and ecological plans but certainly is not the main contributor to power generation in many countries yet. Implementing and realizing these plans cannot be achieved overnight and therefore still impede a fleet-wide electrification [297]. Consequently,

politicians and researchers are looking for actions to reduce CO_2 emissions quickly. An action that is meant to instantly reduce CO_2 emissions is the introduction of speed limits on public streets.

To allow for a better understanding of the political debate in general, we take a closer look at the following question: How do speed limits affect CO_2 emissions? Speed limits directly influence and, in most cases, reduce the average velocity of motorized vehicles [298,299], even if not every driver can be expected to obey the restrictions [300]. Since the amount of energy required to move a conventional vehicle at a specific speed directly results in liters of fossil fuel burned, which in turn leads to carbon dioxide emissions, the total amount of pollution created by a vehicle is heavily correlated to the velocity it is moving at [273,301,302]. Therefore, in theory a restriction in maximum allowed speed significantly reduces the maximum amount of CO_2 produced on a per-kilometer basis. This correlation between speed limits and CO_2 reductions has been researched extensively [300,303–307].

Furthermore, a general speed limit can smooth out the velocity across network participants, leading, theoretically, to a smoothed traffic flow, which requires less braking and accelerating [308]. Since the amount of fuel burned during acceleration is much higher than during cruising speeds, this in turn results in less air pollution by CO_2 emissions [305,307] while also decreasing the likelihood of accidents caused by speeding within the traffic network as well as noise emissions [103,105,223].

As a result, one key argument that is heavily controversial within the German parliament and public opinion alike is the introduction of a general speed limit on the German autobahn. This stems from the fact that carbon dioxide emissions generally increase disproportionally above 120 kph and the German autobahn is one of the last motorway networks worldwide where it is legally allowed to drive at unrestricted speeds throughout large parts of the network. Studies cited in favor of speed reductions on urban streets as well as highways presented substantial savings in CO_2 emissions in the range of 5 to 30%, depending on the intensity of traffic congestion [306,307]. Additionally, the German Environment Agency (GEA) recently published a study to evaluate the consequences of a general speed limit on German motorways. According to this official study, the proposed reduction to a maximum velocity of 120 kph should result in yearly total CO_2 savings of 2.6 million tons. These savings assume that 55.5% of the entire motorway network flow is unrestricted and driving speeds along these unrestricted edges average at about 124.7 kph [309]. Critics question the validity of the proposed savings in terms of the assumptions made and the methodology used, since the official study partly relied on old data from 2010 as well as non-public information.

When reading the referenced study [310], three suggestions for improvement regarding the estimation of vehicle velocities stand out that should be considered and improved upon:

1. The study references data from nearly one decade ago to estimate an underlying distribution of vehicle velocities throughout the network. According to the study, additional data were gathered from 2010 to 2014 to measure velocity but this information has never received an update and could be outdated, since road conditions and construction sites have a significant impact on network velocity and could very well change within the span of 10 years. Therefore, more recent data should be included.
2. The aforementioned information was gathered via measuring points directly installed on individual motorway edges. However, the number of measuring points was very limited. In sequence for the years 2010 to 2014, the number of measuring points that were working as intended and generating data was 80, 102, 108, 114 and 116 points, respectively. Comparing the number of measuring stations to the total motorway network length of 25,665 km, one measuring point had to cover approximately 221 km. Due to this small coverage, relevance of the provided velocity estimations on a large scale is questionable and requires validation.
3. The last argument for an in-depth review of these velocity estimations is one concerning data transparency. The raw data basis as well as the presented estimations have never been published in detail, which inflicts doubts on the credibility of the used methodology and implementation.

Due to the shortcomings of the previously published study by the GEA as well as the general necessity to regularly update such assessments in a perpetually changing field of research [311], the following article aims to validate or disprove political and ecological statements transparently by using publicly available up-to-date data from providers such as OpenStreetMap and TomTom. Within our context, publicly available means the source of the information allows access to the information by anyone upon request. We aim to evaluate whether the actual driving speeds as measured by navigation devices throughout the entirety of the road network are as high as presented during previous selected studies based on historical averages. Based on this evaluation, we compute possible savings via the introduction of a speed limit into the network by referencing general emission curves for motorized passenger vehicles. The general research question to be answered via this methodology can therefore be formulated as follows:

How can road networks be enriched by publicly available real-world data to enable CO_2 emission calculations?

The remainder of this article is structured as follows: Section 2 describes and applies our methodology to generate representative and routable (road) networks from publicly available data. We begin by retrieving geographical street data via OpenStreetMap to build the network and continue by supplementing the network by means of static, official traffic count and traffic distribution data provided by the GEA. In addition to this static information, we reference and map historically averaged traffic flow information from the TomTom API onto our network to approximate network usage on a per-edge basis throughout any given day. Section 3 continues by outlining the calculations applied to this enhanced network to derive results in terms of CO_2 emission reductions achievable by introducing speed limits into the traffic network. Finally, Section 4 discusses the results of our calculations in comparison to the previously published study by the GEA, while Section 5 discusses our findings in relation to previous studies on dynamic traffic speed limits and road participant acceptance in different countries.

4.2. Generating Routable Networks from Publicly Available Data

4.2.1. Extracting Data from OSM

At its core, the methodology to be presented is based on a programmatic analysis of traffic networks. Within this context, a traffic network is defined as a combination of nodes and edges, while edges are defined as a direct link between a set of exactly two nodes. One key component of mapping traffic information onto network data structures is the assumption of directed connections. Therefore, two-way streets are defined by different nodes and edges for each individual direction. This fact plays a crucial role in our need to develop auxiliary functions to correctly map external data onto the right nodes and edges within our network.

Building such networks from scratch would require mapping any relevant street within the network as a connection of nodes and edges while also adding geospatial information to each data point. Due to the sheer size of a country-wide motorway network, this would require hours upon hours of manual and labor-intensive work. This is where open-data platforms like OpenStreetMap come into play. These platforms use crowdsourcing to keep information up to date and openly accessible. Especially for primary road networks, this approach results in a high coverage and accuracy [312,313].

Unsurprisingly, these data pools are used regularly by researchers and practitioners alike to extract detailed topological information. One such framework to create spatial networks from OSM data is the Python package OSMnx by Geoff Boeing [136]. By using this package, we extracted the relevant motorway network, in the example defined via bounding box and saved the network to disk as a GraphML file. This GraphML file not only contained information about nodes and edges, which, in their sum, define the network, but also included additional information from OSM such as, for

example, speed limits as enforced by traffic signs as well as the length in meters for any given edge throughout the network. Note, however, that this information is entirely crowdsourced and might therefore include errors or missing details if no OSM user has added a specific parameter to the platform yet. Nonetheless, this first step left us with a fully connected and routable road network that already contained most basic information. In our context, fully connected and routable describes the fact that the network topology enables the construction of routes from a source to a destination both defined by separate nodes via an uninterrupted path containing several edges. Since every node at least contains information about its geospatial location in the form of latitude–longitude coordinate pairs, we can already visualize the retrieved network as depicted in Figure 23.

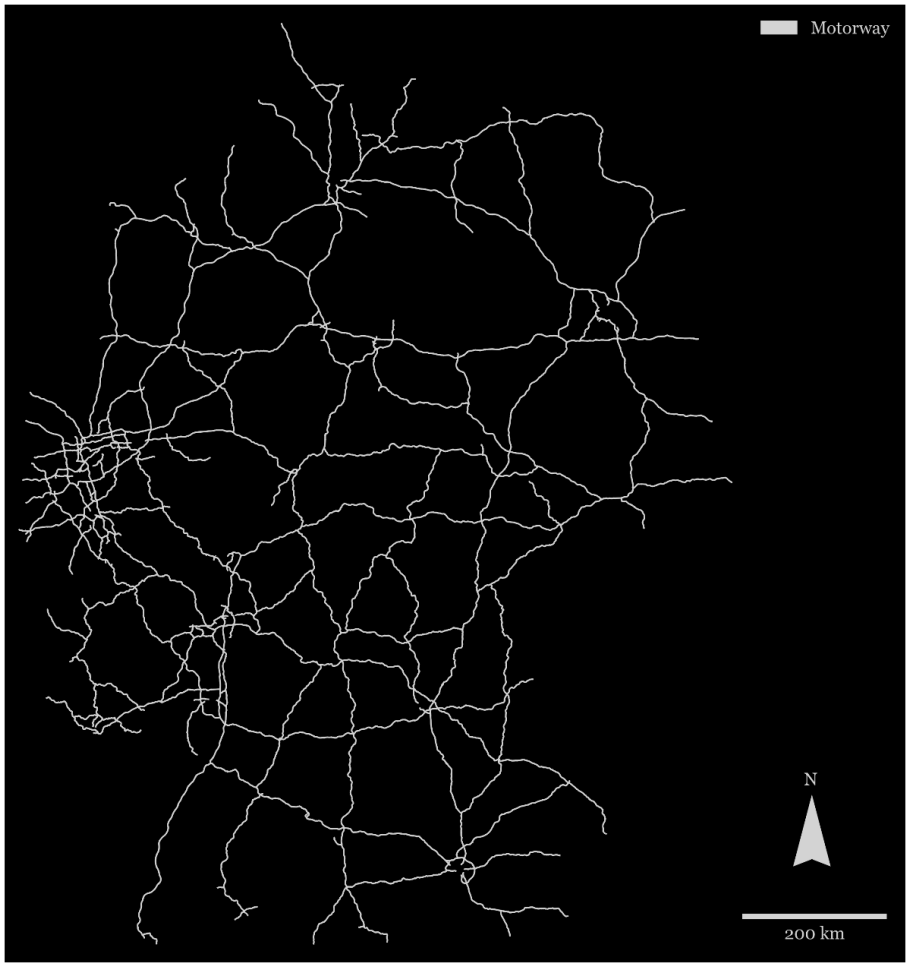

Figure 23 German motorway network defined by nodes and edges as retrieved from OpenStreetMap (OSM) using OSMnx.

4.2.2. Adding Official Traffic Count Data

We began enhancing the information density of the network by adding traffic count data to identify estimated total quantities of cars on a per-edge basis for any average day. In case of the German motorway network, the "Bundesanstalt für Straßenwesen" (BASt), a governmental institution, regularly measures traffic counts on German primary and secondary roads via a total of 1913 counting points. For application in different countries or regions, corresponding local data sources must be identified accordingly. Of these 1913 counting points throughout Germany, 1125 are located on motorways.

The most recent data available at the time of this writing were from the year 2018. Data was exported as a comma-separated values (.csv) file. It was then imported into the Python workspace

where the network resides. By using a getNearestNode function from the OSMnx package with a maximum cutoff radius of 5 km, we mapped the traffic count data (which include latitude/longitude coordinate pairs for every counting point) onto their respective nodes in the network. The contextually relevant information included in this data was comprised of

- the average daily quantity of cars measured by the counting point,
- as well as the average daily quantity of trucks measured by the counting point.

After successful mapping, these data were incorporated into the network and could be referenced as a data dictionary for every node's unique ID. Figure 24 depicts all nodes that now contained traffic data information in yellow.

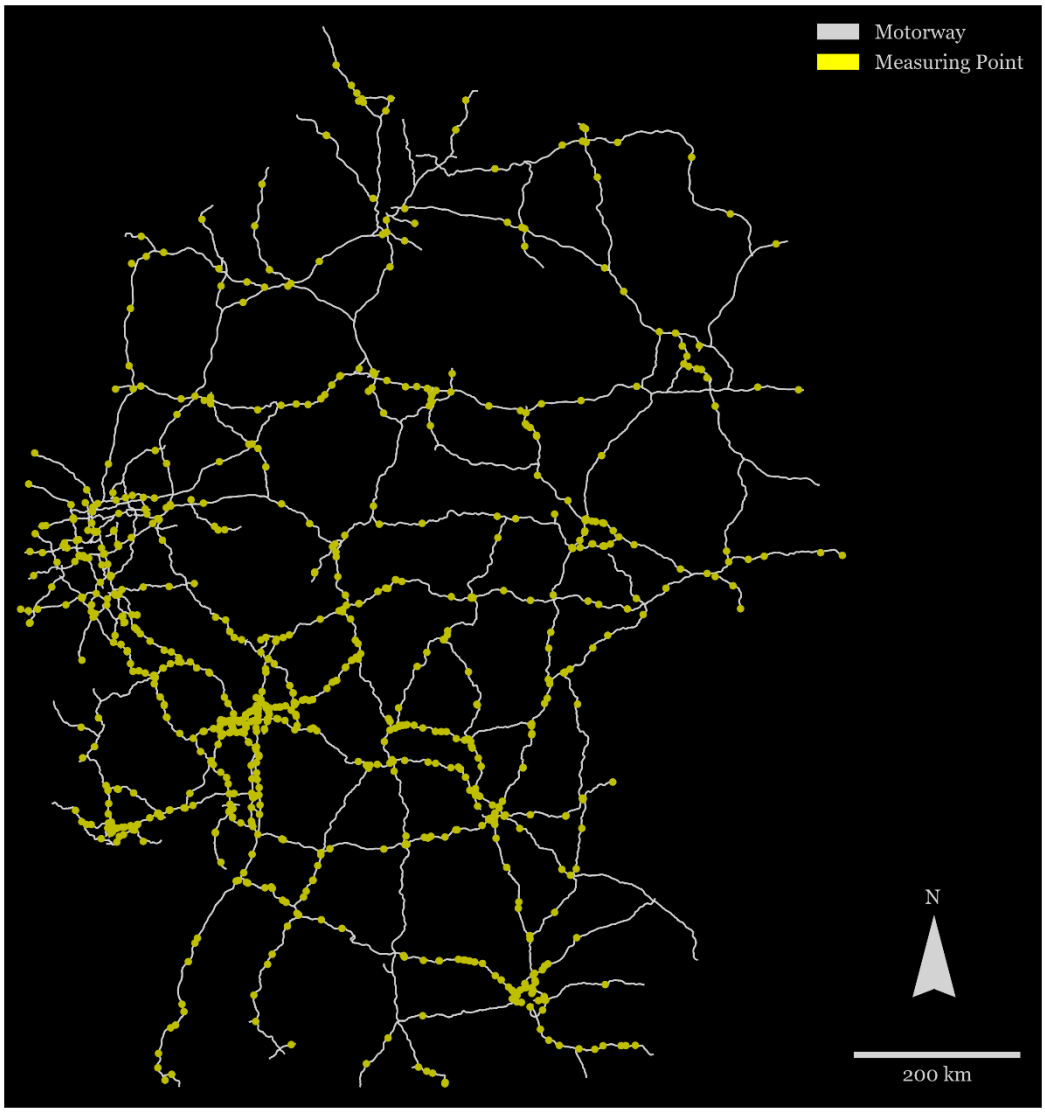

Figure 24 Depiction of traffic count data mapped onto the network. Yellow nodes contain traffic count data.

Since we only mapped data onto the individual closest node identified via getNearestNode, as can be seen in Figure 24, we needed to enrich all remaining nodes throughout our network as well. We achieved this by iterating over all nodes without data and identifying the closest node that contained traffic count data via great-circle distance. Therefore, all nodes around the individual nodes we mapped traffic count data onto were supplied with the same traffic count information. Since our analysis was mostly concerned with actual road sections instead of selective points, we needed to

derive a methodology to approximate the traffic count for every edge between two nodes. Throughout multiple iterations of this process, we found that a simple average calculation led to satisfactory and sensible results. Therefore, the formula to estimate the traffic count (TC) for any given edge E defined by one start- and endnode (n_1, n_2) inside the network is the simple average of both its adjacent nodes. By applying this logic to every edge in the network, we arrived at the first intermediate result of our methodology: A road network enriched by daily traffic count data.

$$\mathrm{TC}_{\mathrm{E(n1,n2)}} = \frac{1}{2}(\mathrm{TC}_{\mathrm{n1}} + \mathrm{TC}_{\mathrm{n2}}). \tag{15}$$

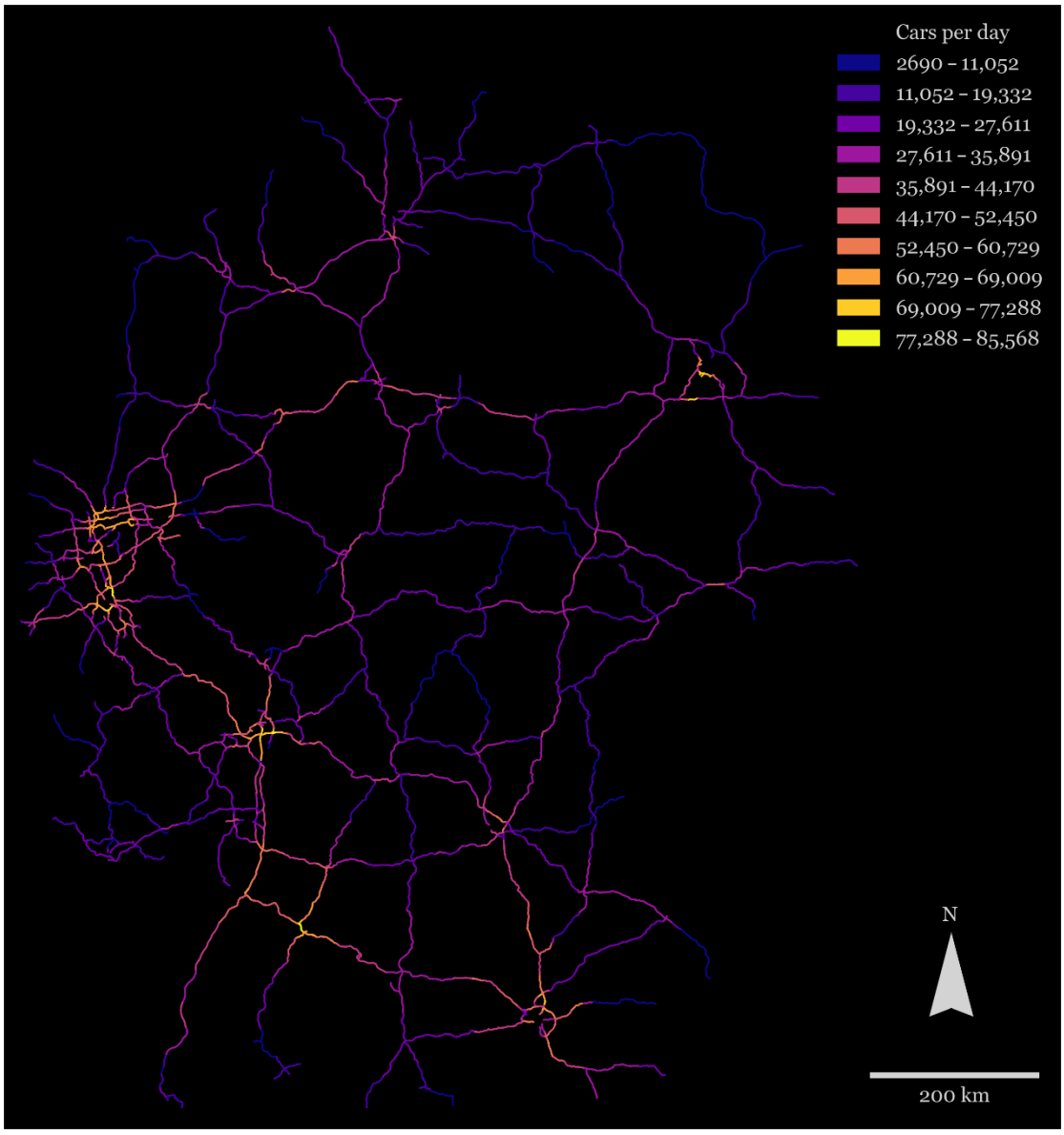

Figure 25 Visualization of traffic count within the network. Network edges are colored based on their daily quantity of cars. Brighter color corresponds to higher traffic count.

As can be seen in Figure 25, throughout Germany, certain areas showed a specifically high traffic count. The western area, mainly the state of North Rhine–Westphalia, as well as the areas around Frankfurt, Stuttgart, Berlin and Munich, depicted a higher-than-average traffic count, which was to be expected since these geographical areas are known socioeconomic conurbations and therefore are central traffic turnstiles throughout the German traffic landscape. Note, however, that by now, the

network only contained averaged daily traffic count information for every edge. To perform a thorough and time-specific case study, region-specific car distribution data on an hourly or even a 30-min interval basis needed to be added. Otherwise, all calculations performed within the network would need to be averaged for an entire day. This would require the assumption that traffic was evenly distributed throughout any given day, ignoring the existence of rush hours.

4.2.3. Adding Additional Traffic Distribution Information throughout the Day

To be able to divide the daily total traffic count per edge into 30-min intervals, a distribution function was derived using another set of officially published BASt data. This second data set is a more detailed version of the previously used traffic count data set and includes hourly data points for the same traffic counting points. We grouped this data by hour and extracted bidirectional traffic counts, derived the average hourly traffic count and used linear interpolation to approximate data for every half-hour mark. This results in the distribution shown in Figure 26.

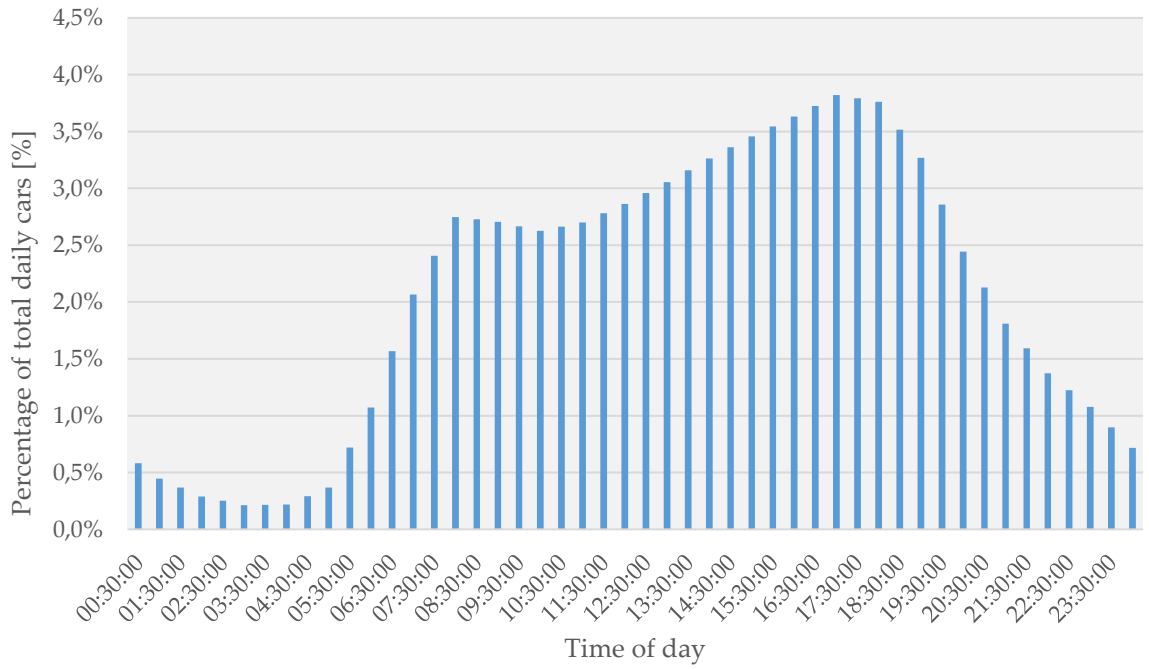

Figure 26 German motorway traffic distribution throughout the day. Two peaks can be identified, corresponding to daily commuting rush hours.

As expected, two major peaks were identified, corresponding to the daily commuting rush hours across the German motorway network. At 8:00 a.m., on average, 3% of the total daily number of vehicles were traveling along any given edge. Between 9:00 a.m. and 7:00 p.m., the average percentage of daily vehicles on edge varied between 2.5 and 4%, peaking in between 5:00 p.m. and 6:30 p.m. Between 11 p.m. and 4:00 a.m., only a marginal amount of daily traffic occurred on German motorways. This distribution later allowed for a more precise calculation of flow kilometers across edges for any given timestamp within the network. The total quantity of daily cars per edge (see Section 2.2 and Figure 25) was therefore multiplied by the average percentage from Figure 26. By applying this transformation, specific travel speeds could be weighted by the total sum of applicable flow kilometers. A detailed description of the flow kilometer calculation is given in Section 3.1.

In case no suitable, region-specific data set to estimate a daily traffic distribution is available, the distribution provided in Figure 26 can be used as a reference for countries with comparable size and similar official working hours.

4.2.4. Adding Real-World Traffic Flow Information to the Network

Continuing, the next part of our methodology was concerned with adding external real-world traffic flow information, in this case using the TomTom Routing Application Programming Interface (API) into the network. Real-world information refers to historical data gathered under practical circumstances, in this case via navigation devices. In comparison, the official (in this case mostly governmental) data sources used in previous studies by the GEA were mostly estimations from small-scale data samples or simulation based. Therefore, the accuracy of real-world data was considered significantly higher on a wide scale. Data that adhered to this definition could be retrieved programmatically by sending HTTP-compliant GET-requests to a remote API endpoint provided by TomTom. The endpoint allowed access to a database of navigation information supplemented by historical data gathered via personal and commercial navigation devices. Every route request, excluding free quotas provided to experiment with the API, required authentication and incurred a cost. To request and incorporate this data efficiently, we first needed to generate routes such that, at best, every edge included in the network was also included in at least one or more TomTom routing calls while minimizing the total number of routes required.

4.2.4.1. Generating Network Routes Requestable via TomTom Routing API

A TomTom route is defined by a single source and destination coordinate pair. In between these two points, up to 148 points along the route can be inserted. By trial and error, we devised a five-step process to generate a list of 958 routes in total, which resulted in a network coverage of 98.79% of all relevant motorway nodes. These five steps can be summarized as follows:

1. Identify all motorway endpoints by filtering for network nodes with only one adjacent motorway edge.
2. For every node identified in such a way (destination), apply the Dijkstra algorithm to calculate the shortest path from the network's central node (source) identified via degree centrality. The result is a sequence of nodes comprising the shortest path.
3. Since the network is defined as a directed graph, Step 1 only handled one direction. Therefore, apply the same logic from Step 1 in reverse to all endpoints that have not yet been found in any route from Step 1.
4. For every remaining endnode, calculate the shortest path from the endnode (source) to the central node (destination).
5. After applying Steps 1 and 2, a total of 3630 nodes (out of 13,763 network nodes) were still not included in any path, since these nodes did not lie on any shortest path to or from the previously identified network endpoints in combination with the central node. To handle these nodes as well, we derived the following logic: Select new start- and endpoints within all remaining nodes by identifying nodes that border on exactly one node already included in paths from Steps 1 and 2. For every start- and endnode pairing identified this way, once again create the shortest paths using the Dijkstra algorithm. Figure 27 depicts the different stages of route coverage described above.

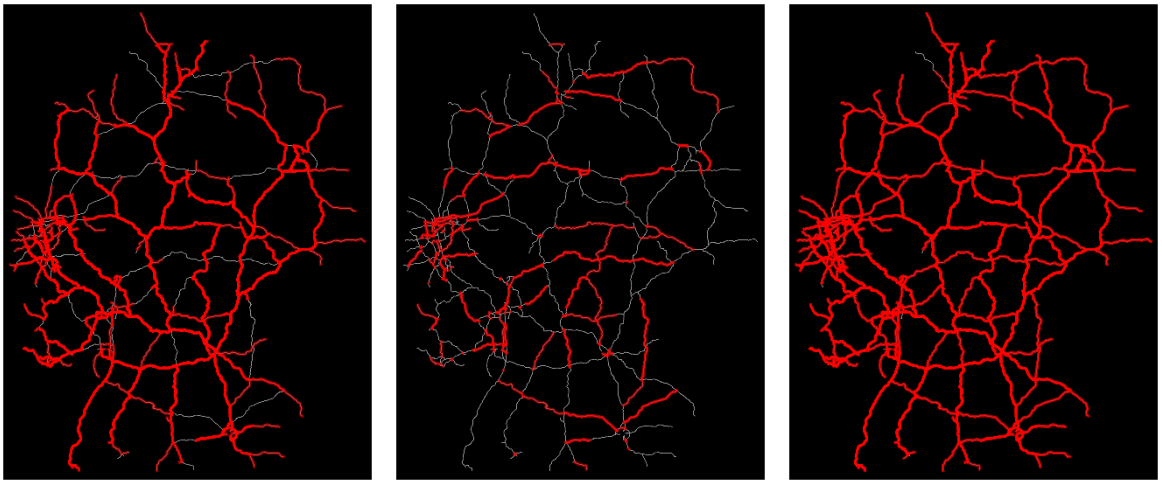

(a) (b) (c)

Figure 27 Different stages of network coverage after Steps 2 (a), 4 (b) and 5 (c). The rightmost image depicts the final network coverage. Road sections highlighted in red are traversed by at least one route request.

As a next step, all 958 routes needed to be converted to a suitable format to use with the TomTom Routing API. In its most basic form, the API requires a route as a colon-delimited list of successive coordinate pairs. We therefore retrieved the latitude and longitude attribute for every node along a route and added them together as a text string in the format.

$$routeString_{1\ to\ n} = lat_1 : lon_1; lat_2 : lon_2; \ldots; lat_n : lon_n. \quad (16)$$

Since the maximum number of points contained within any given TomTom route is restricted to 150, we only added one coordinate pair for every motorway exit along the route, since these exit nodes were the only possible change in direction on a motorway. In case a route contained more than 150 individual points, we divided the full route into individual slices, resulting in multiple API calls for full route coverage. An additional restriction was added in the form of a minimum aerial distance of 100 m between consecutive coordinate pairs. This was incorporated to compensate for slight discrepancies between our network coordinates and TomTom's routing network, which in the case of high-granularity routing led to mismatches and unwanted detours. The resulting list of routes comprised of coordinate pairings as specified and required for use with the TomTom Routing API was then saved to disk as a .csv file.

4.2.4.2. Mapping TomTom Routing API Data onto the Network

Using the comma-separated values file created during the previous paragraph, a total of 45,984 API requests were necessary to retrieve all relevant data via the Routing API. The total amount was comprised of 958 requests per individual pass. One pass equaled the request of all routes throughout the network for a single timestamp on any future date, in this case, a future Monday. Requesting a future date led to the calculation of historical averages by TomTom. We observed a timeframe from 0:00 a.m. to 11:30 p.m. in 30-min intervals, leading to 48 separate API passes. One important parameter that must be set is the *sectionType = motorway* parameter. Using this optional parameter, the TomTom response included additional information describing which of the return legs, corresponding to network edges, lay on the motorway network. This was necessary because, as previously mentioned, the TomTom routing network marginally deviates from the underlying OSM network data. In some cases, this led to TomTom mapping the provided coordinate pairs slightly off to the side of

any actual motorway, resulting in high deviations of route length caused by significant detours to navigate to the next freeway ramp and get back on route. Since we did not want to map any of these detours onto our network, we eliminated this problem by using the *sectionType* parameter.

The result for any individual API call was saved to disk as a JSON file. Every JSON response file contained multiple trip legs. Every leg contained multiple successive coordinate points. Additionally, every leg contained information such as length of the leg in meters, travel time in seconds required to fully traverse the leg, the associated travel speed in kilometers per hour as well as historically averaged counterparts and information about traffic-induced delays. All of these details remained to be incorporated into the local OSM network. To do this, we derived the following logic, which was applied to every response file:

1. Iterate through all legs within the response file;
2. Check if the entirety of points inside a leg are included in a motorway section (meaning the leg is entirely located on a motorway and therefore relevant);
3. If true, calculate the shortest paths from start- to endpoint of the leg within the OSM network, resulting in a list of network nodes along the TomTom leg;
4. If leg length and corresponding OSM network path length deviate by less than 10%, a correct mapping is found;
5. Therefore, iterate across all edges of this path and update the edge attributes with TomTom leg traffic flow information.

By running this logic, we created a data dictionary for every edge contained in the OSM network with a single index for every timestamp during which the edge was traversed by the API response data. This allowed for indexing by specific timestamps and retrieving the average travel speed for any given edge for a specific time of the day.

In total, this methodology reached a traffic flow information coverage across the OSM network of 81.5% of all edges.

4.2.5. Translating Average Speed into Estimated Actual Speed

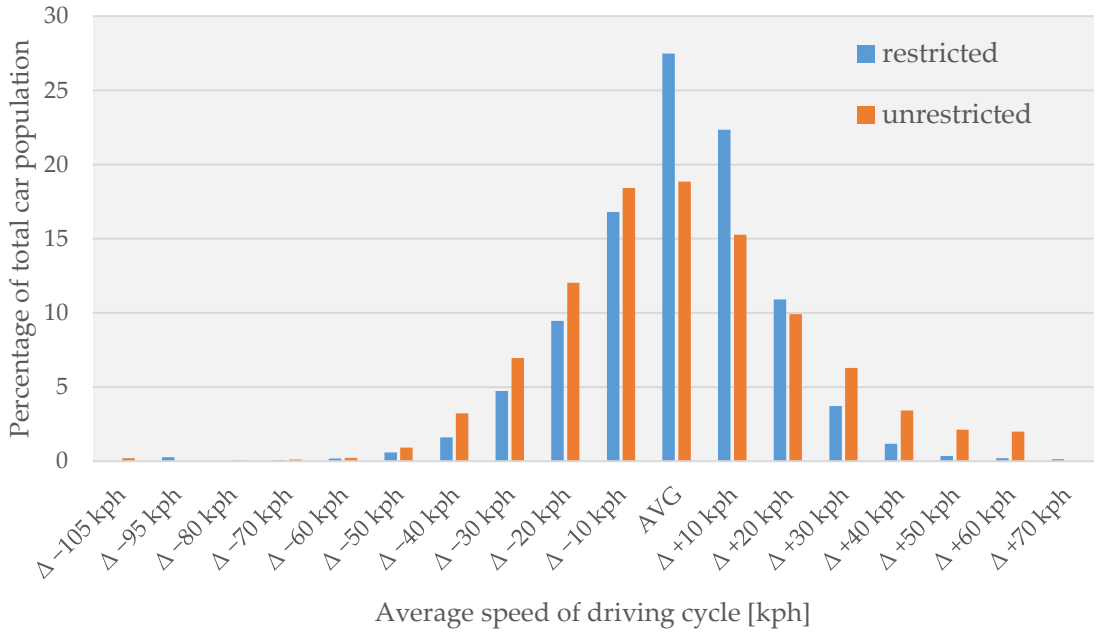

Figure 28 Averaged speed distribution for restricted (as in derived from sections with a legally allowed maximum speed of 130 kph) and unrestricted network state, according to the German Environment Agency.

Up to this point, all calculations were based on a single average travel speed for any given edge at a specified time *t*. Gathering reliable data on travel speed distributions for motorway networks is a laborious task and is, to the best of our knowledge, only undertaken by governmental organizations in small sample sizes. To adjust our calculations, we therefore needed to rely on individually published excerpts of a non-public data set by the GEA. Depicted in Figure 28 is an averaged version of the original speed distribution according to the GEA. By applying this speed distribution to the historically averaged travel speeds returned by TomTom, a more realistic indication of network speeds on any given edge was estimated.

4.3. Case Study: Calculating CO_2 Emissions

The methodology provided in the previous section can be applied to any region that can be defined either via a geographical bounding box or a unique literal identifier like "Bavaria, Germany" to create a programmatically analyzable traffic network as long as general traffic information, OSM and TomTom data are available. The types of analyzes possible are predefined solely by the type of additional data that can be gathered. For this case study, we focused on CO_2 emission calculations, but the necessary steps can easily be modified to include traffic-induced noise emissions or similar data as well.

4.3.1. Establishing General Key Parameters for CO_2 Calculations

According to the DIN EN 16258:2013-03 norm, every Megajoule of petroleum burned produces 75.2 g of CO_2 equivalents (CO_2e), while one Megajoule of diesel leads to 71.0 g of CO_2e emissions [272]. According to the European Automobile Manufacturers Association, one liter of diesel fuel has an energy density of 36.9 Megajoule, while one liter of petroleum has an energy density of 33.7 Megajoule. Therefore, both engine types produce roughly the same amount of CO_2e emission on a per-kilometer basis, depending on the exact composition of the fuel and drivetrain efficiency. Due to this fact, the different fuel types were not analyzed separately.

To quantify the total amount of possible CO_2 savings resulting from the introduction of a speed limit, it was necessary to compute the total emissions by any given vehicle in relation to its velocity. As a basis for this calculation, we concurred with the recommendation of the German Environment Agency by referencing adjusted driving cycles provided by the Handbook Emission Factors for Road Transport (HBEFA). For all driving cycles, CO_2 emissions on a per-kilometer basis were calculated using the Passenger Car and Heavy-Duty Emission Model (PHEM). For this model, modern Euro-6 passenger vehicles were used as a baseline. Euro-6 vehicles have a nearly identical fleet average of CO_2 emissions in day-to-day usage compared to older vehicles adhering to previous Euro-3 to Euro-5 norms [309]. Since more than 90% of registered vehicles in Germany adhered to at least Euro-3 standard and newer, we considered PHEM as representative and generally applicable for this analysis. Since most emission models, PHEM included, are only defined for velocities up to 130 kph, the GEA provides unpublished "further driving cycles" up to 190 kph inside their study, which we could neither validate nor disprove but adhered to for comparability between both studies. Figure 29 depicts the final regression model used to estimate CO_2 emissions by means of averaged travel speeds.

Applying this regression to all edges within the network resulted in the total amount of CO_2 g emitted on any average Monday throughout the German motorway network. Unfortunately, this result only held true under the previous assumption that all traffic is evenly distributed across the day. It was therefore prone to error because travel speeds as well as traffic delays vary throughout the day, as can be measured by inspecting the specific attributes across edges throughout the day. Given the fact that during a possible morning rush hour, the travel speed on a specific edge is much lower than during the rest of the day, this should be weighted accordingly by also including the percentage of daily cars that need to traverse the edge at this specific time of the day into the calculation (see Section 2.3).

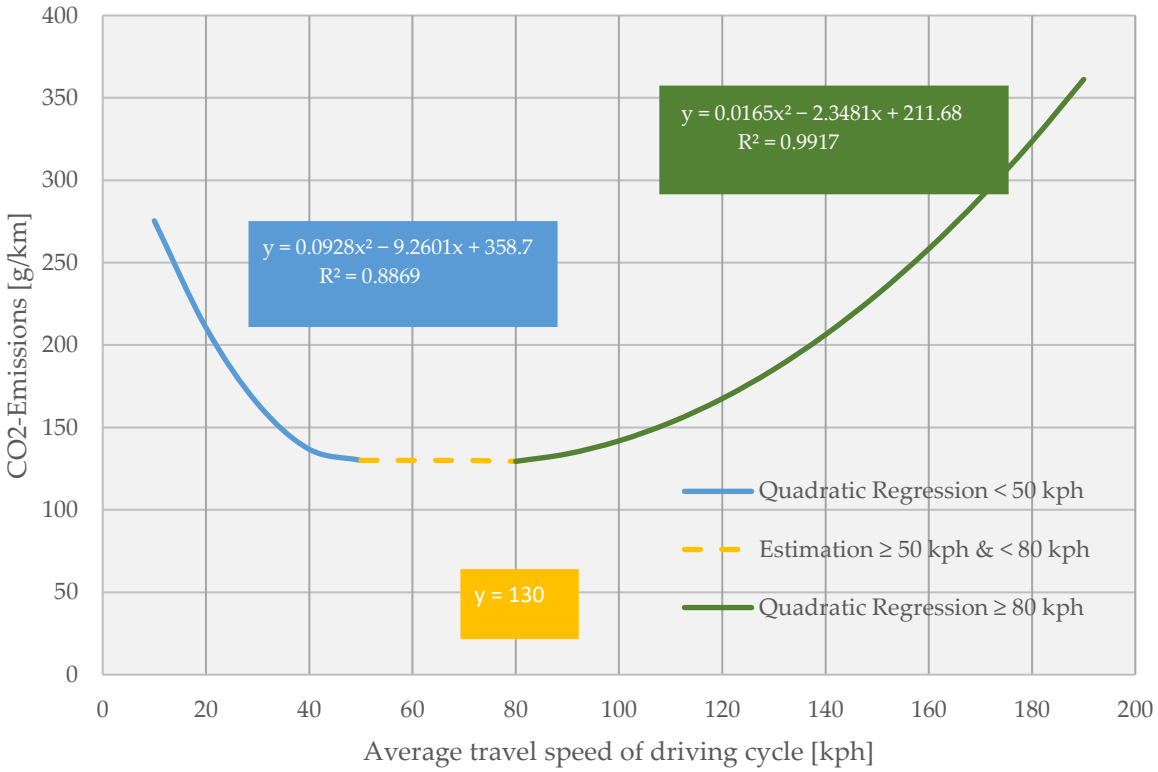

Figure 29 Threefold regression model based on Handbook Emission Factors for Road Transport (HBEFA) and Passenger Car and Heavy-Duty Emission Model (PHEM), according to the German Environment Agency.

The measurement of kilometers travelled along an edge multiplied by the number of total applicable cars at any specific time t was therefore defined as the edge flow kilometers of any edge at time t. Due to this, the total edge flow kilometers (TEFK) of any edge can be calculated via the formula

$$TEFK = \sum_{t=1}^{48} \frac{edge\ \ length\ \ [m]}{1000} * (Percentage\ \ of\ \ daily\ \ cars(t) * TC_E) \quad (17)$$

which enables weighting of time-specific edge calculations based on their proportion of total edge flow kilometers. All following calculations and results depicted were based on these weighted flow kilometers.

4.3.2. Applying Speed Limits to the Network

Introducing a speed limit into the network was as simple as defining a cutoff-threshold that was applied at time of calculation. During unrestricted state, every network edge contained several average travel speeds—one value per timestamp. By defining an exemplary threshold of 120 kph, we simply cut off any average travel speeds above 120 kph on a per-unrestricted-edge basis. Any edge with a speed below the threshold remained unchanged while sections above the threshold were limited to the threshold when included in any calculation. This simplified introduction of a speed limit could therefore be compared to the introduction of legally binding, static traffic signs on the motorway network. As depicted in Figure 28, not all network participants could be expected to implicitly

comply with the legal restrictions. Therefore, we additionally applied the speed distribution in restricted state (see Figure 28, depicted in blue) to arrive at a more realistic speed distribution for any given edge at specified time *t*. A thorough discussion of the results achieved by introducing different speed thresholds into the network can be found in the upcoming section.

4.4. Results

In this section, we examine the results presented by the German Environment Agency within the official study and compare these results to calculations derived directly via the network.

4.4.1. Network Benchmark

We began by comparing basic statements concerning the general motorway infrastructure, its state of restriction and general usage-patterns to establish a baseline similarity between both the official study and our programmatical analysis. The results of this comparison are shown in Table 17.

Table 17 Benchmark between general motorway infrastructure according to the German Environment Agency (GEA) and proposed methodology for network analysis.

Speed Limit [kph]	Ø Travel Speed GEA [kph]	Affected Flow GEA [%]	Ø Travel Speed Network Analysis [kph]	Affected Flow Network Analysis [%]
100	103.3	10.95	102.9	8.38
120	115.6	17.17	114.24	25
130	118.3	7.4	118.82	8.8
Unrestricted	124.7	55.5	126.77	53.5
Network-wide	116.5	-	119.37	-

According to the GEA, 55.5% of the German motorway flow across the network currently has no permanent speed restriction (e.g., static traffic signs) in place. In cases of no speed restriction, hereby defined as "open" sections, the average travel speed across network participants is measured at 124.7 kph. A total of 10.95% of network flow is permanently restricted to 100 kph with a measured average travel speed of 103.3 kph. The largest part of the restricted network flow is statically restricted to 120 kph with an average travel speed slightly below the allowed maximum speed at 115.6 kph. Another 7.4% of network flow is presented as currently restricted to 130 kph with an average travel speed of 118.3 kph. The remaining 8.9% of network flow belongs to speed categories below 100 kph, as is the case with inner-city motorways or permanent construction sites. On average, travel speed across all network flow is 116.5 kph, according to the GEA.

By retrieving the same statistics programmatically via the motorway network, we arrived at comparable results for speed restrictions of 100 kph, 130 kph and for non-restricted traffic flow with 8.38% and 102.9 kph, 8.8% and 118.82 kph as well as 53.5% and 126.77 kph, respectively. In the case of network flow permanently restricted to 120 km, our results differed significantly from the official study. The network analysis resulted in 25% of flow kilometers that were currently restricted to 120 kph instead of the previously cited 17.2%. In terms of average speed on these sections, the results converged again with the network analysis, resulting in 114.24 kph compared to 115.6 kph. This difference was most likely caused by including versus omitting dynamic traffic signs during the analysis. While we have no specific information on how dynamic traffic signs were handled by the GEA, our network defaulted to assuming an average restriction of 120 kph. Across all flow kilometers, the network calculated an average travel speed of 119.37 kph.

4.4.2. Theoretical Versus Practical Speed Restrictions

By definition, a restriction only occurs if the historically averaged travel speed is higher than the threshold at which the speed limit would occur. This means that it is entirely possible that even though a particular section of the motorway network legally allows for a maximum speed of 130 kph, meaning that it would in theory be restricted by a speed threshold of 120 kph, in reality the historically achieved travel speed averages at about 118 kph. What this in turn means is that even though on first glance, a road previously limited to 130 kph might be restricted by a general speed limit, in reality most network participants on this road section are never able to reach travel speeds above the speed limit throughout most of the day, meaning the restriction would not affect them at all but would also not contribute to any CO_2 savings resulting from a general speed limit. While critics of general speed restrictions base their argumentation of heavy incursions on personal freedom on the first aspect of currently allowed maximum speed limits, the more relevant aspect in terms of CO_2 reductions is the analysis of practical, real-world facts as recorded by navigation devices.

Putting these claims to the test by adding the previously retrieved historical traffic details from TomTom into the equation, our network analysis revealed that only 7.19% of all flow kilometers allow for high-speed driving. High-speed driving is defined as the circumstance that a road section is currently not restricted by any traffic signs ("unrestricted" or "open") and has no traffic-induced delays, for example, caused by traffic jams or construction sites. Comparing this 7.19% of *practically* "unlimited" flow kilometers according to real-world TomTom data (where it is indeed possible to achieve high speeds in day-to-day driving) to the previously described 53.5% of *theoretically* unrestricted flow according to traffic signs, a major gap between theory and practice became obvious.

Additionally, a total of 65.61% of all flow kilometers on average do not reach their legally allowed travel speed (according to traffic signs) due to general traffic volume as well as traffic jams. To put it simply, most motorway sections operate at suboptimal performance due to traffic delays induced by too many network participants simultaneously claiming usage of the same finite infrastructure. Additionally, another 1.61% of all flow kilometers operate below their legally allowed speed limits without any traffic-induced delays at all. On the other hand, for 22.5% of flow kilometers, the average daily travel speed exceeds the legally allowed speed limit, leading to illegal speeding on certain motorway sections. It therefore appears that major reductions in CO_2 emissions can already be achieved by enforcing current speed limitations more strictly.

Referencing the speed limit of 120 kph as proposed by the GEA, the introduction of such a general speed limit across the entire network would restrict 50.74% of practical flow kilometers, leading to a decrease in average speed of 4.1 kph or 2.94% compared to the status quo.

4.4.3. Analysis of Possible CO_2 Reductions by Inducing Speed Limits

Now that we have established that a general speed limit of 120 kph across all German motorways would restrict 50.74% of total daily flow kilometers based on real-world traffic data, the question remains as to what proportions of CO_2 emission savings would result from such measures.

During the second major part of the analysis, we identified potential emission savings on a per-edge basis by calculating the total CO_2 emissions with and without a speed limit threshold in place. To achieve this, we calculated CO_2 emissions by inserting the historical travel speeds as measured by TomTom, adjusted by applying the travel speed distribution previously depicted in Figure 28 into the regression model and retrieved the respective CO_2 emissions. If the historic travel speed was higher than the introduced speed threshold, the value of the threshold was inserted instead. According to our traffic data network coverage of 81.5%, we scaled up the results of our calculations by dividing each absolute CO_2 value by.815, such that the remaining 18.5% of network edges not covered by any TomTom data were likewise included within the results to be presented.

By applying this logic to the network, total daily CO_2 savings of 7.43% compared to the unrestricted network can be achieved, while the aforementioned 50.74% of flow kilometers throughout

the German motorway network would practically be restricted. In absolute measures, this would save 9796.37 tons of CO_2 emission per day or 3,575,675.95 tons of CO_2 per year within the transport sector. To calculate yearly savings, we assumed a historically averaged Monday is representative for any given weekday. Future research might focus on analyzing network characteristics depending on different days of the week, especially Monday to Friday versus the weekend.

Table 18 Sensitivity analysis of different speed limit thresholds and their impact on network speed compared to CO_2 savings. Highlighted in blue is the scenario of 120 kph referenced during most of this article.

Speed Threshold [kph]	Restricted Flow Kilometers [%]	Ø Speed Restriction [kph]	Ø Speed Restriction [%]	CO_2 Savings [%]	CO_2 Savings [tons]
60	96.91	57.52	46.73	28.04	36,965.63
70	96.91	47.83	38.37	27.45	36,184.47
80	92.06	38.26	30.54	25.98	34,251.81
90	87.92	28.77	22.66	23.16	30,536.46
100	80.68	19.51	15.1	18.94	24,963.77
110	69.23	10.95	8.27	13.49	17,777.05
120	50.74	4.10	2.94	7.43	9796.37
130	35.23	−0.14	−0.26	2.39	3144.28

The same procedure was carried out for several different thresholds ranging from 60 kph to 130 kph, comparing potential CO_2 savings to network restrictions necessary to achieve these savings. The results are shown in Table 18.

One interesting result from Table 18 is the fact that a speed limit of 130 kph would result in a negative change of average speed (meaning an average speed increase) throughout the network. On first sight, this appears to be counterintuitive. Nonetheless, these results are a good indicator for the underlying assumption that the introduction of a speed limit would implicitly result in road participants adhering to these new regulations. Due to the previously described average speed throughout the network of 119.38 km an hour, adhering to the speed limit would require the general road user to increase their average driving speed. Since the current average network travel speed results not only from driver preference but also primarily from infrastructural performance of the network in general, it is highly unlikely that such a broad change could be realized.

To allow for a representative comparison between both studies it was important to keep in mind that while the GEA cited the total amount of CO_2 emitted by motorized vehicles as 44.5 million tons annually, a calculation within our network returned a total of 48.12 million tons, based on official and supplemented traffic count information as well as navigation service provider data. Therefore, percentage-wise comparison required normalization as provided within Table 19.

Table 19 Comparison between results presented by the German Environment Agency (GEA) versus results generated by programmatically analyzing the network.

Speed Threshold [kph]	CO_2 Savings GEA [m tons]	CO_2 Savings GEA [%]	CO_2 Savings Network Analysis [m tons]	CO_2 Savings Network Analysis* [%]
100	6.2	13.93	9.1	20.45
120	2.9	6.52	3.6	8.09
130	2.2	4.94	1.1	2.47

* Percentage-values normalized to 44.5 million tons according to the GEA.

The estimated CO_2 savings for a targeted speed limit of 120 kph differed by 1.57 percentage points, based on the absolute difference of 700,000 tons annually between our analysis and the results presented by the GEA. This gap is a direct result of the different methodologies applied. While the GEA used a fixed set of measuring points to extrapolate traffic flow information across the network, the methodology presented in this article referenced real-world traffic data provided by navigation devices across 81% of the network. Results differed more significantly for the remaining two cases of 100 and 130 kph. These variations stemmed from the fact that Löhe [310], the major data source for the GEA analysis, only provides data from measuring points for restricted sections with a speed limit of 120 kph. Therefore, the GEA was only able to provide general estimations for scenarios of 100 and 130 kph, while our data-driven methodology could draw from broad navigation service provider data to estimate a more realistic speed distribution for these additional thresholds.

4.4.4. On the Way to Well-Chosen Speed Limits

While the goal of minimizing CO_2 emission is generally accepted as beneficial, discussions on the dimensions of restrictions necessary and acceptable to achieve these savings continue. To better compare the proportions of restrictions necessary for achievable CO_2 savings, the parallel coordinate plot in Figure 30 is used.

A completely parallel line in Figure 30 equates to a directly proportional relation between two parameters. An example for this is the left-hand side for a speed limit of 90 km (black line). To achieve percentage-based CO_2 savings of 23.16% compared to the unrestricted network state, the average speed across the network must be reduced by 22.66%. In contrast to that, a steeper line in any direction (upward or downward slope) indicates a non-proportional relation between two attributes. The steeper the line, the more disproportional the relation is. Coming back to the major example of this article, the blue line indicates a speed limit of 120 km per hour. While the left-hand side relation between the average speed to be restricted and the potential savings is a positive one (an average speed reduction of 2.94% results in average daily CO_2 savings of 7.43%), the right-hand side supports claims of disproportionate incisions as 50.74% of total flow kilometers would require restrictions to achieve this 7.43% of CO_2 savings. The same can be said for any of the other thresholds considered during this case study.

To seek a mutually acceptable compromise for both parties—supporters and opponents of general speed restrictions—we took a closer look at the 120 kph restriction. In the case of 120 kph, 50.74% of traffic flow would practically be restricted. The total CO_2 emissions could be reduced by 7.43%, equaling 9796.37 tons per day. Figure 31 indicates the consequences of partial restrictions. The street sections have been ordered by the corresponding percentage of reduced CO_2 emissions in the case of a 120 kph restriction. A restriction of the top 19% of street sections in terms of percentage of CO_2 savings would lead to absolute CO_2 savings of 5000 tons daily, which equals about 50% of total possible savings considering a speed limit of 120 kph.

Figure 30 Parallel coordinate plot visualizing average network restrictions in comparison to potential CO_2 savings.

One fact worth mentioning while examining Figure 31 is the plateau value at approximately 72% of cumulated flow regulated by traffic signs, whereas our previous calculations showed a maximum restriction of 50.74% of flow kilometers. This stems from the fact that the conceptualized restrictions we applied to the network would be time-independent via the introduction of static and permanent speed signs on road sections, but the level of speed and therefore the classification of whether specific flow kilometers within the network will be restricted or not are highly time-dependent. In fact, a high amount of flow would theoretically be regulated by traffic signs, but in practice would not reach the threshold of 120 kph (i.e. originally unrestricted flow at rush hours). This suggests establishing dynamic traffic signs to adjust speed limits throughout different times of the day, based on actual traffic volume at specified time *t*.

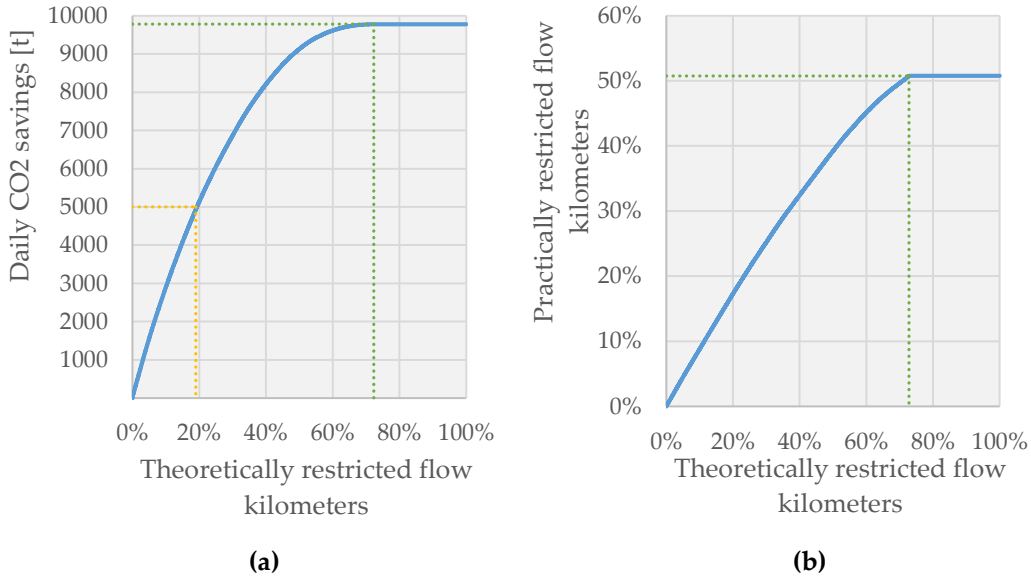

Figure 31 Depiction of the (a) direct relation between daily CO_2 savings in tons and the necessary percentage-based restriction of network flow and the (b) ratio of theoretical (static) restriction versus practical (dynamic) restriction considering a 120 kph speed limit.

Therefore, the *x*-axis of Figure 31 indicates the flow that is driven on edges with potential speed signs, but its practical restriction depends on the daytime-specific actual driving speeds. As a result, the amount of flow kilometers that are theoretically restricted is higher than the amount of flow kilometers that are practically restricted. This is worth mentioning since speed limit opponents will

argue based on a 72% restriction extracted from Figure 31, which in fact distorts the proportion of restricted flow kilometers and ignores dynamic real-world conditions. A more in-depth analysis and discussion on the topic of dynamic traffic regulation can be found in the upcoming section.

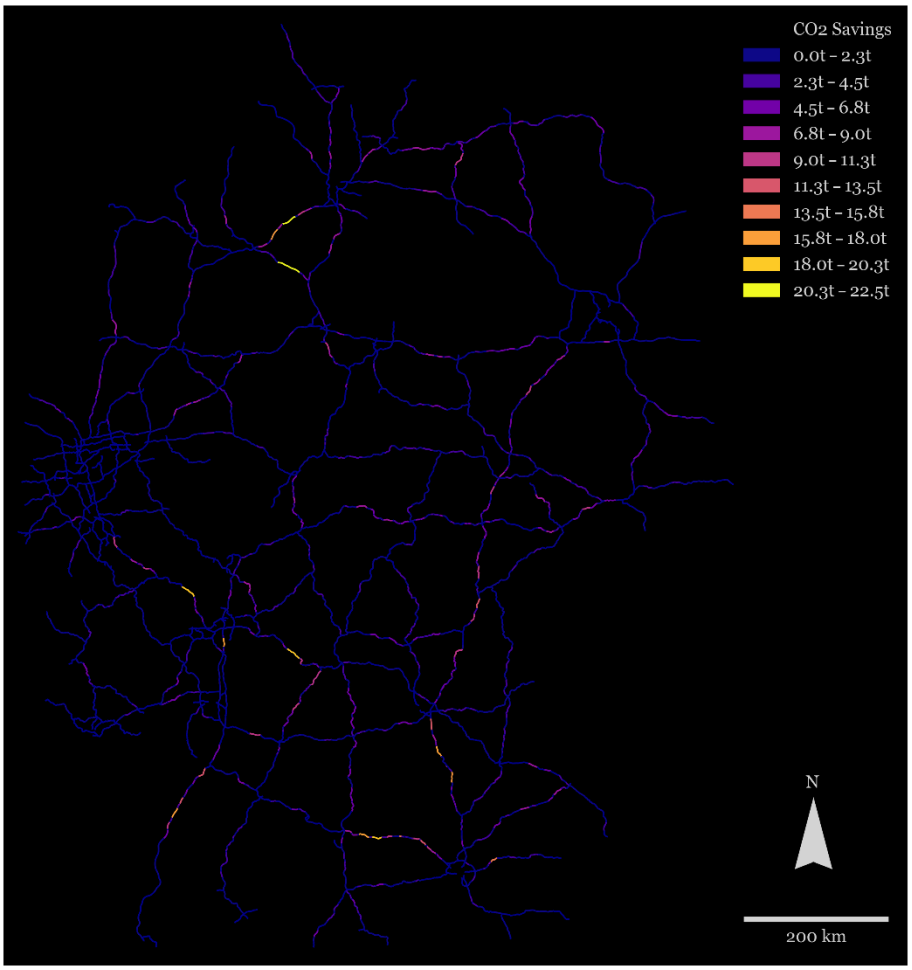

Figure 32 Network edges colored by the amount of daily CO_2 savings per edge resulting from a general speed limit of 120 kph. Brighter areas correspond to higher savings.

Figure 32 depicts the result in terms of absolute CO_2 savings per network edge (with an average edge length of 1.8 km) throughout the German motorway network according to our network analysis. Unsurprisingly, the highest savings are to be found on motorway edges in between large cities. As proximity to city centers increases, only marginal savings, if any, exist, which is to be expected since most of the traffic converges at these network intersections before it splits into different directions. Therefore, these highly used parts of the network predominately suffer from traffic jams, decreasing the historically averaged travel speed. Due to this decrease in average travel speed, most motorways located in close proximity to major cities are not affected by a speed limit since their default travel speed is already below the maximum speed allowed via the introduction of a speed threshold, resulting in no noteworthy CO_2 savings on these network edges.

4.5. Discussion

Our results verify the assumption that a general speed limit throughout the German motorway network can help reduce the annual amount of CO_2 emission by reducing average travel speeds. The

range of achievable savings calculated using our proposed methodology is in line with previous governmental studies by the German Environment Agency as well as the body of literature on this topic [24,28,30,36]

The methodology presented in this paper delivers a coherent guide on how to programmatically leverage official governmental data, historical traffic information as well as open-data platforms to improve on many of the shortcomings of previous studies, mainly on the issue of non-published data sets as well as the lack of transparency and reproducibility caused by it.

As discussed in Section 4, it is not necessary to apply speed limits to the whole network. Instead of this, we suggest the usage of so-called Variable Speed Limits (VSL). In addition to reducing the obstacle of perceived justification, VSL contribute significant further side effects, mainly flow optimization, reduced travel times, a decrease in traffic shock waves as well as an increase in road safety in general [314–321].

Unfortunately, motorists generally do not adhere to speed limits [322]. Because of that, VSL still require enforcement to realize many of their implied benefits [323–325], which results in high upfront and maintenance costs. It is therefore necessary to precisely evaluate the benefits resulting from these investments. In our case, Sections 3 and 4 focused on environmental benefits in terms of CO_2 emission savings. The calculated savings of 3.6 million tons annually (by implementing a speed limit of 120 kph) would require 50.74% of daily flow kilometers to be restricted throughout the network. However, this estimation resides on the lower end of the spectrum since it currently neglects the positive impacts of VSL previously described. Due to this, a wide-scale implementation of Variable Speed Limits could lead to reduced road occupancy, resulting in a smoothed traffic flow, which transfers to better driving patterns that require less acceleration and braking throughout a journey, decreasing the fuel consumption of any given vehicle, which directly correlates to fewer fossil fuels burned and less CO_2 emitted throughout the network.

Unfortunately, the proposed introduction of VSL into the network highlights a major limitation of our methodology, since these effects cannot currently be determined because we adhered to simplifications and assumptions provided by the GEA for the sake of comparability. Due to this, future research might focus on improving on these assumptions and supplementing the network via more specific and scientifically verifiable calculations. Some key points to be approved upon can therefore be summarized as follows:

We adopted the average-based CO_2 emission functions derived by the GEA. Since data on how the underlying driving cycles have been calculated are non-public, we suggest building transparent CO_2 emission functions. To achieve this, vehicle registration data can be analyzed to extract the distribution of different vehicle types moving on German motorways. In addition to that, open access frameworks like COPERT could be utilized to differentiate CO_2 emission curves by vehicle and fuel type [274]. The biggest issue that needs addressing is the fact that CO_2 emission functions often have a limited definition range. COPERT functions are currently only defined up to velocities of 130 kph. Therefore, one crucial part is finding or developing emission functions that adhere to the following two requirements: (1) they should be detailed enough to differentiate between vehicle and fuel types and (2) must be robust at higher speeds, which are driven on legally unrestricted motorways.

Additionally, the applicability and reliability of the traffic distribution functions provided by the GEA depicted in Figure 28 require further validation. Since the introduction of a general speed limit might significantly impact the driving patterns throughout the network, leading to increased travel times and longer lengths of stay within the network, future studies could focus on a simulation-based approach to validate the assumed distribution functions and their impact on network-wide CO_2 emission savings. Microscopic traffic simulation would also allow for the inclusion of VSL-based calculations [326–328], drastically improving on the applicability of our methodology to practical debates and potentially offsetting concerns on the topic of negative changes in driving patterns.

4.6. Conclusions

The contribution of this paper is a methodology to allow for transparent data analysis in road networks by enriching OpenStreetMap (OSM) data with publicly available traffic information on a dynamic scale.

We apply our methodology to contribute to the discussion of possible CO_2 emission savings via the introduction of a speed limit to the German motorway network by comparing our programmatical results to the official study by the German Environment Agency published in 2020. The comparison reveals that while the key facts and estimations in terms of network infrastructure as presented by the GEA hold true, major differences between the theoretical assumptions of network performance in terms of possible travel speeds and practical data gathered by navigation service providers can be identified.

We have quantified and shown that the introduction of a flat-rate speed limit of 120 kilometers per hour would result in a theoretical restriction of about 70% of total flow kilometers across the German motorway network, saving 3,575,675.95 tons of annual CO_2 emissions within the transport sector. More importantly, we quantify that nearly 100% of these savings could already be realized by restricting only 50.74% of all network sections dynamically throughout the day due to significant variations in time-dependent road utilization. Additional calculations for speed limits from 60 kph to 130 kph were provided as a means of sensitivity analysis to our findings.

Since we adopted multiple simplifying assumptions provided by the GEA for sake of comparability, future research might focus on speed distribution patterns in the context of 100 and 130 kph as well as on validating the presented driving cycles to calculate the speed-induced CO_2 emissions. In addition to that, the influence of Variable Speed Limits on traffic flow smoothness and its consequences, such as the level of CO_2 emissions and the probability of accidents, are currently not included and should be analyzed in detail.

5. Final Conclusion

A multitude of available data sources can enable the development of new methodologies to find solutions for unanswered questions. In addition to that, already established solutions can be validated with the use of new information and tools. The cost analysis of road freight transportation networks is based on information about transport activities and their intensities. Consequently, a lot of dynamic data is needed to elaborate on the impacts of transport costs. On its own, the existence of large amounts of data is worthless if there are no adequate methods to retrieve, transform and analyze them. The goal of this thesis was to show scientifically based case studies on how to put data and algorithms to use to gain insightful and practically relevant knowledge in the field of road transport. Several data sources and methodologies were considered, applications on practical problems were shown and the results were put into the context of the scientific community.

5.1. Implications

Due to the fact that this thesis consists of three separately published manuscripts, every manuscript leads to a conclusion or discussion where implications and further research are discussed. To draw a broader picture of the presented research, theoretical and practical implications are summarized in the following section. The implications are structured as follows: Every section starts with general implications in the context of this thesis. In addition to that, specific implications derived from the manuscripts are listed with bullet points.

5.1.1. Implications of manuscript 1

Manuscript 1 "Bringing economies of integration into the pricing of groupage freight" shows the solution to a new problem by leveraging existing historical shipment data. The manuscript is the first publication to formulate and answer the new consignor integration problem which deals with a new consignor entering a shipment structure of existing consignors. The overall goal is to find a suitable tariff for the consignor's shipments. This problem is solved by focusing on the nodes within a distribution network and analyzing their potential impacts on the overall cost structure. Information needed regarding the edges of the network is replaced by assumptions to keep complexity relatively low. This manuscript can be seen as basic research on how to handle data in the context of road freight transportation. The presented methodology can easily be reproduced by any stakeholder dealing with the NCIP. This manuscript implies remarkable findings for practitioners and researchers alike:

- Economies of integration substantially deviate from economies of scale. In the context of road freight transportation, economies of integration dictate the costs of a new consignor. They are heavily impacted by the number of shipments, payload, certainty, drop factor, tour and area density of the existing shipment structure.
- To impact the overall cost structure, a new consignor needs to add a certain volume of shipments into the existing structure. When crossing this threshold, a new consignor usually reduces the costs for all existing consignors within the network.
- General recommendations for tariff negotiations are formulated as follows: A consignor who adds less than 1% of shipments of the existing shipment structure should not pay less than the standard tariff. If a consignor is offered a discount, this discount should not exceed the reduction of costs per shipment derived from the proposed methodology.
- Large consignors can also negatively impact the costs per shipment. Resulting from this fact, the historical shipments of a new consignor should always be analyzed in the context of the existing shipment structure even if no tariff negotiation is planned. Simply applying the standard tariff for a new consignor could lead to less or negative margins.

5.1.2. Implications of manuscript 2

Manuscript 2 "Towards Sustainable Cities: Utilizing Floating Car Data to Support Location-Based Road Network Performance Measurements" solves the problem of measuring road network performance by utilizing a navigations service provider API called "Reachable Range". By the time of publication, this API and its potential have been studied by very few researchers. Consequently, the contribution of this paper is the integration of a new data source to solve an already studied question in a more efficient way. Road network performance can be measured very precisely with small effort when isoline calculations based on traffic data are integrated. Since isoline calculations need a start point and calculate reachable points via edges, this methodology is focusing on both the nodes and edges of a road network. The start point is considered very crucial as a small shift in a certain direction can lead to significant differences in results. Likewise to the methodology presented in manuscript 1, the calculation procedure can be reproduced very easily. The implications for different stakeholders are stated below:

- The time of departure highly impacts the travel time required from origin to destination. This stems from the fact that traffic intensity fluctuates within a day, week and year. The analysis shows that most travel time is needed in rush hours in the morning and early afternoon, whereas the hours around midnight are considered traffic-free. These hours can be used as a reference when talking about the so-called free flow state.
- The term free flow is slightly misleading since free flow is characterized by an accepted delay. This means that even when no traffic is occurring on the edges, restrictions such as infrastructure and traffic signs lead to a lower average travel speed than speed limits alone would induce.
- Little attention in research is given to the detour factor. The proportion of travel distance and air distance to be covered has a significant impact on travel costs. Therefore, it is important to collect information about the detour function. The detour factor is not static. In fact, it is distance-dependent because the more air distance is to be covered the more highways can be incorporated into route planning. Highways are often straight-lined edges with a small detour factor.
- Travel costs are always a product of air distance, detour factor and travel speed. To compare different starting points, all these variables must be considered to deliver meaningful and correct evidence.
- Different start points and different regions lead to significantly different travel costs. This is important when thinking about location problems like building a new distribution center. Distribution centers are approached and departed by many trucks on every workday within many years. This long-term planning horizon leads to a multiplication of every cost factor occurring while operating such a DC. Saving or expending "a few cents" per truck can lead to significant differences in margins impacted by the choice of location.

5.1.3. Implications of manuscript 3

Manuscript 3 "Speed Limit Induced CO_2 Reduction on Motorways: Enhancing Discussion Transparency through Data Enrichment of Road Networks" supplements the debate on implementing general speed limits on German motorways. Therefore, the Python library OSMnx, OpenStreetMap data, official street count data and the TomTom routing API are combined to deliver detailed information about the CO_2 emission on network edges. While this manuscript does not deal with road freight at first glance, the methodology can easily be adopted to gather and store information about edge speeds within a network. This manuscript shows the integration of several data sources as well as the first step towards gaining independence from online-only data sources by mapping information into an offline available network. The results are used to validate statements made by politicians. It is proven that their claims about CO_2 reduction are based on incomplete information

and can be more precise by incorporating additional data sources and methodologies. This finding can be translated to the context of road freight as significant insights can be found by using historical shipment structures only (manuscript 1), but results get increasingly more precise and reliable as multiple data sources and data analysis methods are combined. Besides these insights, which are more deeply discussed in the section Further research, some specific implications can be derived from manuscript 3:

- The results show that a general speed limit throughout the German motorway network would lead to significant CO_2 reductions. This is in line with recent literature. In contrast to that, a few minor improvements were made compared to the official study from the German Environment Agency.
- A flat rate speed limit would impact 70% of total flow kilometer driven whereas 3,575,675 tons of CO_2 can be saved annually. These savings could be realized by restricting only 50.74% of all network sections which could possibly lead to much greater acceptance by network participants.
- The calculated CO_2 savings can be seen as a bottom-line estimation. The amount of reduced pollution is potentially much higher as slower driving leads to fewer shock waves, better flow, less braking and fewer accidents.

5.2. Further research

This thesis shows important contributions for practitioners and researchers alike. From a critical standpoint, the published manuscripts do not max out every data source's potential. Therefore, the next section will conclude the presented research with an outlook on further research in the field of road transport.

5.2.1. Data source combinations

As it is shown in manuscript 3, research and practitioners can benefit immensely from combining different data sources and methodologies. Every source of information can help make results more robust and precise. Therefore, it would be useful to integrate more data sources into manuscript 1 and manuscript 2. Manuscript 1 could be extended by using edge-specific information to model the transport between points of distribution. Precise information about travel distance and travel speed could help to emulate real-world costs more accurately and lower cost estimation errors. When thinking about manuscript 2, the results could be validated by developing an alternative algorithm based on other routing APIs than the reachable range. In addition to that, historical shipments could be integrated to modify general reachable ranges and weigh the retrieved polygon points by the closeness of potential recipients. In general, it can be stated that the existing research questions should be elaborated on with the possibilities of additional APIs to achieve the best results possible. Manuscript 3 clearly shows that estimations based on static data can lead to huge differences in specific outcomes in comparison to estimations based on dynamic data.

5.2.2. Structural comparison of data sources

Another perspective regarding the available data source providers can be taken. In some cases, it can be useful to compare data from different providers. The choice of API is based on specific needs like precision, data quality and coverage. There is no peer-reviewed research found about the structural comparison of navigation service providers. Further research could develop specific key performance indicators and test them for different providers, APIs and regions. This would support researchers and practitioners in terms of choosing the right provider for future case studies.

5.2.3. Future developments

During the writing process of this thesis, the available APIs changed several times in terms of retrieval logic or delivered data (structure). Besides this development, completely new APIs emerged

which lead to more opportunities in putting data to use. Consequently, future research should always check for new providers or APIs. The goal of this thesis was to search for questions and to deliver better or new answers based on dynamic data sources. This goal can be pursued in further research by analyzing existing APIs, looking for new developments and matching the respective data onto (existing) problems.

Another aspect to mention under the headline of future developments is the ever-changing circumstances a transportation network is operated in. Road transportation is a very dynamic field of research in terms of underlying assumptions and environmental characteristics. Traffic increases year by year which leads to changing travel times. Infrastructure is modified which directly impacts the detour factor, travel distances as well as delays to be accounted for. Therefore, it is mandatory to check historical calculations in fixed time intervals. This means that, in contrast to the methodology, which holds true in the future, the experimental results in this thesis' case studies could be outdated by the time of reading this final publication.

5.2.4. From offline to online and reverse

Every manuscript of this thesis uses online APIs to derive better insights than conventional methods do. Whether it is geocoding, routing or retrieval of OpenStreetMap networks, the results are heavily dependent on the availability of certain providers' data. Most of the providers offer so-called "Freemium" models. Every user is provided with a free contingent of calls up to a limited threshold. When this threshold is reached, every API call is invoiced. This procedure can lead to extensive costs very fast. Google Maps already switched to an exclusive "paid only" model where every API call is invoiced immediately. To gain independence from providers, future research should focus on the offline storage and analysis of the latest data. In contrast to that advice, road transport is considered a very dynamic field of research which relies on recent up-to-date data. Consequently, future research should focus also on the estimation of prospective information that is currently retrieved by the time needed with the help of described providers.

5.2.5. Estimation of shipment costs

When discussing distribution in road freight networks, a very complex problem is the future pricing of individual shipments. This stems from the fact that the future shipment structure is not known in advance, network characteristics are very dynamic and shipment costs arise during joint production. Joint production in the context of transportation means that individual shipments are combined to tours to save costs and increase operational efficiency. These tours as well as the underlying network characteristics are not known for future scenarios. An interesting research topic for practitioners and researchers alike is the determination of shipment costs with stochastic tours and network characteristics. This would enable a new level of pricing of shipments. Every single shipment could be evaluated in advance, based on specific characteristics regarding network structure and traffic situations. This thesis builds the basis on how to use APIs to get detailed information about the historical shipment structure (manuscript 1) and traffic information (manuscript 2 & 3) to estimate different types of costs. This information should be analyzed, filtered and applied to model the stochastic costing of shipments. This would lead to shipment-specific pricing, improved cost control for logistic service providers and cost-induced allocation between consignors within the same tour. In addition to that, an advanced information basis for precise tariff negotiations could be built.

To summarize the above-mentioned opportunities for further research, this thesis can be considered as another step into a more digitalized field of road transportation. **Nevertheless, a lot of work lies ahead to exploit the given potentials within the transportation industry.**

References

1. Furtado, P.; Frayret, J.-M. Proposal Sustainability Assessment of Resource Sharing in Intermodal Freight Transport with Agent-based Simulation. *IFAC-PapersOnLine* **2015**, *48*, 436–441, doi:10.1016/j.ifacol.2015.06.120.
2. Bask, A.; Rajahonka, M. The role of environmental sustainability in the freight transport mode choice. *IJPDLM* **2017**, *47*, 560–602, doi:10.1108/IJPDLM-03-2017-0127.
3. Meixell, M.J.; Norbis, M. A review of the transportation mode choice and carrier selection literature. *IJLM* **2008**, *19*, 183–211, doi:10.1108/09574090810895951.
4. Alacam, S.; Sencer, A. Using Blockchain Technology to Foster Collaboration among Shippers and Carriers in the Trucking Industry: A Design Science Research Approach. *Logistics* **2021**, *5*, 37, doi:10.3390/logistics5020037.
5. Zgonc, B.; Tekavčič, M.; Jakšič, M. The impact of distance on mode choice in freight transport. *Eur. Transp. Res. Rev.* **2019**, *11*, 43, doi:10.1186/s12544-019-0346-8.
6. Farquharson, N.; Mageto, J.; Makan, H. Effect of internet of things on road freight industry. *Journal of Transport and Supply Chain Management* **2021**, *15*, doi:10.4102/jtscm.v15i0.581.
7. Pernestål, A.; Engholm, A.; Bemler, M.; Gidofalvi, G. How Will Digitalization Change Road Freight Transport? Scenarios Tested in Sweden. *Sustainability* **2021**, *13*, 304, doi:10.3390/su13010304.
8. Bain, R. Technology and State Government. *American Sociological Review* **1937**, *2*, 860, doi:10.2307/2084365.
9. Xia, F.; Yang, L.T.; Wang, L.; Vinel, A. Internet of Things. *Int. J. Commun. Syst.* **2012**, *25*, 1101–1102, doi:10.1002/dac.2417.
10. Hwang, G.; Lee, J.; Park, J.; Chang, T.-W. Developing performance measurement system for Internet of Things and smart factory environment. *International Journal of Production Research* **2017**, *55*, 2590–2602, doi:10.1080/00207543.2016.1245883.
11. Rudskoy, A.; Ilin, I.; Prokhorov, A. Digital Twins in the Intelligent Transport Systems. *Transportation Research Procedia* **2021**, *54*, 927–935, doi:10.1016/j.trpro.2021.02.152.
12. Shubenkova, K.; Valiev, A.; Shepelev, V.; Tsiulin, S.; Reinau, K.H. Possibility of Digital Twins Technology for Improving Efficiency of the Branded Service System. In *Proceedings, 2018 Global Smart Industry Conference (GloSIC)*, South Ural State University (national research university), Chelyabinsk, Russian Federation, November 13-15, 2018. 2018 Global Smart Industry Conference (GloSIC), Chelyabinsk, 11/13/2018 - 11/15/2018; IEEE: Piscataway, NJ, 2018; pp 1–7, ISBN 978-1-5386-7386-7.
13. Jiang, Y.; Xing, Y.L.; Zhang, C.X.; Wang, B.; Du, L.L. Freight Vehicles Regulatory Assistance System Based on Internet of Things. *AMM* **2014**, *587-589*, 1871–1874, doi:10.4028/www.scientific.net/AMM.587-589.1871.
14. Humayun, M.; Jhanjhi, N.Z.; Hamid, B.; Ahmed, G. Emerging Smart Logistics and Transportation Using IoT and Blockchain. *IEEE Internet Things M.* **2020**, *3*, 58–62, doi:10.1109/IOTM.0001.1900097.
15. Dimokas, N.; Margaritis, D.; Gaetani, M.; Koprubasi, K.; Bekiaris, E. A Big Data Application for Low Emission Heavy Duty Vehicles. *Transport and Telecommunication Journal* **2020**, *21*, 265–274, doi:10.2478/ttj-2020-0021.
16. Hopkins, J.; Hawking, P. Big Data Analytics and IoT in logistics: a case study. *IJLM* **2018**, *29*, 575–591, doi:10.1108/IJLM-05-2017-0109.

17. He, C.R.; Maurer, H.; Orosz, G. Fuel Consumption Optimization of Heavy-Duty Vehicles With Grade, Wind and Traffic Information. *Journal of Computational and Nonlinear Dynamics* **2016**, *11*, doi:10.1115/1.4033895.

18. Meyer, T.; Kuhn, M.; Hartmann, E. Blockchain technology enabling the Physical Internet: A synergetic application framework. *Computers & Industrial Engineering* **2019**, *136*, 5–17, doi:10.1016/j.cie.2019.07.006.

19. Pournader, M.; Shi, Y.; Seuring, S.; Koh, S.L. Blockchain applications in supply chains, transport and logistics: a systematic review of the literature. *International Journal of Production Research* **2020**, *58*, 2063–2081, doi:10.1080/00207543.2019.1650976.

20. Babich, V.; Hilary, G. What Operations Management Researchers Should Know About Blockchain Technology. *SSRN Journal* **2018**, doi:10.2139/ssrn.3131250.

21. Koh, L.; Dolgui, A.; Sarkis, J. Blockchain in transport and logistics – paradigms and transitions. *International Journal of Production Research* **2020**, *58*, 2054–2062, doi:10.1080/00207543.2020.1736428.

22. Yuan, Y.; Wang, F.-Y. Blockchain and Cryptocurrencies: Model, Techniques and Applications. *IEEE Trans. Syst. Man Cybern, Syst.* **2018**, *48*, 1421–1428, doi:10.1109/TSMC.2018.2854904.

23. Subramanian, N.; Chaudhuri, A.; Kayıkcı, Y. Blockchain Applications and Future Opportunities in Transportation. In *Blockchain and Supply Chain Logistics*: *Evolutionary Case Studies*; Subramanian, N., Ed.; Palgrave Macmillan UK: Cham, 2020; pp 39–48, ISBN 978-3-030-47530-7.

24. Astarita, V.; Giofrè, V.P.; Mirabelli, G.; Solina, V. A Review of Blockchain-Based Systems in Transportation. *Information* **2020**, *11*, 21, doi:10.3390/info11010021.

25. Alias, C.; Kalkan, Y.; Koç, E.; Noche, B. Enabling Improved Process Control Opportunities by Means of Logistics Control Towers and Vision-Based Monitoring. In *Proceedings of the ASME International Design Engineering Technical Conferences and Computers and Information in Engineering Conference - 2014*, Presented at ASME 2014 International Design Engineering Technical Conferences and Computers and Information in Engineering Conference; August 17 - 20, 2014, Buffalo, New York, USA. ASME 2014 International Design Engineering Technical Conferences and Computers and Information in Engineering Conference, Buffalo, New York, USA, 8/17/2014 - 8/20/2014; ASME: New York, NY, 2014, ISBN 978-0-7918-4629-2.

26. Irannezhad, E. Is blockchain a solution for logistics and freight transportation problems? *Transportation Research Procedia* **2020**, *48*, 290–306, doi:10.1016/j.trpro.2020.08.023.

27. Frohm, J.; Lindström, V.; Winroth, M.; Stahre, J. Levels of Automation in Manufacturing. *Ergonomia - International Journal of Ergonomics and Human Factors* **2008**, *30*, 181–207.

28. Jaller, M.; Otero-Palencia, C.; Pahwa, A. Automation, electrification and shared mobility in urban freight: opportunities and challenges. *Transportation Research Procedia* **2020**, *46*, 13–20, doi:10.1016/j.trpro.2020.03.158.

29. G. R. Janssen; Jan Zwijnenberg; Iris Blankers; Janiek de Kruijff. Truck platooning: driving the future of transportation **2015**.

30. Reis, V.; Pereira, R.; Kanwat, P. Assessing the potential of truck platooning in short distances: the case study of Portugal. In *Urban freight transportation systems*; Friedrich, C., Pfohl, H.-C., Boltze, M., Elbert, R., Eds.; Elsevier: Amsterdam, Netherlands, 2020; pp 203–222, ISBN 9780128173626.

31. Bergenhem, C.; Shladover, S.; Coelingh, E.; Englund, C.; Tsugawa, S. Overview of platooning systems. In *Proceedings of the 19th ITS World Congress,* Vienna, Austria, Oct. 22-26, 2012, ISBN 978-1-7281-5812-9.

32. Alam, A.; Besselink, B.; Turri, V.; Martensson, J.; Johansson, K. Heavy-Duty Vehicle Platooning for Sustainable Freight Transportation: A Cooperative Method to Enhance Safety and Efficiency. *IEEE Control Syst.* **2015**, *35*, 34–56, doi:10.1109/MCS.2015.2471046.

33. Hamido, S.; Hamamoto, R.; Gu, X.; Itoh, K. Factors influencing occupational truck driver safety in ageing society. *Accid. Anal. Prev.* **2021**, *150*, 105922, doi:10.1016/j.aap.2020.105922.

34. Michael, W.; Wood, L.; Wang, B. Transportation Capacity Shortage Influence on Logistics Performance: Evidence From the Australian Logistics Service Providers' Driver Shortage. *SSRN Journal* **2021**, doi:10.2139/ssrn.3957222.

35. Phares, J.; Balthrop, A. Investigating the role of competing wage opportunities in truck driver occupational choice. *J Bus Logist* **2021**, doi:10.1111/jbl.12285.

36. Trick, S.; Peoples, J.; Ross, A. Driver turnover in the trucking industry: What's the cost of reducing driver quit rates? *Research in Transportation Economics* **2021**, 101129, doi:10.1016/j.retrec.2021.101129.

37. Paddeu, D.; Denby, J. Decarbonising road freight: Is truck automation and platooning an opportunity? *Clean Techn Environ Policy* **2021**, doi:10.1007/s10098-020-02020-9.

38. Paddeu, D.; Parkhurst, G. The potential for automation to transform urban deliveries: Drivers, barriers and policy priorities. *Policy Implications of Autonomous Vehicles*; Elsevier, 2020; pp 291–314, ISBN 9780128201916.

39. Müller, S.; Voigtländer, F. Automated Trucks in Road Freight Logistics: The User Perspective. In *Advances in production, logistics and traffic*: *Proceedings of the 4th Interdisciplinary Conference on Production Logistics and Traffic 2019*; Clausen, U., Langkau, S., Kreuz, F., Eds.; Springer: Cham, 2019; pp 102–115, ISBN 978-3-030-13534-8.

40. Oliveira, C.; Albergaria De Mello Bandeira, Renata; Vasconcelos Goes, G.; Schmitz Gonçalves, D.; D'Agosto, M. Sustainable Vehicles-Based Alternatives in Last Mile Distribution of Urban Freight Transport: A Systematic Literature Review. *Sustainability* **2017**, *9*, 1324, doi:10.3390/su9081324.

41. Ghosh, A. Possibilities and Challenges for the Inclusion of the Electric Vehicle (EV) to Reduce the Carbon Footprint in the Transport Sector: A Review. *Energies* **2020**, *13*, 2602, doi:10.3390/en13102602.

42. González Palencia, J.C.; van Nguyen, T.; Araki, M.; Shiga, S. The Role of Powertrain Electrification in Achieving Deep Decarbonization in Road Freight Transport. *Energies* **2020**, *13*, 2459, doi:10.3390/en13102459.

43. Frieske, B.; Kloetzke, M.; Mauser, F. Trends in vehicle concept and key technology development for hybrid and battery electric vehicles. In *World Electric Vehicle Symposium and Exposition (EVS 27), 2013*, Barcelona, Spain, 17 - 20 Nov. 2013. 2013 World Electric Vehicle Symposium and Exhibition (EVS27), Barcelona, Spain, 11/17/2013 - 11/20/2013; IEEE: Piscataway, NJ, 2013; pp 1–12, ISBN 978-1-4799-3832-2.

44. Hasan, M.K.; Mahmud, M.; Ahasan Habib, A.; Motakabber, S.; Islam, S. Review of electric vehicle energy storage and management system: Standards, issues and challenges. *Journal of Energy Storage* **2021**, *41*, 102940, doi:10.1016/j.est.2021.102940.

45. Karki, A.; Phuyal, S.; Tuladhar, D.; Basnet, S.; Shrestha, B.P. Status of Pure Electric Vehicle Power Train Technology and Future Prospects. *ASI* **2020**, *3*, 35, doi:10.3390/asi3030035.

46. Lebrouhi, B.E.; Khattari, Y.; Lamrani, B.; Maaroufi, M.; Zeraouli, Y.; Kousksou, T. Key challenges for a large-scale development of battery electric vehicles: A comprehensive review. *Journal of Energy Storage* **2021**, *44*, 103273, doi:10.1016/j.est.2021.103273.

47. Lu, M.; Zhang, X.; Ji, J.; Xu, X.; Zhang, Y. Research progress on power battery cooling technology for electric vehicles. *Journal of Energy Storage* **2020**, *27*, 101155, doi:10.1016/j.est.2019.101155.

48. Inkinen, T.; Hämäläinen, E. Reviewing Truck Logistics: Solutions for Achieving Low Emission Road Freight Transport. *Sustainability* **2020**, *12*, 6714, doi:10.3390/su12176714.

49. Napoli, G.; Polimeni, A.; Micari, S.; Dispenza, G.; Antonucci, V.; Andaloro, L. Freight distribution with electric vehicles: A case study in Sicily. Delivery van development. *Transportation Engineering* **2021**, *3*, 100048, doi:10.1016/j.treng.2021.100048.

50. Teoh, T.; Kunze, O.; Teo, C.-C.; Wong, Y. Decarbonisation of Urban Freight Transport Using Electric Vehicles and Opportunity Charging. *Sustainability* **2018**, *10*, 3258, doi:10.3390/su10093258.

51. Taefi, T.T.; Kreutzfeldt, J.; Held, T.; Fink, A. Strategies to Increase the Profitability of Electric Vehicles in Urban Freight Transport. In *E-Mobility in Europe*: *Trends and Good Practice*; Leal Filho, W., Ed.; Springer International Publishing AG: Cham, 2015; pp 367–388, ISBN 978-3-319-13193-1.

52. Christensen, L.; Klauenberg, J.; Kveiborg, O.; Rudolph, C. Suitability of commercial transport for a shift to electric mobility with Denmark and Germany as use cases. *Research in Transportation Economics* **2017**, *64*, 48–60, doi:10.1016/j.retrec.2017.08.004.

53. Monios, J.; Bergqvist, R. The transport geography of electric and autonomous vehicles in road freight networks. *Journal of Transport Geography* **2019**, *80*, 102500, doi:10.1016/j.jtrangeo.2019.102500.

54. Stopka, O.; Stopkova, M.; Lizbetin, J.; Soviar, J.; Caban, J. Development Trends of Electric Vehicles in the Context of Road Passenger and Freight Transport. In *2020 XII International Science-Technical Conference AUTOMOTIVE SAFETY*. 2020 XII International Science-Technical Conference AUTOMOTIVE SAFETY, Kielce, Poland, 21–23 Oct. 2020; IEEE, 2020 - 2020; pp 1–8, ISBN 978-1-7281-5812-9.

55. Taefi, T.T.; Stütz, S.; Fink, A. Assessing the cost-optimal mileage of medium-duty electric vehicles with a numeric simulation approach. *Transportation Research Part D: Transport and Environment* **2017**, *56*, 271–285, doi:10.1016/j.trd.2017.08.015.

56. Huber, R. The Digital Transformation of Freight Forwarders. In *The digital transformation of logistics*: *Demystifying impacts of the fourth industrial revolution*; Sullivan, M., Kern, J., Eds.; Wiley-IEEE Press: Hoboken, New Jersey, 2021; pp 153–167, ISBN 9781119646495.

57. Poniatowska-Jaksch, M.; Nowicka, K. Transport Platforms in the EU towards Sustainable Development. *ERSJ* **2021**, *XXIV*, 779–797, doi:10.35808/ersj/2155.

58. Reuver, M. de; Sørensen, C.; Basole, R.C. The Digital Platform: A Research Agenda. *Journal of Information Technology* **2018**, *33*, 124–135, doi:10.1057/s41265-016-0033-3.

59. Thomas, L.D.W.; Autio, E.; Gann, D.M. Architectural Leverage: Putting Platforms in Context. *AMP* **2014**, *28*, 198–219, doi:10.5465/amp.2011.0105.

60. Stradner, S.; Brunner, U. *Impact of Digitalization on Logistics Provider Business Models*, 2020.

61. Wyman, O. Digital Logistics Startups Are Both Challenge And Opportunity For Industry Incumbents. *Forbes [Online],* July 28, 2017. Available online: https://www.forbes.com/sites/oliverwyman/2017/07/28/digital-logistics-startups-are-both-challenge-and-opportunity-for-industry-incumbents/?sh=2c254f531589 (accessed on 29 November 2021).

62. Mikl, J. Start-ups in the logistics industry: Advancing a framework for the disruptive potential of digital freight forwarder platforms (DFFs). In *Proceedings of The 8th International Conference on New Ideas in Management*, *Economics and Accounting*; ACAVENT, 2021, ISBN 9786094851407.

63. Mikl, J.; Herold, D.M.; Ćwiklicki, M.; Kummer, S. The impact of digital logistics start-ups on incumbent firms : a business model perspective. *IJLM* **2021**, *32*, 1461–1480, doi:10.1108/IJLM-04-2020-0155.

64. Jin, D.-H.; Kim, H.-J. Integrated Understanding of Big Data, Big Data Analysis and Business Intelligence: A Case Study of Logistics. *Sustainability* **2018**, *10*, 3778, doi:10.3390/su10103778.

65. Borgi, T.; Zoghlami, N.; Abed, M.; Naceur, M.S. Big Data for Operational Efficiency of Transport and Logistics: A Review. In *6th IEEE International Conference on Advanced Logistics and Transport*, 24-27 July 2017, Bali, Indonesia : conference proceedings. 2017 6th IEEE International Conference on Advanced Logistics and Transport (ICALT), Bali, 7/24/2017 - 7/27/2017; IEEE: Piscataway, NJ, 2018; pp 113–120, ISBN 978-1-5386-1623-9.

66. Sun, Z.; Sun, L.; Strang, K. Big Data Analytics Services for Enhancing Business Intelligence. *Journal of Computer Information Systems* **2018**, *58*, 162–169, doi:10.1080/08874417.2016.1220239.

67. Gruber, T.R. Toward principles for the design of ontologies used for knowledge sharing? *International Journal of Human-Computer Studies* **1995**, *43*, 907–928, doi:10.1006/ijhc.1995.1081.

68. Holsapple, C.; Lee-Post, A.; Pakath, R. A unified foundation for business analytics. *Decision Support Systems* **2014**, *64*, 130–141, doi:10.1016/j.dss.2014.05.013.

69. Rincon-Garcia, N.; Waterson, B.J.; Cherrett, T.J. Requirements from vehicle routing software: perspectives from literature, developers and the freight industry. *Transport Reviews* **2018**, *38*, 117–138, doi:10.1080/01441647.2017.1297869.

70. Konstantakopoulos, G.D.; Gayialis, S.P.; Kechagias, E.P. Vehicle routing problem and related algorithms for logistics distribution: a literature review and classification. *Oper Res Int J* **2020**, doi:10.1007/s12351-020-00600-7.

71. Gayialis, S.P.; Konstantakopoulos, G.D.; Papadopoulos, G.A.; Kechagias, E.; Ponis, S.T. Developing an Advanced Cloud-Based Vehicle Routing and Scheduling System for Urban Freight Transportation. In *Advances in Production Management Systems. Smart Manufacturing for Industry 4.0*; Moon, I., Lee, G.M., Park, J., Kiritsis, D., Cieminski, G. von, Eds.; Springer International Publishing: Cham, 2018; pp 190–197, ISBN 978-3-319-99706-3.

72. Alvarez, P.; Lerga, I.; Serrano-Hernandez, A.; Faulin, J. The impact of traffic congestion when optimising delivery routes in real-time. A case study in Spain. *International Journal of Logistics Research and Applications* **2018**, *21*, 529–541, doi:10.1080/13675567.2018.1457634.

73. do C. Martins, L.; Hirsch, P.; Juan, A.A. Agile optimization of a two-echelon vehicle routing problem with pickup and delivery. *Intl. Trans. in Op. Res.* **2021**, *28*, 201–221, doi:10.1111/itor.12796.

74. Sbai, I.; Krichen, S. A real-time Decision Support System for Big Data Analytic: A case of Dynamic Vehicle Routing Problems. *Procedia Computer Science* **2020**, *176*, 938–947, doi:10.1016/j.procs.2020.09.089.

75. van der Spoel, S.; Amrit, C.; van Hillegersberg, J. Predictive analytics for truck arrival time estimation: a field study at a European distribution centre. *International Journal of Production Research* **2017**, *55*, 5062–5078, doi:10.1080/00207543.2015.1064183.

76. Zhao, J.; Gao, Y.; Yang, Z.; Li, J.; Feng, Y.; Qin, Z.; Bai, Z. Truck Traffic Speed Prediction Under Non-Recurrent Congestion: Based on Optimized Deep Learning Algorithms and GPS Data. *IEEE Access* **2019**, *7*, 9116–9127, doi:10.1109/ACCESS.2018.2890414.

77. Lv, Y.; Duan, Y.; Kang, W.; Li, Z.; Wang, F.-Y. Traffic Flow Prediction With Big Data: A Deep Learning Approach. *IEEE Trans. Intell. Transport. Syst.* **2014**, 1–9, doi:10.1109/TITS.2014.2345663.

78. van Lint, J.W. Reliable Real-Time Framework for Short-Term Freeway Travel Time Prediction. *J. Transp. Eng.* **2006**, *132*, 921–932, doi:10.1061/(ASCE)0733-947X(2006)132:12(921).

79. Wang, Z.; Goodchild, A.V.; McCormack, E. Freeway truck travel time prediction for freight planning using truck probe GPS data. European Journal of Transport and Infrastructure Research, Vol 16 No 1 (2016) **2016**, doi:10.18757/EJTIR.2016.16.1.3114.

80. Tsekeris, T.; Tsekeris, C. Demand Forecasting in Transport: Overview and Modeling Advances. *Economic Research-Ekonomska Istraživanja* **2011**, *24*, 82–94, doi:10.1080/1331677X.2011.11517446.

81. Mrowczynska, B.; Ciesla, M.; Krol, A.; Sladkowski, A. Application of Artificial Intelligence in Prediction of Road Freight Transportation. *PROMET* **2017**, *29*, 363–370, doi:10.7307/ptt.v29i4.2227.

82. Yang, Y. Development of the regional freight transportation demand prediction models based on the regression analysis methods. *Neurocomputing* **2015**, *158*, 42–47, doi:10.1016/j.neucom.2015.01.069.

83. Fite, J.T.; Don Taylor, G.; Usher, J.S.; English, J.R.; Roberts, J.N. Forecasting freight demand using economic indices. *IJPDLM* **2002**, *32*, 299–308, doi:10.1108/09600030210430660.

84. Yin, S.; Jiang, Y.; Tian, Y.; Kaynak, O. A Data-Driven Fuzzy Information Granulation Approach for Freight Volume Forecasting. *IEEE Trans. Ind. Electron.* **2017**, *64*, 1447–1456, doi:10.1109/TIE.2016.2613974.

85. Mentzer, J.T. Determining motor carrier backhaul markets. *Industrial Marketing Management* **1986**, *15*, 237–243, doi:10.1016/0019-8501(86)90033-7.

86. Seiler, T. *Operative Transportation Planning;* Physica-Verlag HD: Heidelberg, 2012, ISBN 978-3-7908-2791-0.

87. Defee, C.C.; Hanna, J.B.; Overstreet, R. LTL pricing: Looking back to the future. *JOTM* **2011**, *22*, 45–58, doi:10.22237/jotm/1317427440.

88. Miller, J.W.; Scott, A.; Williams, B.D. Pricing Dynamics in the Truckload Sector: The Moderating Role of the Electronic Logging Device Mandate. *J Bus Logist* **2021**, *42*, 388–405, doi:10.1111/jbl.12256.

89. Lin, K.Y. Dynamic pricing with real-time demand learning. *European Journal of Operational Research* **2006**, *174*, 522–538, doi:10.1016/j.ejor.2005.01.041.

90. Qiao, B.; Pan, S.; Ballot, E. Dynamic Pricing for Carriers in Physical Internet with Peak Demand Forecasting. *IFAC-PapersOnLine* **2019**, *52*, 1663–1668, doi:10.1016/j.ifacol.2019.11.439.

91. Qiao, B.; Pan, S.; Ballot, E. Dynamic pricing model for less-than-truckload carriers in the Physical Internet. *J Intell Manuf* **2019**, *30*, 2631–2643, doi:10.1007/s10845-016-1289-8.

92. Figliozzi, M.A.; Mahmassani, H.S.; Jaillet, P. Pricing in Dynamic Vehicle Routing Problems. *Transportation Science* **2007**, *41*, 302–318, doi:10.1287/trsc.1070.0193.

93. Sun, L.; Karwan, M.H.; Gemici-Ozkan, B.; Pinto, J.M. Estimating the long-term cost to serve new customers in joint distribution. *Computers & Industrial Engineering* **2015**, *80*, 1–11, doi:10.1016/j.cie.2014.11.012.

94. Kellner, F.; Otto, A.; Brabänder, C. Bringing infrastructure into pricing in road freight transportation – A measuring concept based on navigation service data. *Transportation Research Procedia* **2017**, *25*, 794–805, doi:10.1016/j.trpro.2017.05.458.

95. Biggs, N.; Lloyd, E.K.; Wilson, R.J. *Graph theory*: *1736 - 1936*, 1. Reprint. with corr., der 1. Paperback-Ausgabe; Clarendon Press: Oxford, 1998, ISBN 9780198539162.

96. Riaz, F.; Ali, K.M. Applications of Graph Theory in Computer Science. In *2011 Third International Conference on Computational Intelligence, Communication Systems and Networks.* 2011 3rd International Conference on Computational Intelligence, Communication Systems and Networks

(CICSyN 2011), Bali, Indonesia, 26–28 Jul. 2011; IEEE, 2011; pp 142–145, ISBN 978-1-4577-0975-3.

97. Klapka, P.; Kraft, S.; Halás, M. Network based definition of functional regions: A graph theory approach for spatial distribution of traffic flows. *Journal of Transport Geography* **2020**, *88*, 102855, doi:10.1016/j.jtrangeo.2020.102855.

98. Janic, M. Modelling the full costs of an intermodal and road freight transport network. *Transportation Research Part D: Transport and Environment* **2007**, *12*, 33–44, doi:10.1016/j.trd.2006.10.004.

99. Porta, S.; Crucitti, P.; Latora, V. The network analysis of urban streets: A dual approach. *Physica A: Statistical Mechanics and its Applications* **2006**, *369*, 853–866, doi:10.1016/j.physa.2005.12.063.

100. Ahmadzai, F.; Rao, K.; Ulfat, S. Assessment and modelling of urban road networks using Integrated Graph of Natural Road Network (a GIS-based approach). *Journal of Urban Management* **2019**, *8*, 109–125, doi:10.1016/j.jum.2018.11.001.

101. Verhoef, E. External effects and social costs of road transport. *Transportation Research Part A: Policy and Practice* **1994**, *28*, 273–287, doi:10.1016/0965-8564(94)90003-5.

102. Kuhlman, T.; Farrington, J. What is Sustainability? *Sustainability* **2010**, *2*, 3436–3448, doi:10.3390/su2113436.

103. Casado-Sanz, N.; Guirao, B.; Attard, M. Analysis of the Risk Factors Affecting the Severity of Traffic Accidents on Spanish Crosstown Roads: The Driver's Perspective. *Sustainability* **2020**, *12*, 2237, doi:10.3390/su12062237.

104. Ohiduzzaman, M.D.; Sirin, O.; Kassem, E.; Rochat, J. State-of-the-Art Review on Sustainable Design and Construction of Quieter Pavements—Part 1: Traffic Noise Measurement and Abatement Techniques. *Sustainability* **2016**, *8*, 742, doi:10.3390/su8080742.

105. Park, T.; Kim, M.; Jang, C.; Choung, T.; Sim, K.-A.; Seo, D.; Chang, S. The Public Health Impact of Road-Traffic Noise in a Highly-Populated City, Republic of Korea: Annoyance and Sleep Disturbance. *Sustainability* **2018**, *10*, 2947, doi:10.3390/su10082947.

106. Shah, S.A.R.; Ahmad, N. Road Infrastructure Analysis with Reference to Traffic Stream Characteristics and Accidents: An Application of Benchmarking Based Safety Analysis and Sustainable Decision-Making. *Applied Sciences* **2019**, *9*, 2320, doi:10.3390/app9112320.

107. Sirin, O. State-of-the-Art Review on Sustainable Design and Construction of Quieter Pavements—Part 2: Factors Affecting Tire-Pavement Noise and Prediction Models. *Sustainability* **2016**, *8*, 692, doi:10.3390/su8070692.

108. Zhu, L.; Lu, L.; Zhang, W.; Zhao, Y.; Song, M. Analysis of Accident Severity for Curved Roadways Based on Bayesian Networks. *Sustainability* **2019**, *11*, 2223, doi:10.3390/su11082223.

109. Barth, M.; Boriboonsomsin, K. Real-World Carbon Dioxide Impacts of Traffic Congestion. *Transportation Research Record* **2008**, *2058*, 163–171, doi:10.3141/2058-20.

110. Armah, F.; Yawson, D.; Pappoe, A.A.N.M. A Systems Dynamics Approach to Explore Traffic Congestion and Air Pollution Link in the City of Accra, Ghana. *Sustainability* **2010**, *2*, 252–265, doi:10.3390/su2010252.

111. Blagoiev, M.; Gruicin, I.; Ionascu, M.-E.; Marcu, M. A Study on Correlation Between Air Pollution and Traffic. In *26th Telecommunications Forum (TELFOR).* 26th Telecommunications Forum (TELFOR), 2018; pp 420–425.

112. Figliozzi, M.A. The impacts of congestion on commercial vehicle tour characteristics and costs. *Transportation Research Part E: Logistics and Transportation Review* **2010**, *46*, 496–506, doi:10.1016/j.tre.2009.04.005.

113. Zhang, K.; Batterman, S. Air pollution and health risks due to vehicle traffic. *Sci. Total Environ.* **2013**, *450-451*, 307–316, doi:10.1016/j.scitotenv.2013.01.074.

114. Dewees, D.N. Estimating the Time Costs of Highway Congestion. *Econometrica* **1979**, *47*, 1499, doi:10.2307/1914014.

115. Figliozzi, M.A. The impacts of congestion on commercial vehicle tour characteristics and costs. *Transportation Research Part E: Logistics and Transportation Review* **2010**, *46*, 496–506, doi:10.1016/j.tre.2009.04.005.

116. Konur, D.; Geunes, J. Analysis of traffic congestion costs in a competitive supply chain. *Transportation Research Part E: Logistics and Transportation Review* **2011**, *47*, 1–17, doi:10.1016/j.tre.2010.07.005.

117. McKinnon, A.; Edwards, J.; Piecyk, M.; Palmer, A. Traffic congestion, reliability and logistical performance: a multi-sectoral assessment. *International Journal of Logistics Research and Applications* **2009**, *12*, 331–345, doi:10.1080/13675560903181519.

118. McKinnon, A. The Effect of Traffic Congestion on the Efficiency of Logistical Operations. *International Journal of Logistics Research and Applications* **1999**, *2*, 111–128, doi:10.1080/13675569908901576.

119. Mondschein, A.; Taylor, B.D. Is traffic congestion overrated? Examining the highly variable effects of congestion on travel and accessibility. *Journal of Transport Geography* **2017**, *64*, 65–76, doi:10.1016/j.jtrangeo.2017.08.007.

120. Weisbrod, G.; Vary, D.; Treyz, G. Measuring Economic Costs of Urban Traffic Congestion to Business. *Transportation Research Record* **2003**, *1839*, 98–106, doi:10.3141/1839-10.

121. *Highway capacity manual*: *A guide for multimodal mobility analysis*, Sixth edition; Transportation Research Board: Washington, D.C, 2016, ISBN 9780309369978.

122. Cottrill, C.D.; Derrible, S. Leveraging Big Data for the Development of Transport Sustainability Indicators. *Journal of Urban Technology* **2015**, *22*, 45–64, doi:10.1080/10630732.2014.942094.

123. HERE Technologies. Build apps with HERE Maps API and SDK Platform Access | HERE Developer. Available online: https://developer.here.com/ (accessed on 11 February 2022).

124. TomTom. TomTom Developer Portal | Maps APIs and SDKs for Location Applications. Available online: https://developer.tomtom.com/ (accessed on 11 February 2022).

125. Google. Google Maps Platform | Google Developers. Available online: https://developers.google.com/maps (accessed on 11 February 2022).

126. Mapbox. Documentation | Mapbox. Available online: https://docs.mapbox.com/ (accessed on 11 February 2022).

127. Bing. Bing Maps Dev Center - Bing Maps Dev Center. Available online: https://www.bingmapsportal.com/ (accessed on 11 February 2022).

128. Hoffmann, S. Nominatim Documentation. Available online: https://nominatim.org/release-docs/develop/ (accessed on 11 February 2022).

129. ESRI. ArcGIS Developer. Available online: https://developers.arcgis.com/ (accessed on 11 February 2022).

130. MapQuest. MapQuest Developer Network | Mapping, Geocoding, Routes, Traffic | MapQuest Developer Network. Available online: https://developer.mapquest.com/ (accessed on 11 February 2022).

131. Ruci, E. Geocode.xyz API. Available online: https://geocode.xyz/api (accessed on 11 February 2022).

132. Inrix. INRIX for Developers - INRIX. Available online: https://inrix.com/developers/ (accessed on 11 February 2022).

133. OpenStreetMap. OpenStreetMap. Available online: https://www.openstreetmap.org/#map=19/22.84199/89.65966 (accessed on 11 February 2022).

134. Goeff Boeing. OSMnx 1.1.2 — OSMnx 1.1.2 documentation. Available online: https://osmnx.readthedocs.io/en/stable/ (accessed on 11 February 2022).

135. Boeing, G. OSMnx: A Python package to work with graph-theoretic OpenStreetMap street networks. *JOSS* **2017**, *2*, 215, doi:10.21105/joss.00215.

136. Boeing, G. OSMnx: New methods for acquiring, constructing, analyzing and visualizing complex street networks. *Computers, Environment and Urban Systems* **2017**, *65*, 126–139, doi:10.1016/j.compenvurbsys.2017.05.004.

137. Boeing, G. Urban Street Network Analysis in a Computational Notebook. *REGION* **2019**, *6*, 39–51, doi:10.18335/region.v6i3.278.

138. Boeing, G. A multi-scale analysis of 27,000 urban street networks: Every US city, town, urbanized area and Zillow neighborhood. *Environment and Planning B: Urban Analytics and City Science* **2020**, *47*, 590–608, doi:10.1177/2399808318784595.

139. Hermanns, G.; Kulkov, I.N.; Hemmerle, P.; Rehborn, H.; Koller, M.; Kerner, B.S.; Schreckenberg, M. Simulations of Synchronized Flow in TomTom Vehicle Data in Urban Traffic with the Kerner-Klenov Model in the Framework of the Three-Phase Traffic Theory. In *Traffic and Granular Flow '13*; Chraibi, M., Boltes, M., Schadschneider, A., Seyfried, A., Eds.; Springer International Publishing: Cham, 2015; pp 563–569, ISBN 978-3-319-10628-1.

140. Stanojevic, R.; Abbar, S.; Mokbel, M. MapReuse: Recycling Routing API Queries. In *2019 20th IEEE International Conference on Mobile Data Management (MDM).* 2019 20th IEEE International Conference on Mobile Data Management (MDM), Hong Kong, Hong Kong, 10–13 Jun. 2019; IEEE, 2019; pp 279–287, ISBN 978-1-7281-3363-8.

141. Dimitrov Berov, T. A vehicle routing planning system for goods distribution in urban areas using google maps and genetic algorithm. *IJTTE* **2016**, *6*, 159–167, doi:10.7708/ijtte.2016.6(2).04.

142. Li, R.; Cheng, C.; Qi, M.; Lai, W. Design of dynamic vehicle routing system based on online map service. In *2016 13th International Conference on Service Systems and Service Management (ICSSSM).* 2016 13th International Conference on Service Systems and Service Management (ICSSSM), Kunming, China, 24–26 Jun. 2016; IEEE, 2016; pp 1–5, ISBN 978-1-5090-2842-9.

143. Pearce, H.; Gong, Z.; Cai, X.; Bloss, W. Using routing apps to model real-time road traffic emissions. *Weather* **2020**, *75*, 341–346, doi:10.1002/wea.3729.

144. Nunzio, G. de; Ben Gharbia, I.; Sciarretta, A. A Time- and Energy-Optimal Routing Strategy for Electric Vehicles with Charging Constraints. In *2020 IEEE 23rd International Conference on Intelligent Transportation Systems (ITSC).* 2020 IEEE 23rd International Conference on Intelligent Transportation Systems (ITSC), Rhodes, Greece, 20–23 Sep. 2020; IEEE, 2020; pp 1–8, ISBN 978-1-7281-4149-7.

145. Santos, L.; Coutinho-Rodrigues, J.; Antunes, C.H. A web spatial decision support system for vehicle routing using Google Maps. *Decision Support Systems* **2011**, *51*, 1–9, doi:10.1016/j.dss.2010.11.008.

146. Levermore, T.; Sahinkaya, M.; Zweiri, Y.; Neaves, B. Real-Time Velocity Optimization to Minimize Energy Use in Passenger Vehicles. *Energies* **2017**, *10*, 30, doi:10.3390/en10010030.

147. Luxen, D.; Vetter, C. Real-time routing with OpenStreetMap data. In *Proceedings of the 19th ACM SIGSPATIAL International Conference on Advances in Geographic Information Systems - GIS '11.* the

19th ACM SIGSPATIAL International Conference, Chicago, Illinois, 01–04 Nov. 2011; Cruz, I., Agrawal, D., Eds.; ACM Press: New York, New York, USA, 2011; p 513, ISBN 9781450310314.

148. Hentschel, M.; Wagner, B. Autonomous robot navigation based on OpenStreetMap geodata. In *13th International IEEE Conference on Intelligent Transportation Systems.* 2010 13th International IEEE Conference on Intelligent Transportation Systems - (ITSC 2010), Funchal, Madeira Island, Portugal, 19–22 Sep. 2010; IEEE, 2010; pp 1645–1650, ISBN 978-1-4244-7657-2.

149. Bischoff, J.; Marquez-Fernandez, F.J.; Domingues-Olavarria, G.; Maciejewski, M.; Nagel, K. Impacts of vehicle fleet electrification in Sweden – a simulation-based assessment of long-distance trips. In *2019 6th International Conference on Models and Technologies for Intelligent Transportation Systems (MT-ITS).* 2019 6th International Conference on Models and Technologies for Intelligent Transportation Systems (MT-ITS), Cracow, Poland, 05–07 Jun. 2019; IEEE, 2019; pp 1–7, ISBN 978-1-5386-9484-8.

150. Chen, Y.; Rajabifard, A.; Day, J. An Advanced Web API for Isochrones Calculation Using OpenStreetMap Data. In *Planning Support Science for Smarter Urban Futures*; Geertman, S., Allan, A., Pettit, C., Stillwell, J., Eds.; Springer International Publishing: Cham, 2017; pp 185–205, ISBN 978-3-319-57818-7.

151. Alattar, M.A.; Cottrill, C.; Beecroft, M. Modelling cyclists' route choice using Strava and OSMnx: A case study of the City of Glasgow. *Transportation Research Interdisciplinary Perspectives* **2021**, *9*, 100301, doi:10.1016/j.trip.2021.100301.

152. Dingil, A.E.; Schweizer, J.; Rupi, F.; Stasiskiene, Z. Road network extraction with OSMNx and SUMOPy. In . SUMO 2018- Simulating Autonomous and Intermodal Transport Systems; EasyChair, 2018; 111-103.

153. Brabänder, C.; Braun, M. Bringing economies of integration into the costing of groupage freight. *Journal of Revenue and Pricing Management* **2020**, *12*, 191, doi:10.1057/s41272-020-00237-3.

154. Braun, M.; Kunkler, J.; Kellner, F. Towards Sustainable Cities: Utilizing Floating Car Data to Support Location-Based Road Network Performance Measurements. *Sustainability* **2020**, *12*, 8145, doi:10.3390/su12198145.

155. Kunkler, J.; Braun, M.; Kellner, F. Speed Limit Induced CO2 Reduction on Motorways: Enhancing Discussion Transparency through Data Enrichment of Road Networks. *Sustainability* **2021**, *13*, 395, doi:10.3390/su13010395.

156. Baker, J.A. Emergent pricing structures in LTL transportation. *Journal of Business Logistics* **1991**, *Vol. 12*, 191–202.

157. Özkaya, E.; Keskinocak, P.; Roshan Joseph, V.; Weight, R. Estimating and benchmarking Less-than-Truckload market rates. *Transportation Research Part E: Logistics and Transportation Review* **2010**, *46*, 667–682, doi:10.1016/j.tre.2009.09.004.

158. Bretzke, W.-R. *Logistische Netzwerke*, 1. Aufl.; Springer-Verlag: Berlin, Heidelberg, 2008, ISBN 3540779302.

159. Daganzo, C.F. The Break-Bulk Role of Terminals in Many-to-Many Logistic Networks. *Operations research* **1987**, *35*, 543–555, doi:10.1287/opre.35.4.543.

160. Lohre, D.; Monning, W. Erstellung von Haustarifen für Systemverkehre. In *Praxis des Controllings in Speditionen,* 1st ed.; Lohre, D., Ed.; Bildungswerk Spedition und Logistik: Frankfurt am Main, 2007; pp 197–219, ISBN 9783938995471.

161. Boone, N.; Quisbrock, T. Modelling Post-carriage Transport Costs in Groupage Networks. In *Advanced Manufacturing and Sustainable Logistics*: *8th International Heinz Nixdorf Symposium, IHNS 2010, Paderborn, Germany, April 21-22, 2010. Proceedings*; Dangelmaier, W., Blecken, A., Delius,

R., Klöpfer, S., Eds.; Springer-Verlag Berlin Heidelberg: Berlin, Heidelberg, 2010; pp 332–344, ISBN 978-3-642-12461-7.

162. Harrington, L.H. The abc's of motor carrier economics: Understanding a Carrier's Rate Structure is Key to Getting the Best Service and Price. *Transportation & Distribution* **1997**, *38*.
163. Ying, J.S.; Keeler, T.E. Pricing in a Deregulated Environment: The Motor Carrier Experience. *The RAND Journal of Economics* **1991**, *22*, 264, doi:10.2307/2601022.
164. Smith, L.D.; Campbell, J.F.; Mundy, R. Modeling net rates for expedited freight services. *Transportation Research Part E: Logistics and Transportation Review* **2007**, *43*, 192–207, doi:10.1016/j.tre.2005.11.001.
165. Bø, E.; Hammervoll, T. Cost-based pricing of transportation services in a wholesaler–carrier relationship: an MS Excel spreadsheet decision tool. *International Journal of Logistics Research and Applications* **2010**, *13*, 197–210, doi:10.1080/13675560903271203.
166. Bokor, Z. Calculation model for transport costing. *Per. Pol. Transp. Eng.* **2011**, *39*, 43, doi:10.3311/pp.tr.2011-1.08.
167. Wittenbrink, P. *Transportmanagement*: *Kostenoptimierung, Green Logistics und Herausforderungen an der Schnittstelle Rampe*, 2nd ed.; Gabler: Wiesbaden, 2014, ISBN 978-3834933768.
168. Kaplan, R.S.; Anderson, S.R. Time-Driven Activity-Based Costing. *SSRN Journal* **2003**, doi:10.2139/ssrn.485443.
169. Keeler, T.E. Deregulation and Scale Economies in the U. S. Trucking Industry: An Econometric Extension of the Survivor Principle. *The Journal of Law & Economics* **1989**, *32*, 229–253.
170. Fleischmann, B. Designing distribution systems with transport economies of scale. *European Journal of Operational Research* **1993**, *70*, 31–42, doi:10.1016/0377-2217(93)90230-K.
171. Lin, C.-C.; Lin, D.-Y.; Young, M.M. Price planning for time-definite less-than-truckload freight services. *Transportation Research Part E: Logistics and Transportation Review* **2009**, *45*, 525–537, doi:10.1016/j.tre.2008.12.004.
172. Giordano, J.N. Economies of scale after deregulation in LTL trucking: a test case for the survivor technique. *Manage. Decis. Econ.* **2008**, *29*, 357–370, doi:10.1002/mde.1411.
173. McMullen, B.S.; Tanaka, H. An Econometric Analysis of Differences between Motor Carriers: Implications for Market Structure. *Quarterly Journal of Business and Economics* **1995**, *34*, 16–29.
174. Shah, R.; Ward, P.T. Defining and developing measures of lean production. *Journal of Operations Management* **2007**, *25*, 785–805, doi:10.1016/j.jom.2007.01.019.
175. Mandziuk, J. New Shades of the Vehicle Routing Problem: Emerging Problem Formulations and Computational Intelligence Solution Methods. *IEEE Trans. Emerg. Top. Comput. Intell.* **2019**, *3*, 230–244, doi:10.1109/TETCI.2018.2886585.
176. Cordeau, J.-F.; Gendreau, M.; Laporte, G.; Potvin, J.-Y.; Semet, F. A guide to vehicle routing heuristics. *J Oper Res Soc* **2002**, *53*, 512–522, doi:10.1057/palgrave/jors/2601319.
177. Clarke, G.; Wright, J.W. Scheduling of Vehicles from a Central Depot to a Number of Delivery Points. *Operations research* **1964**, *12*, 568–581, doi:10.1287/opre.12.4.568.
178. Bräysy, O.; Gendreau, M. Vehicle Routing Problem with Time Windows: Part I: Route Construction and Local Search Algorithms. *Transportation Science* **2005**, *39*, 104–118.
179. Bräysy, O.; Gendreau, M. Vehicle Routing Problem with Time Windows: Part II: Metaheuristics. *Transportation Science* **2005**, *39*, 119–139.
180. Thomas, A.L. *The allocation problem in financial accounting theory;* American Accounting Association: Sarasota, 1969.

181. Thomas, A.L. *The allocation problem: Part two;* American Accounting Association: Sarasota, 1974.

182. Fishburn, P.C.; Pollak, H.O. Fixed-Route Cost Allocation. *The American Mathematical Monthly* **1983**, *90*, 366–378, doi:10.1080/00029890.1983.11971234.

183. Young, H.P. Cost allocation. In *Handbook of Game Theory with Economic Applications*; Young, H.P., Ed.; Elsevier, 1994; pp 1193–1235, ISBN 1574-0005.

184. Kellner, F.; Otto, A. Allocating CO2 emissions to shipments in road freight transportation. *Journal of Management Control* **2012**, *22*, 451–479, doi:10.1007/s00187-011-0143-6.

185. Kellner, F.; Otto, A.; Lienland, B. Cost assignment paradox: Indirect tooling costs and production orders. In *Advances in management accounting*; Epstein, M.J., Lee, J.Y., Eds.; Emerald: Bingley, U.K, 2014; pp 211–251, ISBN 978-1-78350-632-3.

186. Balachandran, B.V.; Ramakrishnan, R.T.S. Joint Cost Allocation: A Unified Approach. *The Accounting Review* **1981**, *56*, 85.

187. Hartmann, H. *Kosten- und Leistungsrechnung in der Spedition*: *Grundlagen und praktische Anwendungen*, 3., aktualisierte und erweiterte Auflage; De Gruyter Oldenbourg: Berlin/Boston, 2019, ISBN 978-3-11-055947-7.

188. Cividino, S.; Halbac-Cotoara-Zamfir, R.; Salvati, L. Revisiting the "City Life Cycle": Global Urbanization and Implications for Regional Development. *Sustainability* **2020**, *12*, 1151, doi:10.3390/su12031151.

189. Ameen, R.F.M.; Mourshed, M. Urban sustainability assessment framework development: The ranking and weighting of sustainability indicators using analytic hierarchy process. *Sustainable Cities and Society* **2019**, *44*, 356–366, doi:10.1016/j.scs.2018.10.020.

190. Huang, S.-L.; Wong, J.-H.; Chen, T.-C. A framework of indicator system for measuring Taipei's urban sustainability. *Landscape and Urban Planning* **1998**, *42*, 15–27, doi:10.1016/S0169-2046(98)00054-1.

191. Tang, J.; Zhu, H.-L.; Liu, Z.; Jia, F.; Zheng, X.-X. Urban Sustainability Evaluation under the Modified TOPSIS Based on Grey Relational Analysis. *Int. J. Environ. Res. Public Health* **2019**, *16*, doi:10.3390/ijerph16020256.

192. Verma, P.; Raghubanshi, A.S. Urban sustainability indicators: Challenges and opportunities. *Ecological Indicators* **2018**, *93*, 282–291, doi:10.1016/j.ecolind.2018.05.007.

193. Gillis, D.; Semanjski, I.; Lauwers, D. How to Monitor Sustainable Mobility in Cities? Literature Review in the Frame of Creating a Set of Sustainable Mobility Indicators. *Sustainability* **2016**, *8*, 29, doi:10.3390/su8010029.

194. Shen, L.-Y.; Jorge Ochoa, J.; Shah, M.N.; Zhang, X. The application of urban sustainability indicators – A comparison between various practices. *Habitat International* **2011**, *35*, 17–29, doi:10.1016/j.habitatint.2010.03.006.

195. Li, F.; Su, Y.; Xie, J.; Zhu, W.; Wang, Y. The Impact of High-Speed Rail Opening on City Economics along the Silk Road Economic Belt. *Sustainability* **2020**, *12*, 3176, doi:10.3390/su12083176.

196. Zhang; Guan; Zhu. Analysis of Travel Mode Choice Behavior Considering the Indifference Threshold. *Sustainability* **2019**, *11*, 5495, doi:10.3390/su11195495.

197. Ortega, J.; Tóth, J.; Péter, T.; Moslem, S. An Integrated Model of Park-And-Ride Facilities for Sustainable Urban Mobility. *Sustainability* **2020**, *12*, 4631, doi:10.3390/su12114631.

198. Li, X.-H.; Huang, L.; Li, Q.; Liu, H.-C. Passenger Satisfaction Evaluation of Public Transportation Using Pythagorean Fuzzy MULTIMOORA Method under Large Group Environment. *Sustainability* **2020**, *12*, 4996, doi:10.3390/su12124996.

199. Hamurcu, M.; Eren, T. Strategic Planning Based on Sustainability for Urban Transportation: An Application to Decision-Making. *Sustainability* **2020**, *12*, 3589, doi:10.3390/su12093589.

200. Gumbo, T.; Moyo, T. Exploring the Interoperability of Public Transport Systems for Sustainable Mobility in Developing Cities: Lessons from Johannesburg Metropolitan City, South Africa. *Sustainability* **2020**, *12*, 5875, doi:10.3390/su12155875.

201. Castanho, R.A.; Behradfar, A.; Vulevic, A.; Naranjo Gómez, J.M. Analyzing Transportation Sustainability in the Canary Islands Archipelago. *Infrastructures* **2020**, *5*, 58, doi:10.3390/infrastructures5070058.

202. Fernandes, P.; Vilaça, M.; Macedo, E.; Sampaio, C.; Bahmankhah, B.; Bandeira, J.M.; Guarnaccia, C.; Rafael, S.; Fernandes, A.P.; Relvas, H.; et al. Integrating road traffic externalities through a sustainability indicator. *Sci. Total Environ.* **2019**, *691*, 483–498, doi:10.1016/j.scitotenv.2019.07.124.

203. Mahmoudi, R.; Shetab-Boushehri, S.-N.; Hejazi, S.R.; Emrouznejad, A. Determining the relative importance of sustainability evaluation criteria of urban transportation network. *Sustainable Cities and Society* **2019**, *47*, 101493, doi:10.1016/j.scs.2019.101493.

204. Ruiz, A.; Guevara, J. Sustainable Decision-Making in Road Development: Analysis of Road Preservation Policies. *Sustainability* **2020**, *12*, 872, doi:10.3390/su12030872.

205. Wang, S.; Yu, D.; Kwan, M.-P.; Zhou, H.; Li, Y.; Miao, H. The Evolution and Growth Patterns of the Road Network in a Medium-Sized Developing City: A Historical Investigation of Changchun, China, from 1912 to 2017. *Sustainability* **2019**, *11*, 5307, doi:10.3390/su11195307.

206. Liu, J.; Lu, H.; Chen, M.; Wang, J.; Zhang, Y. Macro Perspective Research on Transportation Safety: An Empirical Analysis of Network Characteristics and Vulnerability. *Sustainability* **2020**, *12*, 6267, doi:10.3390/su12156267.

207. Calvo-Poyo, F.; Navarro-Moreno, J.; Oña, J. de. Road Investment and Traffic Safety: An International Study. *Sustainability* **2020**, *12*, 6332, doi:10.3390/su12166332.

208. Fernie, J.; Pfab, F.; Marchant, C. Retail Grocery Logistics in the UK. *International Journal of Logistics Management* **2000**, *11*, 83–90, doi:10.1108/09574090010806182.

209. Golob, T.F.; Regan, A.C. Traffic congestion and trucking managers' use of automated routing and scheduling. *Transportation Research Part E: Logistics and Transportation Review* **2003**, *39*, 61–78, doi:10.1016/S1366-5545(02)00024-8.

210. Figliozzi, M.A. The impacts of congestion on time-definitive urban freight distribution networks CO2 emission levels: Results from a case study in Portland oregon. *Transportation Research Part C: Emerging Technologies* **2011**, *19*, 766–778, doi:10.1016/j.trc.2010.11.002.

211. Chen, A.; Yang, H.; Lo, H.K.; Tang, W.H. Capacity reliability of a road network: an assessment methodology and numerical results. *Transportation Research Part B: Methodological* **2002**, *36*, 225–252, doi:10.1016/S0191-2615(00)00048-5.

212. Fancello, G.; Carta, M.; Fadda, P. A Modeling Tool for Measuring the Performance of Urban Road Networks. *Procedia - Social and Behavioral Sciences* **2014**, *111*, 559–566, doi:10.1016/j.sbspro.2014.01.089.

213. Jenelius, E.; Mattsson, L.-G. Road network vulnerability analysis of area-covering disruptions: A grid-based approach with case study. *Transportation Research Part A: Policy and Practice* **2012**, *46*, 746–760, doi:10.1016/j.tra.2012.02.003.

214. Milevich, D.; Melnikov, V.; Karbovskii, V.; Krzhizhanovskaya, V. Simulating an Impact of Road Network Improvements on the Performance of Transportation Systems under Critical Load: Agent-based Approach. *Procedia Computer Science* **2016**, *101*, 253–261, doi:10.1016/j.procs.2016.11.030.

215. Loder, A.; Ambühl, L.; Menendez, M.; Axhausen, K.W. Understanding traffic capacity of urban networks. *Sci. Rep.* **2019**, *9*, 16283, doi:10.1038/s41598-019-51539-5.

216. Afrin, T.; Yodo, N. A Survey of Road Traffic Congestion Measures towards a Sustainable and Resilient Transportation System. *Sustainability* **2020**, *12*, 4660, doi:10.3390/su12114660.

217. Luca, S. de; Di Pace, R.; Memoli, S.; Pariota, L. Sustainable Traffic Management in an Urban Area: An Integrated Framework for Real-Time Traffic Control and Route Guidance Design. *Sustainability* **2020**, *12*, 726, doi:10.3390/su12020726.

218. Sun, X.; Lin, K.; Jiao, P.; Lu, H. The Dynamical Decision Model of Intersection Congestion Based on Risk Identification. *Sustainability* **2020**, *12*, 5923, doi:10.3390/su12155923.

219. Russo, F.; Comi, A. Investigating the Effects of City Logistics Measures on the Economy of the City. *Sustainability* **2020**, *12*, 1439, doi:10.3390/su12041439.

220. Baghestani, A.; Tayarani, M.; Allahviranloo, M.; Gao, H.O. Evaluating the Traffic and Emissions Impacts of Congestion Pricing in New York City. *Sustainability* **2020**, *12*, 3655, doi:10.3390/su12093655.

221. Borza, S.; Inta, M.; Serbu, R.; Marza, B. Multi-Criteria Analysis of Pollution Caused by Auto Traffic in a Geographical Area Limited to Applicability for an Eco-Economy Environment. *Sustainability* **2018**, *10*, 4240, doi:10.3390/su10114240.

222. Zhang, W.; Lu, J.; Xu, P.; Zhang, Y. Moving towards Sustainability: Road Grades and On-Road Emissions of Heavy-Duty Vehicles—A Case Study. *Sustainability* **2015**, *7*, 12644–12671, doi:10.3390/su70912644.

223. Kleizienė, R.; Šernas, O.; Vaitkus, A.; Simanavičienė, R. Asphalt Pavement Acoustic Performance Model. *Sustainability* **2019**, *11*, 2938, doi:10.3390/su11102938.

224. Astarita, V.; Giofrè, V.P.; Guido, G.; Vitale, A. A review of traffic signal control methods and experiments based on Floating Car Data (FCD). *Procedia Computer Science* **2020**, *175*, 745–751, doi:10.1016/j.procs.2020.07.110.

225. Creutzig, F.; Franzen, M.; Moeckel, R.; Heinrichs, D.; Nagel, K.; Nieland, S.; Weisz, H. Leveraging digitalization for sustainability in urban transport. *Glob. Sustain.* **2019**, *2*, doi:10.1017/sus.2019.11.

226. Kong, L.; Liu, Z.; Wu, J. A systematic review of big data-based urban sustainability research: State-of-the-science and future directions. *Journal of Cleaner Production* **2020**, *273*, 123142, doi:10.1016/j.jclepro.2020.123142.

227. Yu, B.; Wang, Z.; Mu, H.; Sun, L.; Hu, F. Identification of Urban Functional Regions Based on Floating Car Track Data and POI Data. *Sustainability* **2019**, *11*, 6541, doi:10.3390/su11236541.

228. Sun, D.; Leurent, F.; Xie, X. Floating Car Data mining: Identifying vehicle types on the basis of daily usage patterns. *Transportation Research Procedia* **2020**, *47*, 147–154, doi:10.1016/j.trpro.2020.03.087.

229. Ranieri, L.; Digiesi, S.; Silvestri, B.; Roccotelli, M. A Review of Last Mile Logistics Innovations in an Externalities Cost Reduction Vision. *Sustainability* **2018**, *10*, 782, doi:10.3390/su10030782.

230. Wang, S.; Yu, D.; Ma, X.; Xing, X. Analyzing urban traffic demand distribution and the correlation between traffic flow and the built environment based on detector data and POIs. *Eur. Transp. Res. Rev.* **2018**, *10*, doi:10.1186/s12544-018-0325-5.

231. Wang, S.; Yu, D.; Kwan, M.-P.; Zheng, L.; Miao, H.; Li, Y. The impacts of road network density on motor vehicle travel: An empirical study of Chinese cities based on network theory. *Transportation Research Part A: Policy and Practice* **2020**, *132*, 144–156, doi:10.1016/j.tra.2019.11.012.

232. Saedi, R.; Saeedmanesh, M.; Zockaie, A.; Saberi, M.; Geroliminis, N.; Mahmassani, H.S. Estimating network travel time reliability with network partitioning. *Transportation Research Part C: Emerging Technologies* **2020**, *112*, 46–61, doi:10.1016/j.trc.2020.01.013.

233. Serper, E.Z.; Alumur, S.A. The design of capacitated intermodal hub networks with different vehicle types. *Transportation Research Part B: Methodological* **2016**, *86*, 51–65, doi:10.1016/j.trb.2016.01.011.

234. Lagarda-Leyva, E.A.; Bueno-Solano, A.; Vea-Valdez, H.P.; Machado, D.O. Dynamic Model and Graphical User Interface: A Solution for the Distribution Process of Regional Products. *Applied Sciences* **2020**, *10*, 4481, doi:10.3390/app10134481.

235. Leung, A.; Burke, M.; Cui, J.; Perl, A. Fuel price changes and their impacts on urban transport – a literature review using bibliometric and content analysis techniques, 1972–2017. *Transport Reviews* **2019**, *39*, 463–484, doi:10.1080/01441647.2018.1523252.

236. Santosa, W.; Joewono, T.B. An evaluation of road network performance in Indonesia. *Proceedings of the Eastern Asia Society for Transportation Studies* **2005**, 2418–2433.

237. Berens, W. The suitability of the weighted lp-norm in estimating actual road distances. *European Journal of Operational Research* **1988**, *34*, 39–43, doi:10.1016/0377-2217(88)90453-5.

238. Chowdhury, S.; Ceder, A.; Velty, B. Measuring Public-Transport Network Connectivity Using Google Transit with Comparison across Cities. *JPT* **2014**, *17*, 76–92, doi:10.5038/2375-0901.17.4.5.

239. He, F.; Yan, X.; Liu, Y.; Ma, L. A Traffic Congestion Assessment Method for Urban Road Networks Based on Speed Performance Index. *Procedia Engineering* **2016**, *137*, 425–433, doi:10.1016/j.proeng.2016.01.277.

240. Mohan Rao, A.; Ramachandra Rao, K. Measuring Urban Traffic Congestion - A Review. *IJTTE* **2012**, *2*, 286–305, doi:10.7708/ijtte.2012.2(4).01.

241. Altintasi, O.; Tuydes-Yaman, H.; Tuncay, K. Detection of urban traffic patterns from Floating Car Data (FCD). *Transportation Research Procedia* **2017**, *22*, 382–391, doi:10.1016/j.trpro.2017.03.057.

242. Chen, B.Y.; Lam, W.H.K.; Sumalee, A.; Li, Q.; Shao, H.; Fang, Z. Finding Reliable Shortest Paths in Road Networks Under Uncertainty. *Netw Spat Econ* **2013**, *13*, 123–148, doi:10.1007/s11067-012-9175-1.

243. Thoen, S.; Tavasszy, L.; Bok, M. de; Correia, G.; van Duin, R. Descriptive modeling of freight tour formation: A shipment-based approach. *Transportation Research Part E: Logistics and Transportation Review* **2020**, *140*, 101989, doi:10.1016/j.tre.2020.101989.

244. Moraes Ramos, G. de; Mai, T.; Daamen, W.; Frejinger, E.; Hoogendoorn, S.P. Route choice behaviour and travel information in a congested network: Static and dynamic recursive models. *Transportation Research Part C: Emerging Technologies* **2020**, *114*, 681–693, doi:10.1016/j.trc.2020.02.014.

245. Ciscal-Terry, W.; Dell'Amico, M.; Hadjidimitriou, N.S.; Iori, M. An analysis of drivers route choice behaviour using GPS data and optimal alternatives. *Journal of Transport Geography* **2016**, *51*, 119–129, doi:10.1016/j.jtrangeo.2015.12.003.

246. Romano Alho, A.; Sakai, T.; Chua, M.H.; Jeong, K.; Jing, P.; Ben-Akiva, M. Exploring Algorithms for Revealing Freight Vehicle Tours, Tour-Types and Tour-Chain-Types from GPS Vehicle Traces and Stop Activity Data. Journal of Big Data Analytics in Transportation, 1(2-3), 175-190 **2019**, doi:10.1007/S42421-019-00011-X.

247. Shao, H.; Lam, W.H.; Sumalee, A.; Chen, A. Journey time estimator for assessment of road network performance under demand uncertainty. *Transportation Research Part C: Emerging Technologies* **2013**, *35*, 244–262, doi:10.1016/j.trc.2012.12.002.

248. Greenwood, I.D.; Dunn, R.C.; Raine, R.R. Estimating the Effects of Traffic Congestion on Fuel Consumption and Vehicle Emissions Based on Acceleration Noise. *J. Transp. Eng.* **2007**, *133*, 96–104, doi:10.1061/(ASCE)0733-947X(2007)133:2(96).

249. Thurgood, G.S. Development Of A Freeway Congestion Index Using An Instrumented Vehicle. *Transportation Research Record* **1995**, 21-29.

250. Hansen, I. Determination and Evaluation of Traffic Congestion Costs. *European Journal of Transport and Infrastructure Research* **2001**, *1*, 61–72, doi:10.18757/ejtir.2001.1.1.2627.

251. Sun, D.J.; Liu, X.; Ni, A.; Peng, C. Traffic Congestion Evaluation Method for Urban Arterials. *Transportation Research Record* **2014**, *2461*, 9–15, doi:10.3141/2461-02.

252. Cohn, N. Real-Time Traffic Information and Navigation. *Transportation Research Record* **2009**, *2129*, 129–135, doi:10.3141/2129-15.

253. Sun, D.; Zhang, C.; Zhang, L.; Chen, F.; Peng, Z.-R. Urban travel behavior analyses and route prediction based on floating car data. *Transportation Letters* **2014**, *6*, 118–125, doi:10.1179/1942787514Y.0000000017.

254. Yong-chuan, Z.; Xiao-qing, Z.; li-ting, Z.; Zhen-ting, C. Traffic Congestion Detection Based On GPS Floating-Car Data. *Procedia Engineering* **2011**, *15*, 5541–5546, doi:10.1016/j.proeng.2011.08.1028.

255. Zhao, N.; Yu, L.; Zhao, H.; Guo, J.; Wen, H. Analysis of Traffic Flow Characteristics on Ring Road Expressways in Beijing. *Transportation Research Record* **2009**, *2124*, 178–185, doi:10.3141/2124-17.

256. Wang, X.; Liu, H.; Yu, R.; Deng, B.; Chen, X.; Wu, B. Exploring Operating Speeds on Urban Arterials Using Floating Car Data: Case Study in Shanghai. *J. Transp. Eng.* **2014**, *140*, 4014044, doi:10.1061/(ASCE)TE.1943-5436.0000685.

257. Kong, X.; Xu, Z.; Shen, G.; Wang, J.; Yang, Q.; Zhang, B. Urban traffic congestion estimation and prediction based on floating car trajectory data. *Future Generation Computer Systems* **2016**, *61*, 97–107, doi:10.1016/j.future.2015.11.013.

258. Rempe, F.; Franeck, P.; Fastenrath, U.; Bogenberger, K. A phase-based smoothing method for accurate traffic speed estimation with floating car data. *Transportation Research Part C: Emerging Technologies* **2017**, *85*, 644–663, doi:10.1016/j.trc.2017.10.015.

259. Xu, L.; Yue, Y.; Li, Q. Identifying Urban Traffic Congestion Pattern from Historical Floating Car Data. *Procedia - Social and Behavioral Sciences* **2013**, *96*, 2084–2095, doi:10.1016/J.SBSPRO.2013.08.235.

260. Kellner, F. Insights into the effect of traffic congestion on distribution network characteristics – a numerical analysis based on navigation service data. *International Journal of Logistics Research and Applications* **2016**, *19*, 395–423, doi:10.1080/13675567.2015.1094043.

261. Gong, Y.; Rimba, P.; Sinnott, R. A Big Data Architecture for Near Real-time Traffic Analytics. In *Companion Proceedings of the10th International Conference on Utility and Cloud Computing*. Companion the10th International Conference, Austin, Texas, USA, 12/5/2017 - 12/8/2017; Anjum, A., Ed.; ACM: New York, NY, 2017; pp 157–162, ISBN 9781450351959.

262. Zhang, D.; Shou, Y.; Xu, J. The modeling of big traffic data processing based on cloud computing. In *2016 12th World Congress on Intelligent Control and Automation (WCICA)*, June 12-15, 2016, Guilin, China. 2016 12th World Congress on Intelligent Control and Automation (WCICA), Guilin, China, 6/12/2016 - 6/15/2016; IEEE: Piscataway, NJ, 2016; pp 2394–2399, ISBN 978-1-4673-8414-8.

263. Hirako, K.; Kani, S.; Morisaki, Y.; Fujiu, M.; Nishino, T.; Takayama, J. Estimations of Bus Stop Territories using Reachable Area Analysis Focusing on Travel Behavior of Elderly to Medical Facilities. *International Journal of Engineering Research & Technology* **2020**, *09*, 516–522.

264. Phan, T.-K.; Jung, H.; Kim, U.-M. An efficient algorithm for maximizing range sum queries in a road network. *ScientificWorldJournal.* **2014**, *2014*, 541602, doi:10.1155/2014/541602.

265. Williams, M.J.; Musolesi, M. Spatio-temporal networks: reachability, centrality and robustness. *R. Soc. Open Sci.* **2016**, *3*, 160196, doi:10.1098/rsos.160196.

266. Casadei, G.; Bertrand, V.; Gouin, B.; Canudas-de-Wit, C. Aggregation and travel time calculation over large scale traffic networks: An empiric study on the Grenoble City. *Transportation Research Part C: Emerging Technologies* **2018**, *95*, 713–730, doi:10.1016/j.trc.2018.07.033.

267. Nuzzolo, A.; Comi, A.; Polimeni, A. Urban Freight Vehicle Flows: an Analysis of Freight Delivery Patterns through Floating Car Data. *Transportation Research Procedia* **2020**, *47*, 409–416, doi:10.1016/j.trpro.2020.03.116.

268. Sofwan, A.; Soetrisno, Y.A.A.; Ramadhani, N.P.; Rahmayani, A.; Handoyo, E.; Arfan, M. Vehicle Distance Measurement Tuning using Haversine and Micro-Segmentation. In *2019 International Seminar on Intelligent Technology and Its Applications (ISITIA).* 2019 International Seminar on Intelligent Technology and Its Applications (ISITIA), Surabaya, Indonesia; IEEE; pp 239–243, ISBN 978-1-7281-3749-0.

269. Levinson, H.S.; Lomax, T.J. Developing a Travel Time Congestion Index. *Transportation Research Record* **1996**, *1564*, 1–10, doi:10.1177/0361198196156400101.

270. European Environment Agency. EMEP/EEA air pollutant emission inventory guidebook 2019 **2019**.

271. Kellner, F. Exploring the impact of traffic congestion on CO2 emissions in freight distribution networks. *Logist. Res.* **2016**, *9*, doi:10.1007/s12159-016-0148-5.

272. *DIN EN 16258:2012*: *Methodology for calculation and declaration of energy consumption and GHG emissions of transport services (freight and passengers)*.

273. Lejri, D.; Can, A.; Schiper, N.; Leclercq, L. Accounting for traffic speed dynamics when calculating COPERT and PHEM pollutant emissions at the urban scale. *Transportation Research Part D: Transport and Environment* **2018**, *63*, 588–603, doi:10.1016/j.trd.2018.06.023.

274. O'Driscoll, R.; ApSimon, H.M.; Oxley, T.; Molden, N.; Stettler, M.E.; Thiyagarajah, A. A Portable Emissions Measurement System (PEMS) study of NOx and primary NO2 emissions from Euro 6 diesel passenger cars and comparison with COPERT emission factors. *Atmospheric Environment* **2016**, *145*, 81–91, doi:10.1016/j.atmosenv.2016.09.021.

275. Lisle, S. de. Comparison of Road Traffic Noise Prediction Models: CoRTN, TNM, NMPB, ASJ RTN. *Acoust Aust* **2016**, *44*, 409–413, doi:10.1007/s40857-016-0061-8.

276. Great Britain Department of Transport, Welsh Office. *Calculation of road traffic noise;* H.M.S.O: London, 1988, ISBN 0115508473.

277. Givargis, S.; Mahmoodi, M. Converting the UK calculation of road traffic noise (CORTN) to a model capable of calculating LAeq,1h for the Tehran's roads. *Applied Acoustics* **2008**, *69*, 1108–1113, doi:10.1016/j.apacoust.2007.08.003.

278. O'Malley, V.; King, E.; Kenny, L.; Dilworth, C. Assessing methodologies for calculating road traffic noise levels in Ireland – Converting CRTN indicators to the EU indicators (Lden, Lnight). *Applied Acoustics* **2009**, *70*, 284–296, doi:10.1016/j.apacoust.2008.04.003.

279. Kuramochi, T.; Roelfsema, M.; Hsu, A.; Lui, S.; Weinfurter, A.; Chan, S.; Hale, T.; Clapper, A.; Chang, A.; Höhne, N. Beyond national climate action: the impact of region, city and business

commitments on global greenhouse gas emissions. *Climate Policy* **2020**, *20*, 275–291, doi:10.1080/14693062.2020.1740150.

280. Manne, A.; Richels, R. The Greenhouse Debate: Econonmic Efficiency, Burden Sharing and Hedging Strategies. *EJ* **1995**, *16*, doi:10.5547/ISSN0195-6574-EJ-Vol16-No4-1.
281. Woensel, T.; Creten, R.; Vandaele, N. Managing the environmental externalities of traffic logistics: The issue of emissions. *Production and Operations Management* **2001**, *10*, 207–223, doi:10.1111/j.1937-5956.2001.tb00079.x.
282. Durbin, T.D.; Johnson, K.; Miller, J.W.; Maldonado, H.; Chernich, D. Emissions from heavy-duty vehicles under actual on-road driving conditions. *Atmospheric Environment* **2008**, *42*, 4812–4821, doi:10.1016/j.atmosenv.2008.02.006.
283. Santos, G. Road transport and CO 2 emissions: What are the challenges? *Transport Policy* **2017**, *59*, 71–74, doi:10.1016/j.tranpol.2017.06.007.
284. Liang, Y.; Niu, D.; Wang, H.; Li, Y. Factors Affecting Transportation Sector CO2 Emissions Growth in China: An LMDI Decomposition Analysis. *Sustainability* **2017**, *9*, 1730, doi:10.3390/su9101730.
285. Klumpp, M. To Green or Not to Green: A Political, Economic and Social Analysis for the Past Failure of Green Logistics. *Sustainability* **2016**, *8*, 441, doi:10.3390/su8050441.
286. Hickman, R.; Banister, D. Looking over the horizon: Transport and reduced CO2 emissions in the UK by 2030. *Transport Policy* **2007**, *14*, 377–387, doi:10.1016/j.tranpol.2007.04.005.
287. Haas, T.; Sander, H. Decarbonizing Transport in the European Union: Emission Performance Standards and the Perspectives for a European Green Deal. *Sustainability* **2020**, *12*, 8381, doi:10.3390/su12208381.
288. Lajunen, A.; Kivekäs, K.; Vepsäläinen, J.; Tammi, K. Influence of Increasing Electrification of Passenger Vehicle Fleet on Carbon Dioxide Emissions in Finland. *Sustainability* **2020**, *12*, 5032, doi:10.3390/su12125032.
289. Rietmann, N.; Hügler, B.; Lieven, T. Forecasting the trajectory of electric vehicle sales and the consequences for worldwide CO2 emissions. *Journal of Cleaner Production* **2020**, *261*, 121038, doi:10.1016/j.jclepro.2020.121038.
290. Bienias, K.; Kowalska-Pyzalska, A.; Ramsey, D. What do people think about electric vehicles? An initial study of the opinions of car purchasers in Poland. *Energy Reports* **2020**, *6*, 267–273, doi:10.1016/j.egyr.2019.08.055.
291. Kapustin, N.O.; Grushevenko, D.A. Long-term electric vehicles outlook and their potential impact on electric grid. *Energy Policy* **2020**, *137*, 111103, doi:10.1016/j.enpol.2019.111103.
292. Funke, S.Á.; Sprei, F.; Gnann, T.; Plötz, P. How much charging infrastructure do electric vehicles need? A review of the evidence and international comparison. *Transportation Research Part D: Transport and Environment* **2019**, *77*, 224–242, doi:10.1016/j.trd.2019.10.024.
293. Greene, D.L.; Kontou, E.; Borlaug, B.; Brooker, A.; Muratori, M. Public charging infrastructure for plug-in electric vehicles: What is it worth? *Transportation Research Part D: Transport and Environment* **2020**, *78*, 102182, doi:10.1016/j.trd.2019.11.011.
294. Fridstrøm, L. Who will bell the cat? On the environmental and sustainability risks of electric vehicles: A comment. *Transportation Research Part A: Policy and Practice* **2020**, *135*, 354–357, doi:10.1016/j.tra.2020.03.017.
295. Kawamoto, R.; Mochizuki, H.; Moriguchi, Y.; Nakano, T.; Motohashi, M.; Sakai, Y.; Inaba, A. Estimation of CO2 Emissions of Internal Combustion Engine Vehicle and Battery Electric Vehicle Using LCA. *Sustainability* **2019**, *11*, 2690, doi:10.3390/su11092690.

296. Ram, M.; Child, M.; Aghahosseini, A.; Bogdanov, D.; Lohrmann, A.; Breyer, C. A comparative analysis of electricity generation costs from renewable, fossil fuel and nuclear sources in G20 countries for the period 2015-2030. *Journal of Cleaner Production* **2018**, *199*, 687–704, doi:10.1016/j.jclepro.2018.07.159.

297. Canals Casals, L.; Martinez-Laserna, E.; Amante García, B.; Nieto, N. Sustainability analysis of the electric vehicle use in Europe for CO2 emissions reduction. *Journal of Cleaner Production* **2016**, *127*, 425–437, doi:10.1016/j.jclepro.2016.03.120.

298. Shirazinejad, R.S.; Dissanayake, S. Speed Characteristics in Relation to Speed Limit Increase and Its Influence on Driver's Speed Selection Behavior. *Sustainability* **2020**, *12*, 1369, doi:10.3390/su12041369.

299. Yang, J.; Xu, J.; Gao, C.; Bai, G.; Xie, L.; Li, M. Modeling of the Relationship Between Speed Limit and Characteristic Speed of Expressway Traffic Flow. *Sustainability* **2019**, *11*, 4621, doi:10.3390/su11174621.

300. Fergusson, M. The effect of vehicle speeds on emissions. *Energy Policy* **1994**, *22*, 103–106, doi:10.1016/0301-4215(94)90126-0.

301. Keller, J.; Andreani-Aksoyoglu, S.; Tinguely, M.; Flemming, J.; Heldstab, J.; Keller, M.; Zbinden, R.; Prevot, A.S. The impact of reducing the maximum speed limit on motorways in Switzerland to 80km h−1 on emissions and peak ozone. *Environmental Modelling & Software* **2008**, *23*, 322–332, doi:10.1016/j.envsoft.2007.04.008.

302. Frey, H.C.; Rouphail, N.M.; Zhai, H. Speed- and Facility-Specific Emission Estimates for On-Road Light-Duty Vehicles on the Basis of Real-World Speed Profiles. *Transportation Research Record: Journal of the Transportation Research Board* **2006**, 128–137.

303. Chang, C.-C.; Wang, C.-M. Evaluating the effects of speed reduce for shipping costs and CO2 emission. *Transportation Research Part D: Transport and Environment* **2014**, *31*, 110–115, doi:10.1016/j.trd.2014.05.020.

304. Int Panis, L.; Beckx, C.; Broekx, S.; Vlieger, I. de; Schrooten, L.; Degraeuwe, B.; Pelkmans, L. PM, NOx and CO2 emission reductions from speed management policies in Europe. *Transport Policy* **2011**, *18*, 32–37, doi:10.1016/j.tranpol.2010.05.005.

305. Int Panis, L.; Broekx, S.; Liu, R. Modelling instantaneous traffic emission and the influence of traffic speed limits. *Sci. Total Environ.* **2006**, *371*, 270–285, doi:10.1016/j.scitotenv.2006.08.017.

306. Keuken, M.P.; Jonkers, S.; Wilmink, I.R.; Wesseling, J. Reduced NOx and PM10 emissions on urban motorways in The Netherlands by 80 km/h speed management. *Sci. Total Environ.* **2010**, *408*, 2517–2526, doi:10.1016/j.scitotenv.2010.03.008.

307. Madireddy, M.; Coensel, B. de; Can, A.; Degraeuwe, B.; Beusen, B.; Vlieger, I. de; Botteldooren, D. Assessment of the impact of speed limit reduction and traffic signal coordination on vehicle emissions using an integrated approach. *Transportation Research Part D: Transport and Environment* **2011**, *16*, 504–508, doi:10.1016/j.trd.2011.06.001.

308. Gao, C.; Xu, J.; Li, Q.; Yang, J. The Effect of Posted Speed Limit on the Dispersion of Traffic Flow Speed. *Sustainability* **2019**, *11*, 3594, doi:10.3390/su11133594.

309. Lange, M.; Hendzlik, M.; Schmied, M. *Klimaschutz durch Tempolimit*: *Wirkung eines generellen Tempolimits auf Bundesautobahnen auf die Treibhausgasemissionen*, 2020.

310. Löhe, U. *Geschwindigkeiten auf Bundesautobahnen in den Jahren 2010 bis 2014*: *Schlussbericht zum AP-Projekt F1100.6213001*, 2016.

311. Zhang, S.; Witlox, F. Analyzing the Impact of Different Transport Governance Strategies on Climate Change. *Sustainability* **2020**, *12*, 200, doi:10.3390/su12010200.

312. Haklay, M. How Good is Volunteered Geographical Information? A Comparative Study of OpenStreetMap and Ordnance Survey Datasets. *Environ Plann B Plann Des* **2010**, *37*, 682–703, doi:10.1068/b35097.

313. Jacobs, K.T.; Mitchell, S.W. OpenStreetMap quality assessment using unsupervised machine learning methods. *Transactions in GIS* **2020**, *24*, 1280–1298, doi:10.1111/tgis.12680.

314. Heydecker, B.G.; Addison, J.D. Analysis and modelling of traffic flow under variable speed limits. *Transportation Research Part C: Emerging Technologies* **2011**, *19*, 206–217, doi:10.1016/j.trc.2010.05.008.

315. Khondaker, B.; Kattan, L. Variable speed limit: an overview. *Transportation Letters* **2015**, *7*, 264–278, doi:10.1179/1942787514Y.0000000053.

316. Papageorgiou, M.; Kosmatopoulos, E.; Papamichail, I. Effects of Variable Speed Limits on Motorway Traffic Flow. *Transportation Research Record* **2008**, *2047*, 37–48, doi:10.3141/2047-05.

317. Bertini, R.L.; Boice, S.; Bogenberger, K. Dynamics of Variable Speed Limit System Surrounding Bottleneck on German Autobahn. *Transportation Research Record* **2006**, *1978*, 149–159, doi:10.1177/0361198106197800119.

318. Hegyi, A.; DeSchutter, B.; Hellendoorn, J. Optimal Coordination of Variable Speed Limits to Suppress Shock Waves. *IEEE Trans. Intell. Transport. Syst.* **2005**, *6*, 102–112, doi:10.1109/TITS.2004.842408.

319. Abdel-Aty, M.; Dilmore, J.; Dhindsa, A. Evaluation of variable speed limits for real-time freeway safety improvement. *Accid. Anal. Prev.* **2006**, *38*, 335–345, doi:10.1016/j.aap.2005.10.010.

320. Islam, M.T.; Hadiuzzaman, M.; Fang, J.; Qiu, T.Z.; El-Basyouny, K. Assessing Mobility and Safety Impacts of a Variable Speed Limit Control Strategy. *Transportation Research Record* **2013**, *2364*, 1–11, doi:10.3141/2364-01.

321. Lee, C.; Hellinga, B.; Saccomanno, F. Evaluation of variable speed limits to improve traffic safety. *Transportation Research Part C: Emerging Technologies* **2006**, *14*, 213–228, doi:10.1016/j.trc.2006.06.002.

322. Wilmot, C.G.; Khanal, M. Effect of Speed limits on speed and safety: A review. *Transport Reviews* **1999**, *19*, 315–329, doi:10.1080/014416499295420.

323. Hirst, W.M.; Mountain, L.J.; Maher, M.J. Are speed enforcement cameras more effective than other speed management measures? An evaluation of the relationship between speed and accident reductions. *Accid. Anal. Prev.* **2005**, *37*, 731–741, doi:10.1016/j.aap.2005.03.014.

324. Montella, A.; Imbriani, L.L.; Marzano, V.; Mauriello, F. Effects on speed and safety of point-to-point speed enforcement systems: evaluation on the urban motorway A56 Tangenziale di Napoli. *Accid. Anal. Prev.* **2015**, *75*, 164–178, doi:10.1016/j.aap.2014.11.022.

325. Soole, D.W.; Watson, B.C.; Fleiter, J.J. Effects of average speed enforcement on speed compliance and crashes: a review of the literature. *Accid. Anal. Prev.* **2013**, *54*, 46–56, doi:10.1016/j.aap.2013.01.018.

326. Arnaout, G.M.; Arnaout, J.-P. Exploring the effects of cooperative adaptive cruise control on highway traffic flow using microscopic traffic simulation. *Transportation Planning and Technology* **2014**, *37*, 186–199, doi:10.1080/03081060.2013.870791.

327. Barcel, J.; Codina, E.; Casas, J.; Ferrer, J.L.; Garca, D. Microscopic traffic simulation: A tool for the design, analysis and evaluation of intelligent transport systems. *J Intell Robot Syst* **2005**, *41*, 173–203, doi:10.1007/s10846-005-3808-2.

328. So, J.; Motamedidehkordi, N.; Wu, Y.; Busch, F.; Choi, K. Estimating emissions based on the integration of microscopic traffic simulation and vehicle dynamics model. *International Journal of Sustainable Transportation* **2018**, *12*, 286–298, doi:10.1080/15568318.2017.1363328.